Rheology of Cellulose Nanocrystal Dispersions and Pickering Emulsions Stabilized by Cellulose Nanocrystals

by

Saumay Kinra

A thesis
presented to the University of Waterloo
in fulfillment of the
thesis requirement for the degree of
Master of Applied Science
in
Chemical Engineering

Waterloo, Ontario, Canada, 2023

Author's Declaration

I hereby declare that I am the sole author of this thesis. This is a true copy of the thesis, including any required final revisions, as accepted by my examiners.

I understand that my thesis may be made electronically available to the public.

Abstract

Dispersions and Emulsions are prevalent in our society and can be seen in various applications and industries. These include: (a) the food industry, for various products such as mayonnaise, salad dressings, sauces, and ice cream, (b) the pharmaceutical industry, in drug delivery systems which include both oral and topical medications and (c) many different industrial processes, such as metalworking, lubrication, and cutting fluids. The rheology of emulsions is dependent on a series of factors, including but not limited to droplet size, particle interactions, oil volume fraction, shear rate and salt concentration. Utilizing nanoparticles to create emulsions introduces distinctive rheological properties due to their exceedingly small size and expansive surface area. The nanoparticles of choice used in this study are cellulose nanocrystals (CNCs).

This study investigates the rheology of oil-in-water emulsions (O/W) that are stabilized and thickened by cellulose nanocrystals; also known as nanocrystalline cellulose (NCC). This was investigated over a large range of NCC and oil concentrations. The NCC concentrations varied from 1.03 to 7.41 wt% (weight percent) and the oil concentrations of the emulsions varied from approximately 10 to 70 wt% (weight percent). In the process of making these emulsions, NCC dispersions were made for which a rheological analysis was done as well. Various properties such as the physical appearance, stability, droplet size, and the rheological behaviour were studied as a function of concentration, time, and shear rate in this thesis.

The study indicates that the emulsions produced were highly stable over a period of time with respect to creaming and coalescence. At higher concentrations, the emulsions behaved as non-Newtonian fluids, due to the fact that they exhibited strong shear-thinning behaviour. The rheological data were described using an existing power-law model which introduced two variables: the consistency index (K) and the flow behaviour index (n). These two variables for the emulsions were strongly dependent on the NCC and oil concentrations. Upon fixing the oil concentration, it was observed that the consistency index increased, and the flow behaviour index decreased with an increase in NCC concentration. Similarly, upon

fixing the NCC concentration, it was observed that the consistency index increased, and the flow behaviour index decreased with an increase in the oil concentration.

Acknowledgements

First and foremost, I would like to offer my gratitude to my supervisor, Professor Rajinder Pal, for his guidance and help throughout my Master's study and research. I would like to thank him for his patience and support. I would also like to thank Professor Aiping Yu and Professor Ali Elkamel for taking the time out to read and critique my thesis.

Secondly, I would like to thank Professor Juewen Liu and his student MoMo Zandieh in the Bio-nanotechnology & Interfaces Laboratory for allowing me to use the Malvern Zetasizer instrument for Particle size distribution and Zeta potential measurements.

Moreover, I would like to thank Dr. Nina Heinig and Dr. Lei Zhang at Watlab for their help with obtaining SEM and STEM pictures of my samples.

Lastly, I would like to express my gratitude to Bert Habicher and Richard Hecktus for all their technical expertise and support throughout my research.

Dedication

I would like to dedicate this thesis to my family, my parents, Rajesh and Dr. Anita, and my brother, Rajit, whose unwavering support and encouragement have been the driving force behind my educational journey. Their belief in my abilities, countless sacrifices, and constant encouragement have been instrumental in reaching this milestone. I am also grateful for the guidance and encouragement from my aunt, Dr. Pooja Suneja Madan, who helped me in navigating my studies. I would also like to express my deepest appreciation to my friends and colleagues who have provided support and motivation during this challenging but rewarding academic pursuit.

Table of Contents

List of Figures

List of Tables

Chapter 1: Introduction

1.1 Background

Cellulose may be considered the world's most abundant biopolymer with a wide range of applications[1]. 'Biopolymer' implies that cellulose is an organic compound; with the chemical formula $(C_6H_{10}O_5)_n$ composed of repeating units of glucose linked by β-1,4-glycosidic bonds[2]. Due to this abundance, cellulose and its fibers are considered as a very attractive replacement to conventional reinforcing materials. These advantages include it being of low weight, renewable, biodegradable, and cost-effective. Some disadvantages include absorption of moisture and low thermal stability and electrical conductivity[3,4]. Figure 1 below shows the structure of cellulose and its repeating unit.

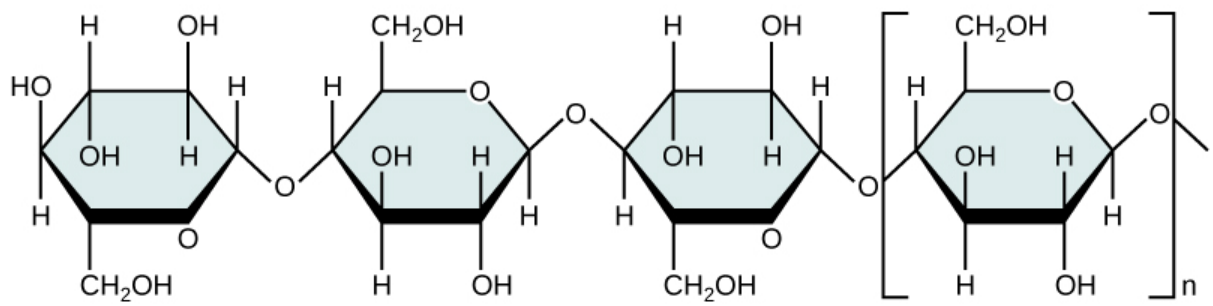

Figure 1 Structure of Cellulose[5]

1.2 Cellulose Nanocrystals (CNC)

Cellulose Nanocrystals can be categorized into three main subcategories, depending on their dimensions and the manufacturing process required which is subsequently on the source. These include Micro-fibrillated cellulose (MFC), Bacterial nano-cellulose (BNC) and Nanocrystalline cellulose (NCC)[2]. In the context of this thesis, the acronym 'CNC' is also used interchangeably with NCC to signify Cellulose nanocrystals. Cellulose is generally linked with being a structural material in the cell wall of green plants. Typical sources of cellulose and NCC include cotton, wood and hemp with cotton being almost the purest form of cellulose. The cellulose content of cotton fiber is >80%, that of wood is 30–60%, and that of dried hemp is >70%[6].

The production of NCC usually involves the sulfuric acid hydrolysis of amorphous portions of cellulose fibers. These cellulose macromolecules then undergo two simultaneous reactions: the hydrolysis of the glycosidic bonds and the esterification of the surface hydroxyl groups. The hydrolysis of the bonds breaks down the cellulose chains to the point where the disordered regions are fully degraded, and the crystalline portions remain[7]. This mechanism can be seen in Figure 2 below.

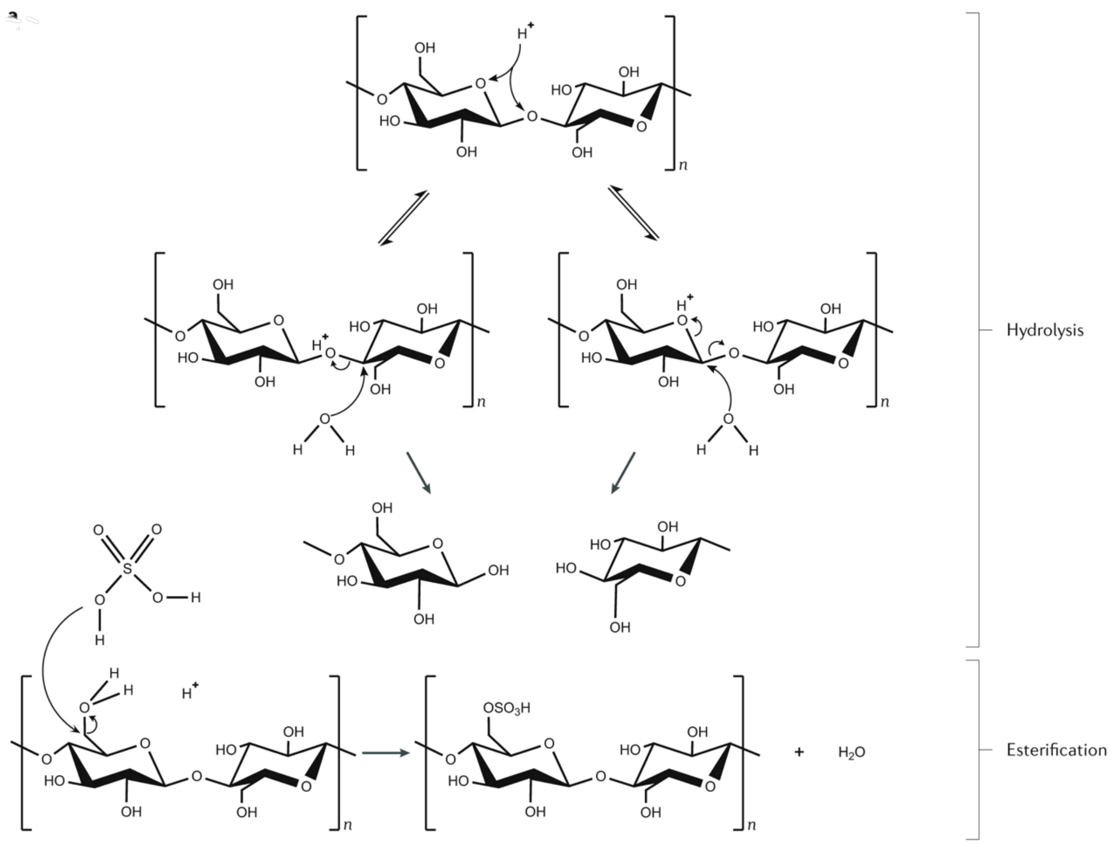

Figure 2 Mechanism to illustrate the hydrolysis and esterification of cellulose[7]

The manufacturing process involving this mechanism is completed in about 2 hours, with yields ranging between 20 and 75%. The sulfuric acid hydrolysis leads to the break down of the glycosidic bonds until the average degree of polymerization decreases to a set levelling off point. This is referred to as the levelling off degree of polymerization (LODP)[8]. This point is generally set at the point at which the rate of decrease plateaus and the degree of polymerization decreases very slowly in comparison to the initial decrease. This is illustrated in Figure 3 below.

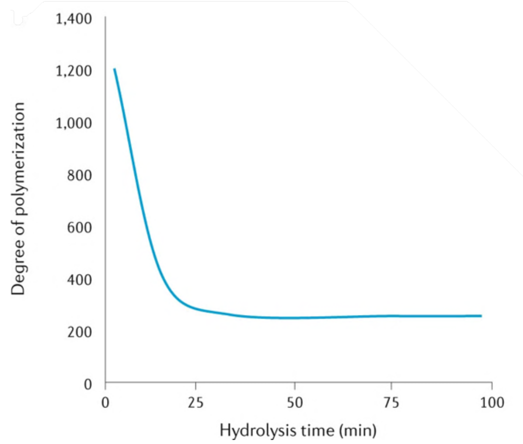

Figure 3 Graph to determine the levelling off degree of polymerization (LODP)[7]

This acid and slurry mixture is then quenched in cold water to terminate the reaction before being centrifuged and dialyzed to remove the acid. The last step in the purification of the nanocrystals is sonication and filtration. A schematic of this process can be found in Figure 4 below[7].

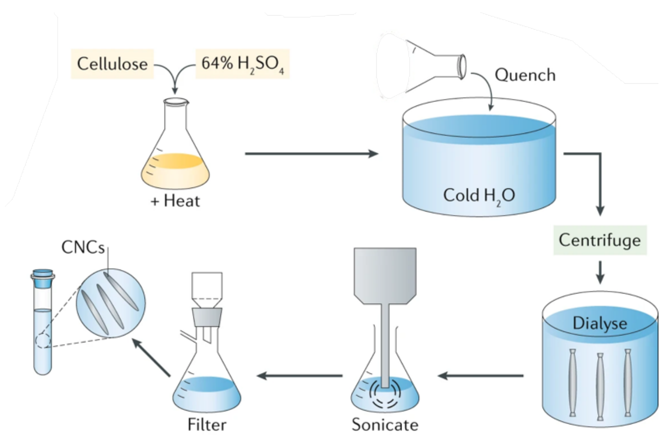

Figure 4 The manufacturing process of Cellulose Nanocrystals (CNCs)[7]

1.3 Applications of Cellulose Nanocrystals

Due to its unique properties and renewable nature, CNCs are very viable candidates for many consumer and industrial applications. Some novel examples include the fabrication of flexible and stretchable strain sensors[9], stretchable electroluminescent devices, flexible triboelectric nanogenerators and recyclable/biodegradable packaging products.

1. **Hydrophobically modified NCC used to disperse Graphene (GN) in flexible and stretchable strain sensors[9]:** These types of sensors have a wide range of applications within the emerging soft electronics industry. To evaluate the operation of these sensors, sensitivity and stretchability are the chosen metrics. Stretchability would then imply the use of a flexible material. The flexible material is a composite material consisting of an extremely flexible elastomer such as polydimethylsiloxane (PDMS) filled with highly conductive filler such as graphene to improve the sensitivity. The issue faced with the use of graphene is that is not easily dispersible in polymer matrix due to weak interactions between GN and the polymer. To combat this issue, NCC is used as it is highly effective in dispersing GN in a polymer matrix. This NCC is first hydrophobically modified to form hydrophobically modified NCC (MNCC). This is then used to form nanocomplexes with GN. The MNCC-GN nanocomplexes are readily dispersible in elastomer due to the strong interaction between the nanocomplexes and the elastomer, leading to an improvement in the interfacial bonding with the PDMS. Thus, this process results in highly flexible and stretchable electrically conductive elastomers suitable for the fabrication of flexible and stretchable strain sensors.
2. **NCC used with Silver Nanowires to form electrodes and fabricate stretchable electroluminescent devices[10]:** Stretchable electroluminescent (EL) devices have garnered significant interest as a pivotal technology for next-generation lighting and display applications. These devices possess the unique ability to maintain their functionality under severe mechanical deformations, due to their exceptional mechanical compliance. In contrast to rigid EL devices, stretchable EL devices offer remarkable flexibility, rendering them highly suitable for applications in biomedical devices and soft interactive display systems. The method proposed involves fabricating

a device with a luminescent layer between electrodes made of silver nanowires-cellulose nanocrystals (CNC II) and a polydopamine-polydimethylsiloxane (PDA-PDMS) matrix. The CNC II acts as a green dispersant, film-forming agent, and antioxidant, significantly enhancing the electrodes' optical, electrical, mechanical, and antioxidant properties. The resulting EL devices exhibit smooth surfaces, low sheet resistance, high transparency, ideal stretchability, and excellent resistance to oxidation. They demonstrate outstanding luminance, flexibility, and stretchability, even in underwater or extreme temperature conditions. Additionally, the devices exhibit intrinsic biocompatibility, making them suitable for wearable display applications and providing insights for advancing flexible electronics.

3. **Nano-cellulose to replace non-renewable synthetic polymers as raw materials for Triboelectric Nanogenerators (TENGs)[11]:** TENGs are a recently proposed mechanical energy conversion technology which combines the two effects of contact electrification and electrostatic induction to transform external mechanical energy into electric energy[12]. It is made up of three parts: the negative and positive triboelectric layer and conductive electrodes. As mentioned earlier, cellulose-based materials possess good biocompatibility and biodegradability which helps in ensuring the sustainability and conservation of the TENGs in the application itself. These functional materials possess desirable characteristics such as optimal surface roughness, lightweight composition, low thermal expansion coefficient, and excellent mechanical properties. Despite the relatively weak triboelectric polarity of nanocellulose, it remains an ideal alternative for active TENGs due to its favorable dielectric properties in addition to the characteristics. When compared to a typical TENG, the output performance of the cellulose-based TENG was equivalent in terms of open-circuit voltage (Voc), short-circuit current (Isc) and power density[13]. Some studies[13,14] have shown that NCC can act as either the positive or negative triboelectric layer based on the material it is paired with. For example, when it is paired with a synthetic polymer with a strong electron acquiring ability, such as Fluoroethylenepropylene (FEP) or Polytetrafluoroethylene (PTFE), it behaves as a positive triboelectric material. On the other hand, when it is paired with a metal, a material with the tendency to lose

electrons, it behaves as a negative triboelectric material. As we saw with the stretchable electroluminescent devices, silver nanowires are good candidates for use as a material in the electrodes and the triboelectric layers[15,16].

4. **Biobased nanomaterials (Cellulose nanocrystals) to be used as a form of biodegradable and recyclable food packaging[17]:** In recent years, there has been a growing consumer demand for healthier food packaging options. Consumers are increasingly aware of the potential health risks associated with certain packaging materials and are seeking alternatives that prioritize their well-being. Healthier food packaging encompasses various aspects, including the use of non-toxic materials, reduced chemical additives, and packaging designs that minimize the risk of contamination or leaching of harmful substances into the food. Consumers are also looking for packaging that is environmentally friendly, recyclable, and made from sustainable materials. This shift in consumer preferences is driving food companies and packaging manufacturers to innovate and develop packaging solutions that align with these health-conscious values, promoting both the safety of the packaged food and the well-being of consumers. Cellulose nanocrystals (NCC) are commonly utilized as reinforcing agents in various materials, often with chemical modifications to enhance compatibility. NCC has been incorporated into food packaging materials such as polyethylene (PET), polypropylene (PP), polylactic acid (PLA), polyvinyl alcohol (PVA), and carboxymethyl cellulose (CMC)[18,19]. For instance, composite films made of PVA/CNC/CMC demonstrated improved mechanical strength, barrier properties, thermal stability, and transparency for food packaging applications[20]. Furthermore, when combined with antimicrobial materials, PLA/nanocellulose composites exhibited antimicrobial properties. These antimicrobial agents include both organic materials, such as organic acids, polymers, or enzymes, and inorganic materials, such as metal and metal oxide nanoparticles[21].

Chapter 2: Literature Review

Dispersions are prevalent in our society and can be observed across in various applications and industries[22]. Dispersions are defined as a mixture or a system in which one material's particles are dispersed in a continuous phase of another material[23]. Their classification is based on the particle sizes and the degree of homogeneity within the mixture. The two main categories of dispersions are suspensions and colloids.

Suspensions are heterogeneous mixtures that contain larger particles compared to solutions. These particles are evenly distributed through mechanical agitation, but they eventually settle out when the agitation ceases. Suspensions typically have particle sizes larger than 1 μm.

On the other hand, colloids are homogeneous but cloudy mixtures that exhibit characteristics between solutions and suspensions. Unlike suspensions, colloidal particles do not settle out when left undisturbed, but they do scatter light when a beam passes through. The particle size of colloids ranges between 1 nm and 1 μm. Colloids can be further categorized into emulsions (liquid-liquid dispersions of immiscible liquids), aerosols (dispersions of solid or liquid particles in a continuous gas phase), foam (dispersion of gas phase in a continuous liquid phase), and hydrosols (dispersions of solid particles in a liquid medium). Examples of dispersions include creams (oil-water dispersions), milk, fog, quicksand, and polymer particles dispersed in a liquid medium such as gelatin.

2.1 Fundamentals of Rheology

Rheology is the branch of science that deals with the study of the flow and deformation of materials under the influence of applied forces or stresses. It encompasses the behavior of materials that exhibit both solid-like and liquid-like properties. Rheology explores how materials respond to various conditions such as shear stress, strain, temperature, and time[24]. By examining the flow characteristics, viscosity, elasticity, and other rheological properties of materials, rheology provides valuable insights into their mechanical behavior and enables the understanding and control of processes involving the flow and deformation of substances, ranging from liquids and polymers to complex fluids and soft matter systems[25]. The field mainly looks at the flow of different complex fluids, including polymers, emulsions, and suspensions. It does so by investigating the relationship between shear stress and shear rate for complex fluids and Newtonian fluids, which generally describe the behavior for simple liquids. These complex fluids tend to be viscous in addition to their important rheological properties which makes them an essential part of rheology[26].

Imagine a layer of fluid moving between two large parallel plates with both plates having the same surface area, *A*, and a distance, *Y*, between them. This can be seen in Figure 5 below:

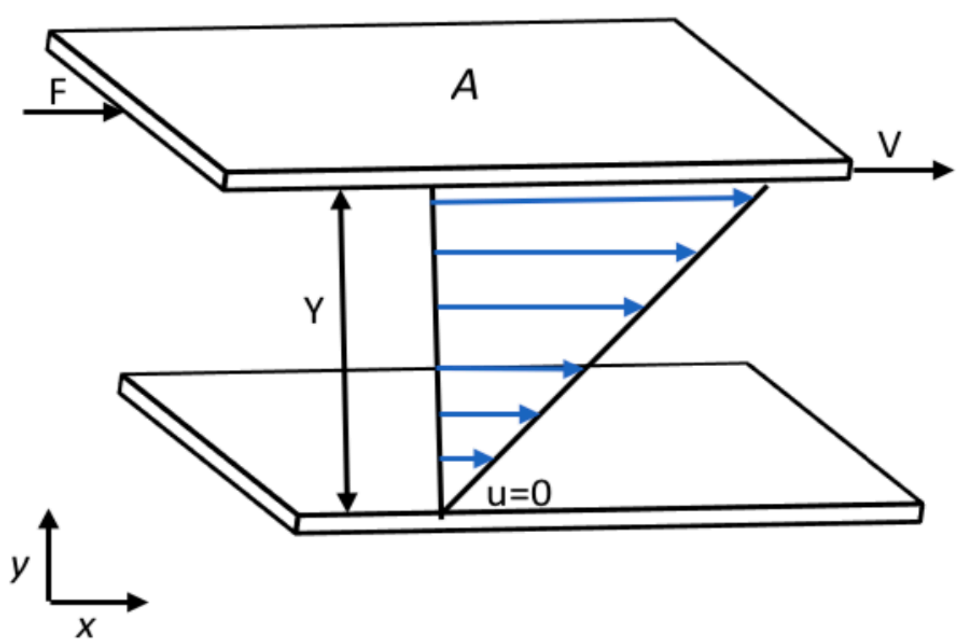

Figure 5 Graphical representation of one directional shear flow

As seen in the figure, the lower plate is to remain stationary while the upper plate starts moving with a constant velocity, *V*, to the right in the positive *x*-direction. Due to this movement, the fluid gains momentum and the other layers in the liquid start moving in the same motion as the upper plate. After some time passes, the system attains a steady state situation where the velocity of the lowest layer of fluid, right above the lower stationary plate, is zero and the velocity of the highest layer of fluid, right below the upper in-motion plate, is the same as the plate at *V*. If we were to look at the velocity profile between the two plates at this steady state, we would be able to see that it increases at a positive *y* slope when going from the lower to the upper plate. To keep the upper plate in motion, a force, *F*, is required. This force per unit surface area, *A*, of the plate is known as the shear stress and is directly proportional to the velocity, *V*, and is inversely proportional to the distance between the two plates, *Y*. This can be represented mathematically below:

$$Shear\ Stress = \frac{F}{A} \propto \frac{V}{Y} \tag{1}$$

To eliminate the proportionality, we can introduce a proportionality constant, μ, which is known as the dynamic viscosity of the fluid. This can be written as:

$$Shear\ Stress = \frac{F}{A} = \mu\frac{V}{Y} \tag{2}$$

Due to the linear velocity profile, Equation 2 can be rewritten for a very small segment fluid, i.e., the differential form of the equation:

$$Shear\ Stress = \tau_{y,x} = -\mu\frac{dV}{dY} \tag{3}$$

Shear stress can be represented using the symbol, $\tau_{y,x}$, to symbolize a force acting in the negative direction on a unit area normal to the *y* direction. The negative sign then signifies that the shear stress acts on a direction that is opposite to the direction of motion of a faster-moving fluid. Equation 3 is also known as *Newton's Law of Viscosity* which states the shear force per unit area (shear stress) is directly proportional to the negative velocity gradient. From the name, it can be inferred that the fluids that follow this law are known as *Newtonian* *fluids.* The complex fluids that we work with, such as dispersions, slurries, and suspensions, generally do not exhibit the same behavior and are called *non-Newtonian fluids.* This behavior can be explained using momentum transfer and a modified form of Equation 3 which uses an incompressible fluid of density, ρ.

$$Shear\ Stress = \tau_{y,x} = -\frac{\mu}{\rho}\frac{d(\rho V_x)}{dY} \tag{4}$$

V_x represents the velocity in the x-direction and the quantity in the parenthesis, ρV_x, represents the momentum per unit volume of fluid. Therefore, $\tau_{y,x}$, then represents the transfer of x-direction momentum in the y-direction which then relates to the subscripts in the symbol. The first fraction in the equation, $\frac{\mu}{\rho}$, is often simplified to another symbol which is known as the fluid property, kinematic viscosity, ν.

$$\nu = \frac{\mu}{\rho} \rightarrow \tau_{y,x} = -\nu\frac{d(\rho V_x)}{dY} \tag{5}$$

The negative sign in this equation relating momentum leads to the understanding that the transfer of momentum happens in the downward direction with respect to velocity. Specifically, in the direction of the higher velocity fluid layer to the lower velocity fluid layer[27,28].

2.2 Flow Behaviour of Dispersions

The most common rheological quantity we encounter is viscosity as it plays a vital role in describing the flow behavior of any liquid. For Newtonian fluids, the viscosity is constant at any given pressure or temperature and is independent of the shear rate (γ). This is not the case for non-Newtonian fluids. For non-Newtonian fluids, the viscosity depends on the shear rate and is generally specified at a given shear rate which is then known as the 'shear viscosity'. This shear viscosity is found by dividing the shear stress with the shear rate. It also depends on a myriad of factors, including flow geometry and any forces that may have acted on the fluid other than the shear rate[29]. In a real-life situation, viscosity mainly depends on the pressure, temperature, and the time the shear is applied. Dispersions show two types of non-Newtonian behavior when subjected to shear rate.

2.1.1 Shear Thinning Behaviour

Shear thinning behavior, also known as pseudo-plastic behavior, refers to a non-Newtonian behavior in which viscosity decreases with an increase in shear rate[30]. One observation in polymeric solution was that for very low shear rates, the apparent viscosity is almost independent of shear rate and is constant. This constant is known as 'zero shear viscosity'.

$$Zero\ shear\ viscosity = \eta_0 = \lim_{shear\ rate \to 0} \frac{Shear\ Stress}{Shear\ Rate} \tag{6}$$

At very high shear rates, the apparent viscosity reaches another constant value known as the 'infinite shear viscosity'.

$$Infinite\ shear\ viscosity = \eta_\infty = \lim_{shear\ rate \to \infty} \frac{Shear\ Stress}{Shear\ Rate} \tag{7}$$

The minimum shear rate value after which a fluid displays shear-thinning behavior is known as the 'critical shear rate value'. This depends on factors like particle shape/size, polymer concentration, and the nature of solvent[29]. The figure below displays the flow behavior for a typical shear-thinning fluid on a log-log scale.

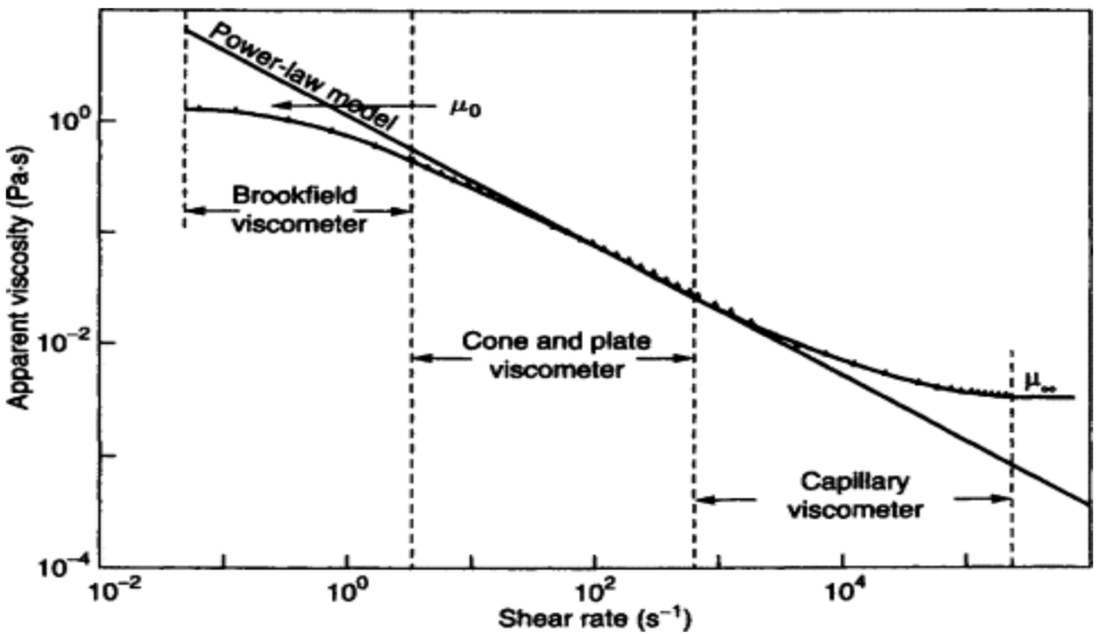

Figure 6 Flow behavior of a typical shear-thinning fluid[31]

2.1.2 Shear Thickening Behaviour

Shear thickening behavior refers to a non-Newtonian behavior in which viscosity increases with an increase in shear rate[32]. This phenomenon occurs as the flow resistance increases with higher shear rates. This behavior is generally observed in concentrated suspensions under high shear rates, although some suspensions may exhibit it even at lower shear rates. Examples include concentrated suspensions of titanium oxide, china clay, and cornstarch in water, among others. Numerous explanations have been proposed to account for shear thickening behavior. One widely accepted explanation is that, at high shear rates, the liquid is unable to effectively fill the void spaces between particles, leading to reduced lubrication and increased frictional forces. This, in turn, manifests as an apparent increase in viscosity[33]. The figure below displays the flow behavior for a typical shear-thickening fluid on a log-log scale.

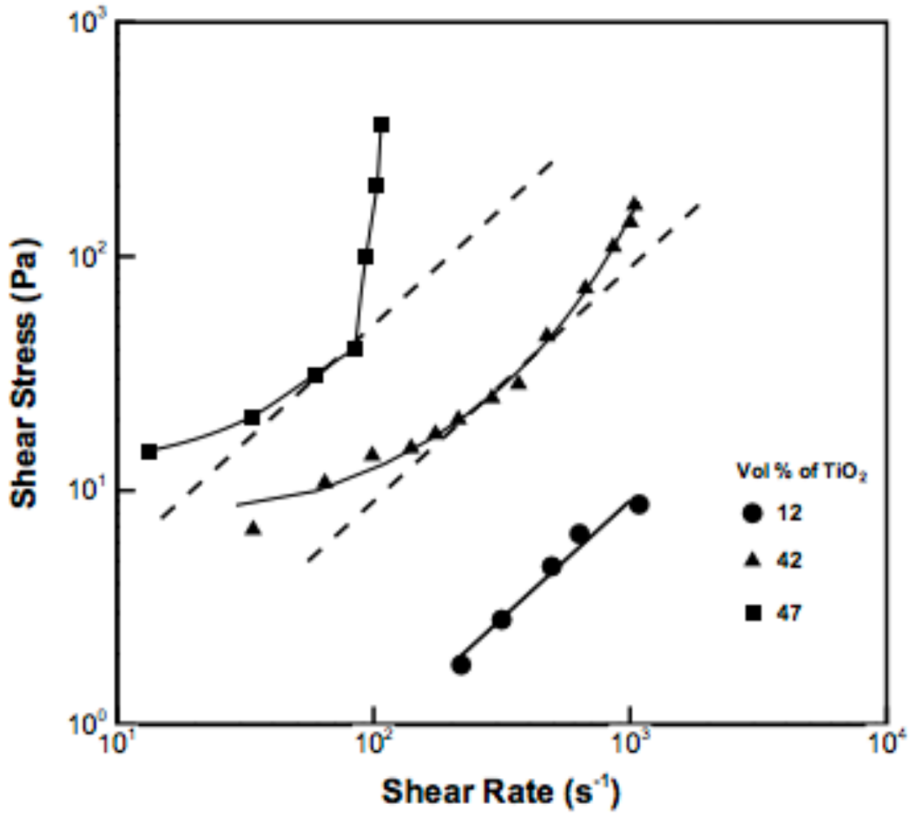

Figure 7 Flow behavior of a typical shear-thickening fluid[34] (TiO_2 suspensions at different particle concentrations)

2.1.3 Power-Law model

The power-law model is one of the most popular models used to approximate fluid behavior. It uses a relation between shear rate and shear stress which can be approximated using a power curve (Equation 8). This is then re-written in terms of shear viscosity and shear rate to get two new empirical parameters, the flow behavior (power-law) index and the consistency index (Equation 9).

$$\tau = K\gamma^n \quad (8)$$

$$\eta = \tau/\gamma = K\gamma^{n-1}$$

(9)

Where,

τ is the shear stress

γ is the shear rate

K is the consistency index

n is the flow behaviour (power-law) index

η is the viscosity

Using a log-log plot of the viscosity versus the shear rate, we can obtain a linear plot which would give us the flow behavior index and the consistency index. The flow behavior index (n) and the consistency index (K) can be determined from the slope and intercept, respectively[35,36].

Below we can see a table with different values for the power-law index and the different fluid behavior it corresponds to.

Table 1 Power Law index values for different fluid behaviour

n **value**	**Fluid behaviour**
$n = 1$	Newtonian Fluid
$n < 1$	Shear Thinning Fluid
$n > 1$	Shear Thickening Fluid

2.3 Stability of Suspended Particles: DLVO Theory

To predict and study the applications of suspended systems, one needs to understand the role played by stability. A popular theory for colloidal stability is the DLVO theory proposed and named by the researchers Landau, Derjaguin, Overbeck and Verwey. The theory focuses on the two major forces acting on charged particles in a liquid medium, i.e., Van der Waals forces and electrostatic forces. As per the theory, the overall interaction between charged particles can be considered as a combination of Van der Waals and columbic interactions, both of which play crucial roles in determining colloidal stability. These interactions form the fundamental foundation for understanding the stability of colloidal systems.

2.1.4 Van der Waals forces

Van der Waals forces, also known as London dispersion forces, are weak intermolecular forces that exist between atoms and molecules. These forces arise due to temporary fluctuations in electron distribution, leading to temporary dipoles. These temporary dipoles induce similar dipoles in neighbouring particles, resulting in attractive forces between them. Van der Waals forces are present in all molecules, regardless of their polarity. Although individually weak, these forces can have a significant cumulative effect, especially in larger molecules or particles with larger surface areas. Van der Waals forces can then be categorized as the total sum of all the interactions between all the neighbouring surfaces with the geometry of the system playing a huge role. A mathematical formula can be applied to approximate the Van der Waals force, F_A, for two spherical particles with a specified radius, R:

$$F_A = \frac{H \times R}{12 \times L^2} \tag{10}$$

Where H is the Hamaker constant L is the distance between the particles. This formula applies for distances that are relatively small; specifically, those that are smaller than the particle radius, R. The Hamaker constant is dependent on material properties, such as density and polarizability, and the medium present[37].

2.1.5 Electrostatic Repulsion Between Particles

Electrostatic repulsion refers to the phenomenon where particles with like charges experience a force that pushes them away from each other. It arises due to the presence of electric charges on the surface of particles. According to Coulomb's law, particles with the same charge will repel each other with a force that is inversely proportional to the square of the distance between them. This repulsive force can prevent particles from coming into proximity and can play a crucial role in stabilizing colloidal systems. Electrostatic repulsion is particularly significant in systems where the charges on particles are mobile or can be influenced by the surrounding environment, such as in the presence of ions or pH changes. By balancing the attractive forces and the electrostatic repulsion, colloidal stability can be maintained, preventing particle aggregation or precipitation. In many cases, the repulsive forces are strong enough to counteract the attractive Van der Waals forces, thereby preventing particle aggregation. There are two mechanisms through which particles can acquire a charge in a liquid medium. Firstly, the surface groups of particles may undergo ionization or dissociation, resulting in the development of a charged surface. Secondly, ions present in the solution can adsorb onto initially uncharged surfaces, thereby imparting a charge to the particles. These mechanisms play a crucial role in establishing and maintaining the electrostatic repulsion between particles in colloidal systems[38].

2.4 Rheology of cellulose nanocrystal dispersions and O/W emulsions stabilised by cellulose nanocrystals

Dispersions and Emulsions are present in various aspects of our daily lives and are utilized in a wide range of everyday products[22]. An example of an emulsion is milk, which is an emulsion of fat globules dispersed in a water-based solution[38]. CNC, or NCC, dispersions are used in various applications and have become increasingly important in recent years[39]. These dispersions consist of highly refined cellulose particles suspended in a liquid medium, often water. The rheology of these Dispersions and the Emulsions made using them (oil-in-water) are of interest to researchers due to the large abundance and availability of cellulose in addition to the fact that it is renewable[39-42].

The dispersions are prepared first by adding the NCC powder (CelluForce Inc.) to a polar liquid such as water. Emulsions are then prepared by adding oil to these dispersions. The NCC particles are amphiphilic, meaning they have both hydrophilic (water-attracting) and hydrophobic (oil-attracting) properties. This is beneficial because it allows for the particles to adsorb at the interface of the oil and water droplets, forming a protective layer around them. This layer of particles acts as a physical barrier, preventing the droplets from coalescing and maintaining stability. The solid particles remain at the interface even if the emulsion is subjected to changes in temperature, pH, or mechanical stress. The use of solid particles in Pickering emulsions offers advantages such as enhanced stability, resistance to coalescence, and the potential for new applications in various industries. However, it is important to note that the choice of particles and their surface properties greatly influence the characteristics and behavior of Pickering emulsions. These surface properties include surface charge, surface area, hydrophilicity/hydrophobicity, particle size and aspect ratio.

Shafiei-Sabet, S. et al (2012) reported that these NCC dispersions are isotropic up until the 3 wt% mark after which the dispersion phase separates into crystalline and isotropic domains at higher NCC concentrations[39]. At these higher concentrations, the dispersions display shear-thinning behaviour over a range of shear rates. This could be attributed to the orientation of crystalline domains and individual rod-shaped nanocrystals in the direction of shear[40-42]. The study also employs the use of ultrasound energy and temperature to understand the effect on the dispersion's rheological properties. It showed that there is a relationship between the ultrasound energy applied and the microstructure of the dispersions. The temperature relationship was of interest as the research in this thesis kept the temperature constant to avoid any external effects on the rheological properties. Shafiei-Sabet, S. et al (2012) showed that the viscosity decreased with an increase in temperature and shear rate until a specific critical concentration was reached upon which temperature had no significant effect on the viscosity[39]. This point was around the 10 wt% mark which is higher than the concentrations investigated in this thesis; the maximum being 7.41 wt%. However, at a high enough temperature (around 50°C), the viscosity seemed to increase.

The thesis referred to the study done by Bai et al (2019) to gauge and diagnose the amount of Sodium Chloride (NaCl) that would be required to screen the surface charge and help with the stability[40]. At the beginning of the research, dispersions were made without any other surfactant and phase separation was observed for which a literature review was done to mitigate this issue. Bai et al (2019) employed the use of high-energy microfluidization to prepare O/W emulsions while varying the microfluidization pressure and environmental factors, such as temperature, pH and NaCl concentration. From this, one could obtain two facts regarding droplet size and stability. First, the droplet size decreases with an increase in microfluidization pressure until a certain point after which it increases (about 19 kpsi). Second, the emulsions exhibited good stability over a range of different pH environments, temperature environments, and low NaCl concentrations with droplet flocculation only occurring in acidic conditions (pH = 2) and high NaCl concentrations[40]. From this paper and bench-top experiments, it was decided to keep 0.06 wt% NaCl as the standard for all emulsions made in the lab.

The following Figure shows the STEM (Scanning Transmission Electron Microscopy) micrograph of a 1 wt% NCC sample. The STEM was performed at WATLab at the University of Waterloo with a Libra 200 MC manufactured by Carl Zeiss using the drop-cast method. The image was obtained with a 200 keV monochromatized electron beam and a High-Angle Annular Dark-Field (HAADF) detector. The white regions of the image show the network of aggregates of rod-shaped nanocrystals.

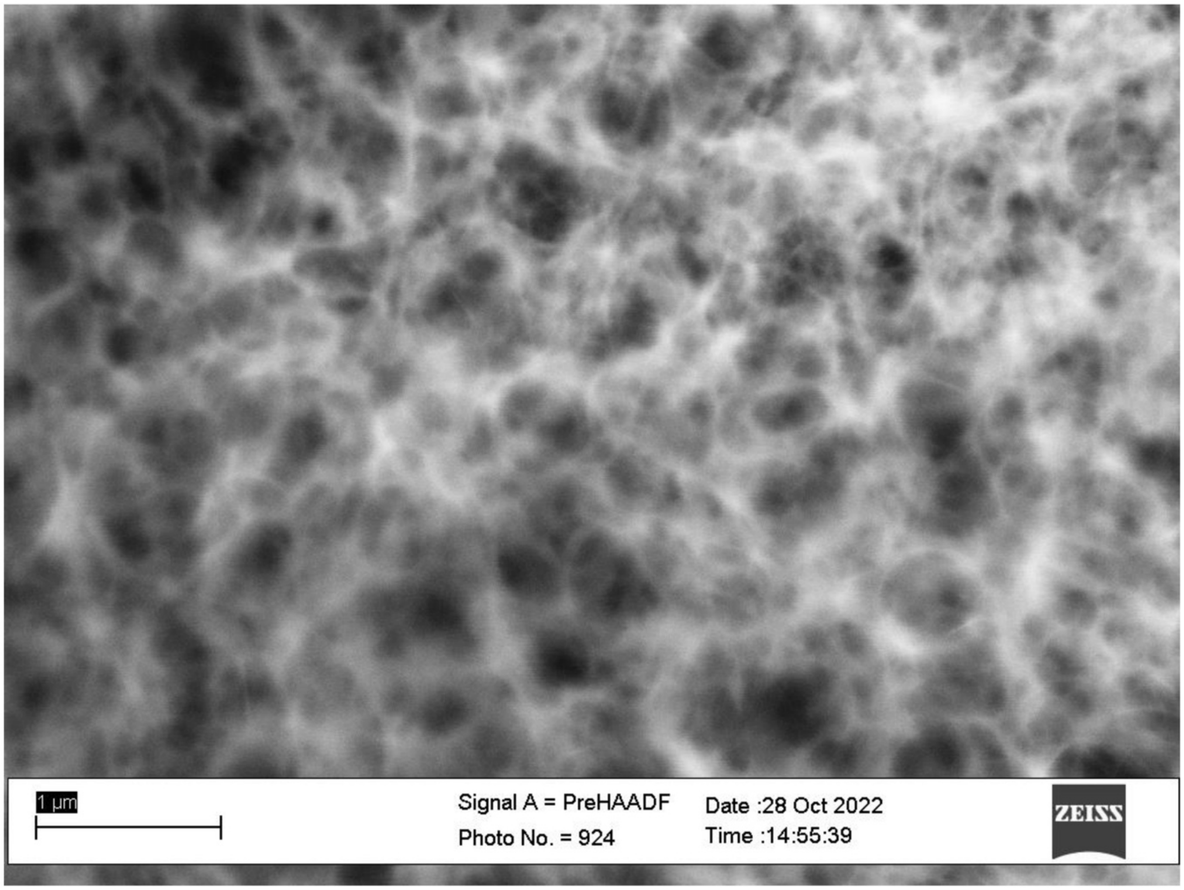

Figure 8 STEM (Scanning Transmission Electron Microscopy) micrograph of 1 wt% NCC solution

Chapter 3: Materials and Methods

3.1 Materials

Oil-in-water (O/W) emulsions were prepared in this study using deionized water, sodium chloride, cellulose nanocrystals, and white mineral oil.

The nanocrystalline cellulose powder (trade name: NCC NCV100-NASD90) was provided by CelluForce Inc., Windsor (ON, Canada). It was produced by the sulfuric acid hydrolysis of wood pulp followed by spray-drying. The cellulose nanocrystals were rod-shaped with a mean length of 76 nm and a mean width of 3.4 nm. The surface area of these nanocrystals was 500 m^2/g, and the crystallinity was 88%[43].

The white mineral oil (Petro-Canada Purity FG WO-15) was supplied by Boucher and Jones Fuels, Waterloo (ON, Canada). The viscosity of the batch of oil used in this study was 27.62 mPa·s at 21 °C. The sodium chloride powder was obtained from Sigma-Aldrich Co. LLC.

3.2 Preparation of Nanocrystalline Cellulose Dispersions

The cellulose nanocrystal dispersions were prepared at room temperature (~22 °C) by adding the powder to about 1000mL deionized water. The cellulose and sodium chloride powder were weighed out as a percentage of the weight of the water used (weight percent, wt%). The sodium chloride was added to the aqueous phase to screen the surface charge of the NCC which would then promote the interfacial packing of nanocrystals at the interface. The concentration of the sodium chloride was fixed at 0.06wt% after a salt analysis was done. Bai et al. (2019) also used the same concentration in preparing NCC-stabilized oil-in-water emulsions[40]. Once the powders were added to the aqueous phase, the mixture was homogenized and agitated using a variable speed homogenizer (Gifford-Wood, model 1L) for about 60 minutes until the nanocrystals were fully dispersed. The dispersion was then allowed to cool down overnight which would also allow for the elimination of any air entrapped during the homogenization. Eight different nanocrystals dispersions were prepared using nanocrystal concentrations ranging from 1.03 to 7.41 wt%. The concentrations were increased in approximately 1 wt% increments. The pH range of all the dispersions was between 7 and 8. The figure below shows the preparation process of these dispersions.

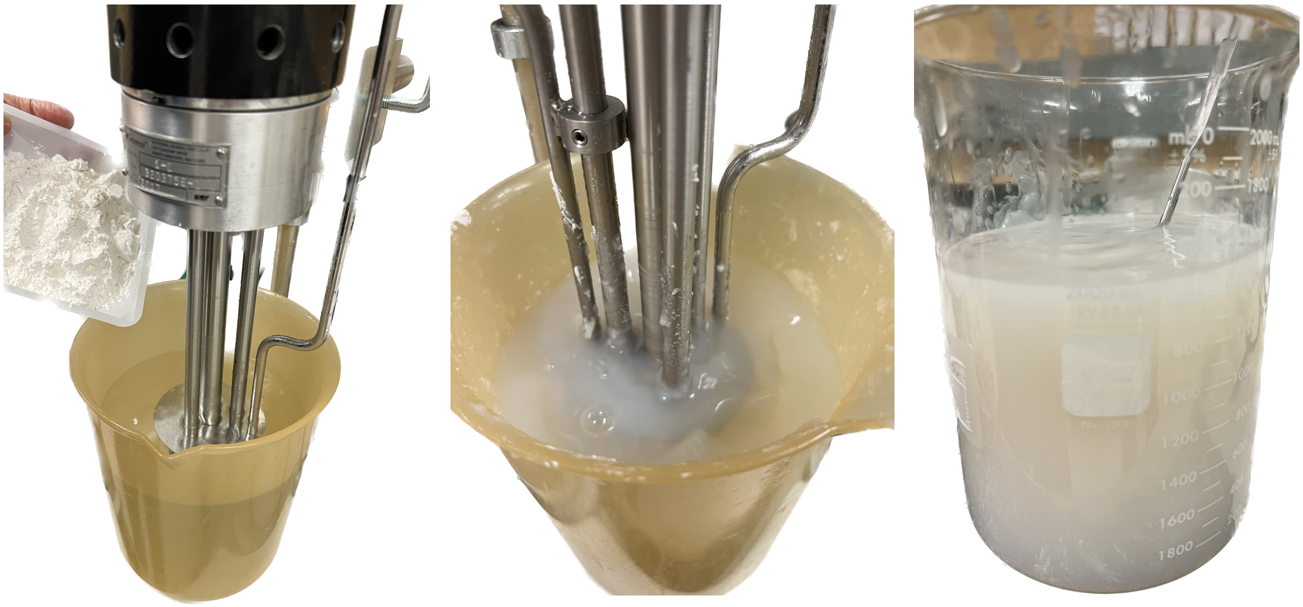

Addition of the nanocrystal and sodium chloride powder to the aqueous phase | **Nanocrystal dispersion during mixing** | **Final dispersion of nanocrystals**

Figure 9 Preparation of cellulose nanocrystals dispersions

3.3 Preparation of Oil-in-water Emulsions

Oil-in-water (O/W) emulsions were prepared at room temperature (~22 °C) by adding a weighed-out amount of oil to a prepared nanocellulose dispersion as discussed in the previous section, whilst being agitated and homogenized using the homogenizer. The homogenizer was run at high speed for about 60 minutes until a homogenous emulsion appeared. The emulsion was then allowed to cool down overnight which would also allow for the elimination of any air entrapped during the homogenization process. The progression towards a higher oil fraction emulsion involved using a known amount of oil which was to be added to an existing lower oil concentration emulsion with mixing in the homogenizer turned on. This also involved running the machine for about 60 minutes.

The oil concentrations were increased in approximately 10 wt% increments until the 60 wt% mark from which the increments changed to approximately 5wt%. About eight different emulsions were made for each nanocrystal dispersions using oil concentrations ranging from 0 to approximately 70 wt%.

The emulsions in the study were of the oil-in-water (O/W) type and no phase inversion to a water-in-oil (W/O) emulsion was observed. This was monitored constantly using an electrical conductivity probe as O/W emulsions are electrically conductive, whereas W/O emulsions are non-conductive[44]. The figure below shows the preparation process of these emulsions.

Previously made nanocrystal dispersion | **O/W emulsion during mixing after oil was added** | **Final O/W emulsion left to cool overnight**

Figure 10 Preparation of O/W emulsions stabilized by cellulose nanocrystals

The table below shows a complete picture of all the dispersions and emulsions investigated in this study and their compositions.

Table 2 Compositions of dispersions and emulsions investigated in this study

NCC Concentration (wt%)	Oil Concentration in Emulsion (wt%)	Oil Concentration in Emulsion (vol%)
1.03	Seven Concentrations: 10.49, 28.42, 40.38, 50.32, 60.28, 65.27, 70.26	Seven Concentrations: 12.17, 31.93, 44.45, 54.47, 64.20, 68.95, 73.62
1.99	Eight Concentrations: 10.10, 20.16, 30.15, 40.13, 50.12, 60.10, 65.10, 70.12	Eight Concentrations: 11.75, 23.03, 33.84, 44.27, 54.35, 64.10, 68.85, 73.55
2.91	Eight Concentrations: 10.01, 20.01, 30.03, 40.05, 50.06, 60.05, 65.07, 70.09	Eight Concentrations: 11.68, 22.92, 33.79, 44.26, 54.37, 64.12, 68.89, 73.59
3.85	Eight Concentrations: 10.03, 20.04, 30.06, 40.05, 50.06, 60.06, 65.07, 70.07	Eight Concentrations: 11.73, 23.01, 33.89, 44.34, 54.45, 64.20, 68.96, 73.73
4.77	Eight Concentrations: 10.05, 20.04, 30.04, 40.05, 50.06, 60.07, 65.07, 70.07	Eight Concentrations: 11.79, 23.07, 33.94, 44.42, 54.53, 64.28, 69.03, 73.69
5.66	Eight Concentrations: 10.02, 20.03, 30.04, 40.07, 50.09, 60.08, 65.08, 70.08	Eight Concentrations: 11.78, 23.11, 34.01, 44.52, 54.64, 64.36, 69.10, 73.75
6.55	Eight Concentrations: 10.01, 20.04, 30.04, 40.05, 50.06, 60.08, 65.08, 70.08	Eight Concentrations: 11.81, 23.17, 34.07, 44.58, 54.68, 64.43, 69.16, 73.81
7.41	Seven Concentrations: 10.03, 20.06, 30.05, 40.07, 50.06, 60.07, 65.07	Seven Concentrations: 11.86, 23.25, 34.15, 44.67, 54.76, 64.49, 69.22

3.4 Rheological Measurements

The rheological measurements included measuring viscosity and emulsion droplet size. The effect of change in shear rate was investigated for different oil and nanocrystal concentrations using two different viscometers, the Haake and the Fann. The emulsion droplet size measurements were done by collecting photomicrographs on a Zeiss optical microscope with transmitted light. These samples were diluted with the aqueous phase before observation under the microscope.

Particle size measurement was performed on a 1 wt% NCC sample. This was done by employing the Dynamic Light Scattering (DLS) method using a Zetasizer Nano ZS90 (Malvern Instruments Ltd., Worcester, UK) with a He-Ne laser operating at 633 nm frequency. The version of software used for measurements was Zetasizer 6.20. The samples were tested in ZEN0112, low volume disposable sizing cuvette at the standard 25 °C temperature with an equilibration time of 120 seconds for the sample analysis with a 10 second delay between different measurements. The mean hydrodynamic diameter of nanocrystals is approximately 24 nm. The figure below shows the size distribution of cellulose nanocrystals.

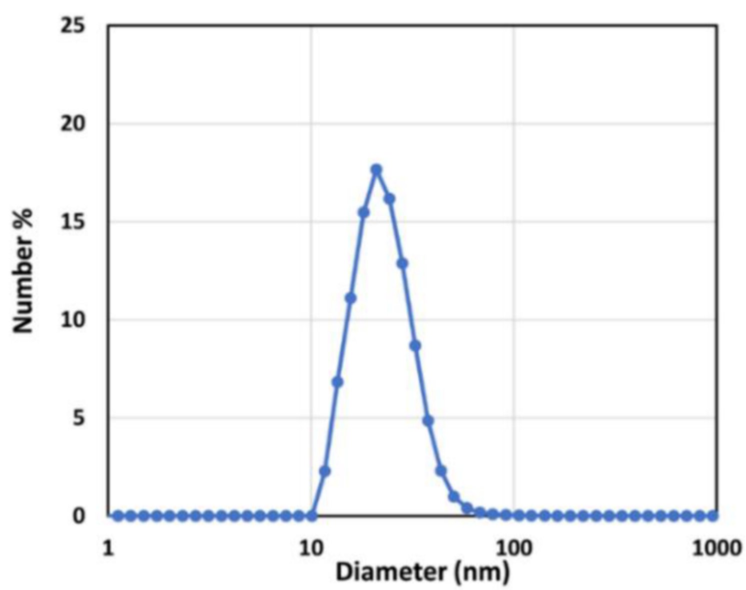

Figure 11 Size distribution of a 1 wt% NCC solution

The equipment is described below.

1. **Fann Viscometer (Model 35A):** This coaxial cylindrical viscometer involves the use of a bob which has an inner and outer cylinder placed in the solution. The inner cylinder is kept stationary while the outer cylinder rotates at 12 different speeds ranging from 0.9 to 600 rpm. When the outer cylinder rotates at a known velocity, a drag force is exerted on the fluid that is trapped between both cylinders. This effect is observed as torque on the bob which gives us a Dial reading on the analog scale. This reading is then related to shear stress to then calculate velocity using the known shear rate values. The figure below shows the Fann Viscometer setup before and during measurement.

Viscometer setup before measurement with inner cylinder (bob) and outer cylinder displayed

Viscometer setup during measurement with inner cylinder (bob) and outer cylinder covered by solution container

Figure 12 Fann viscometer setup

2. **Haake Viscometer (Rotovisco® RV 12):** This coaxial cylindrical viscometer involves the use of a bob which has an inner and outer cylinder placed between a cylindrical annular space that houses the solution. The outer cylinder is kept stationary while the inner cylinder rotates at 30 different speeds ranging from 0.01 to 512 rpm. When the inner cylinder rotates at a known velocity, a momentum is imparted on the fluid. This effect is observed as torque on the fluid and the flow resistance can be estimated. There is a proportional relationship between the torque required to keep the bob running and viscosity. By using this relationship, the magnitude of the torque, the set speed and the bob's geometry, we can calculate the viscosity, shear rate and shear stress. The viscometer displays a reading on a digital screen and is equipped with different bobs. For this study, two different bobs were used in the viscometer, i.e., MV I and MV III**.** The figure below shows the Haake Viscometer setup before and during measurement.

Viscometer setup before measurement with inner cylinder (bob, left) and control panel w/ digital display (right)

Viscometer setup during measurement with inner cylinder (bob) and outer cylinder covered by solution container

Figure 13 Haake viscometer setup

The table below sets out the relevant dimensions of the cylinders used in both viscometers.

Table 3 Relevant dimensions of both viscometers

Device	**Inner Cylinder Radius, R_i (cm)**	**Outer Cylinder Radius, R_o (cm)**	**Length of Inner Cylinder (cm)**	**Gap-Width (cm)**
Fann 35A/SR-12	1.72	1.84	3.8	0.12
Haake Rotovisco® RV 12 with MV I	2.00	2.10	6.0	0.10
Haake Rotovisco® RV 12 with MV III	1.52	2.10	6.0	0.58

3. **pH and Conductivity meter:** All the pH and Conductivity measurements of nanocrystal dispersions and emulsions were conducted using a Fisher Scientific Accumet AE150 pH Benchtop meter and the Thermo Scientific Orion 3-Star Benchtop Conductivity Meter respectively. The pH meter is equipped with both a pH electrode and a temperature electrode to measure pH and temperature readings, respectively. The conductivity meter is also equipped with an electrode to measure electrical conductivity. The pH and conductivity meters are capable of measuring readings as precisely as 0.01 units for pH, 0.1 μS/cm for conductivity, and 0.1 °C for temperature. The electrode is dipped into the solution to obtain a pH/conductivity value. The sensor measures voltage that is then converted into a value that is displayed digitally in the correct units.

Chapter 4: Results and Discussion

The various results obtained for the stability of the emulsions, droplet size of the emulsions and the viscosity of nanocrystalline cellulose dispersions and O/W emulsions stabilized and thickened by the nanocrystalline cellulose are explained in this section.

4.1 Physical Appearance and Stability of O/W Emulsions Stabilized by NCC

The physical appearance of the emulsions was analyzed at two different oil concentrations: the median (50 wt%) and the maximum (70 wt%). These two were chosen as emulsions showed a change in the physical appearance at these points. In the figures below, the collated set of samples can be seen for both oil concentrations increasing in terms of cellulose nanocrystals concentration when going from left to right.

From Figure 14, two observations can be made regarding the physical appearance of the 50 wt% O/W emulsions. Firstly, for low NCC concentrations (less than 4.77 wt% NCC), the consistency of the emulsions is of a mobile fluid. For high NCC concentrations (more than 3.85 wt% NCC), the emulsions exhibit a paste-like consistency.

1.03 wt% NCC **2.91 wt% NCC** **3.85 wt% NCC**

4.77 wt% NCC **5.66 wt% NCC** **6.55 wt% NCC**

Figure 14 O/W emulsion samples at 50 wt% oil concentration for different NCC concentrations

From Figure 15, the main observation that can be made about the physical appearance of the 70wt% O/W emulsions is that the emulsions exhibit a paste-like consistency at all NCC concentrations.

1.99 wt% NCC **2.91 wt% NCC** **3.85 wt% NCC**

4.77 wt% NCC **5.66 wt% NCC** **6.55 wt% NCC**

Figure 15 O/W emulsion samples at 70 wt% oil concentration for different NCC concentrations

To investigate the stability of the emulsions, the emulsions and their respective dispersions were placed in scintillation vials and observed for a duration of four to six months without any stirring or interaction. The investigation involved looking for signs of creaming and coalescence which would indicate instability. In the figures below, the scintillation vials can be seen for all NCC concentrations increasing in terms of oil concentration when going from left to right. From the figures below, the emulsions were highly stable with respect to both phenomena. To indicate creaming, a separate aqueous phase layer should have formed at the bottom of the vials[45]. To indicate droplet coalescence, an oil layer should have formed towards the top of the vials[46].

O/W Emulsions with 1.99 wt% NCC

O/W Emulsions with 2.91 wt% NCC

O/W Emulsions with 3.85 wt% NCC

O/W Emulsions with 4.77 wt% NCC

O/W Emulsions with 5.66 wt% NCC

O/W Emulsions with 6.55 wt% NCC

Figure 16 O/W emulsion samples in scintillation vials for observation over time (NCC concentration range of 1.99 to 6.55 wt%; oil concentration range of 0 to 70 wt%)

4.2 Droplet Size Analysis of O/W Emulsions Stabilized by NCC

A droplet size analysis of the emulsions was performed using a combination of a Zeiss optical microscope and phone camera. These were then used to obtain photomicrographs at each oil concentration from which the diameters of a hundred droplets were obtained. Sauter mean diameter was then utilized as the metric of choice as it provides an average of the particle size. It is calculated using the following formula for a specific oil concentration:

$$Sauter\ mean\ diameter_{oil\ concentration} = \frac{Diameter^3}{Diameter^2} \tag{11}$$

A sample photomicrograph with a scale is attached below. Using the photomicrographs of each emulsion in conjunction with the scale provided with the microscope, the droplet size and the Sauter mean diameter of each emulsion was determined. The range of the Sauter mean diameter values were from 20 μm to 100 μm depending upon the different NCC and oil concentrations.

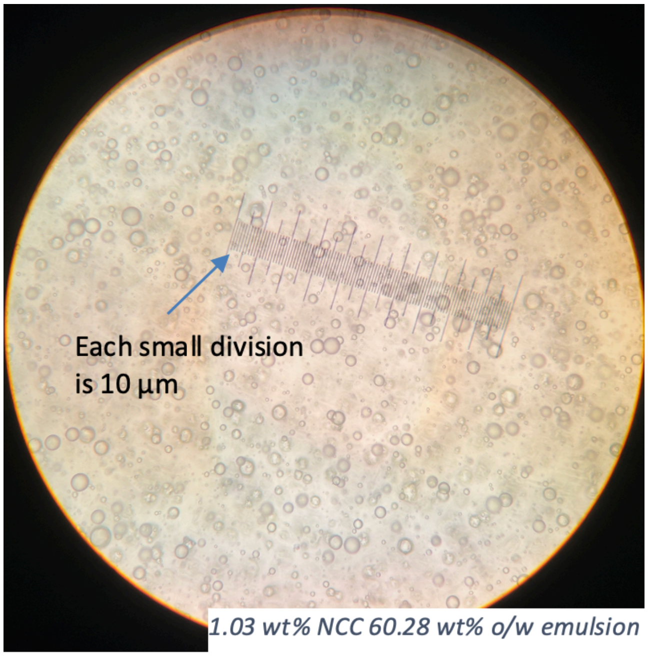

Figure 17 Photomicrograph of O/W Emulsion stabilized by NCC

The following figures show the trends in droplet size when investigating with a basis of a fixed NCC concentration or a fixed oil concentration. At a fixed NCC concentration, the Sauter mean diameter generally increased with an increase in oil concentration. This can be observed in Figure 18 for the different NCC concentrations. At a fixed oil concentration, the Sauter mean diameter generally decreased with an increase in NCC concentration. This can be observed in Figure 19 for the different oil concentrations.

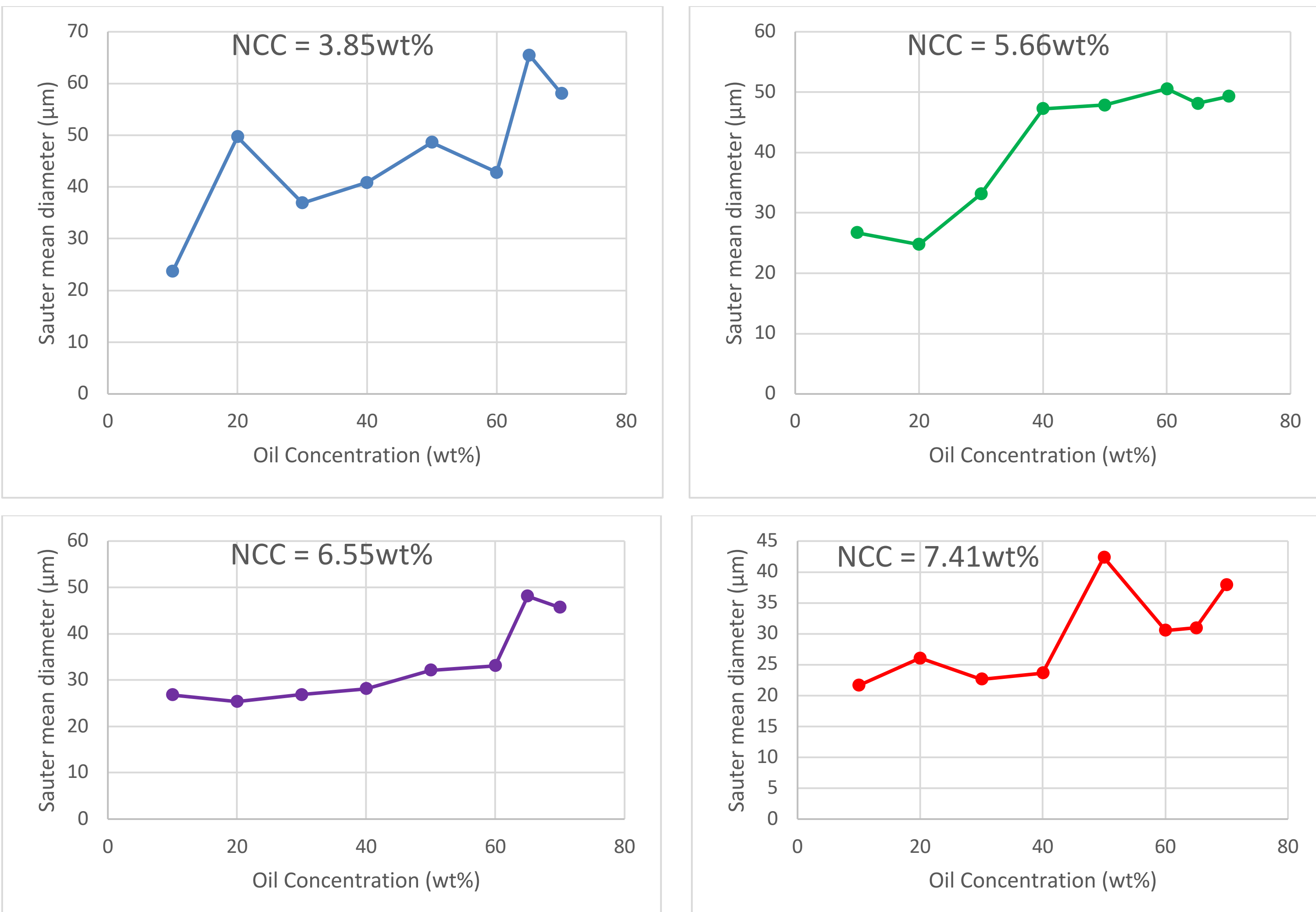

Figure 18 Effect of oil concentration on Sauter mean diameter at fixed NCC Concentrations of 3.85, 5.66, 6.55 and 7.41 wt%

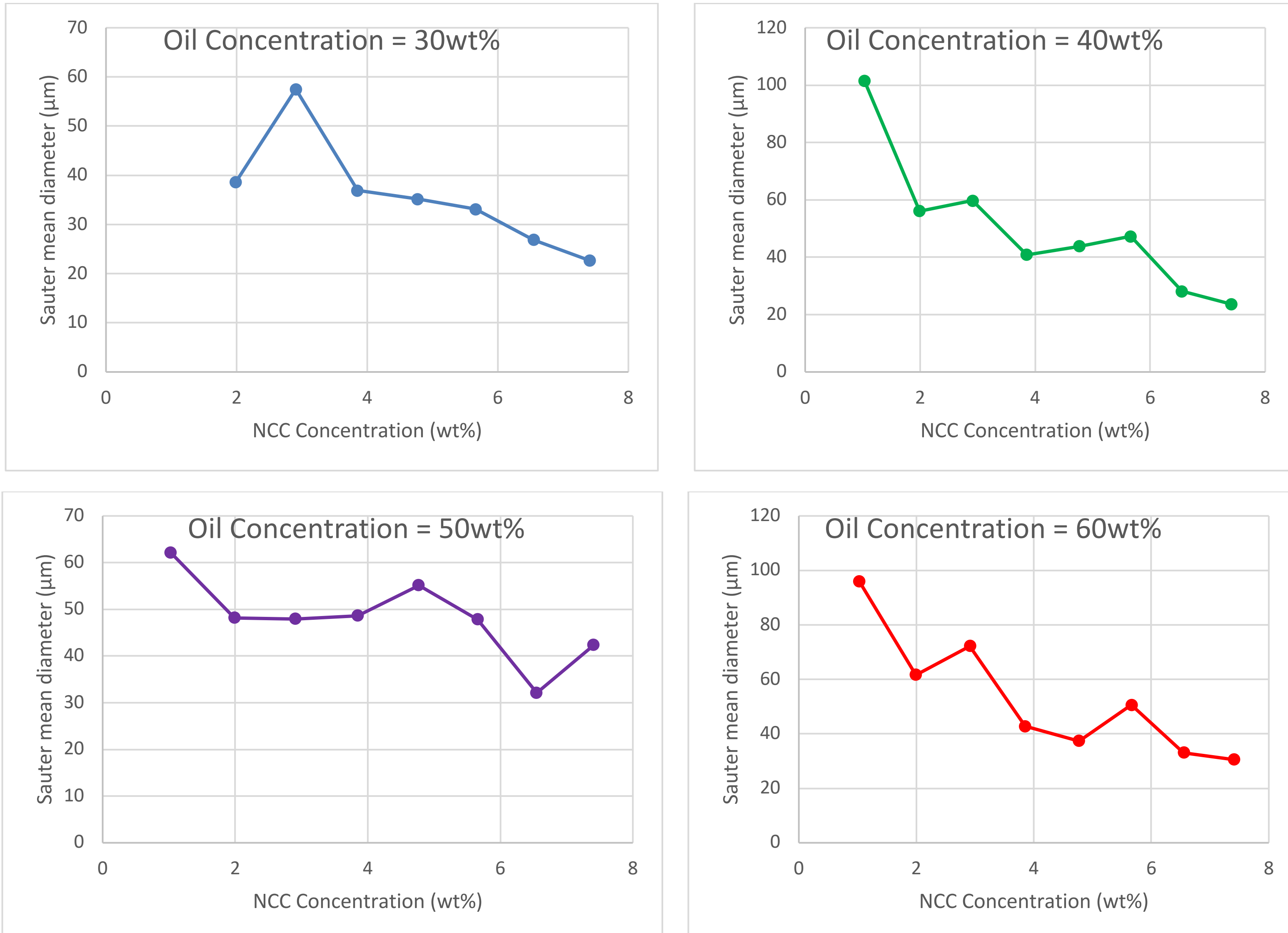

Figure 19 Effect of NCC concentration on Sauter mean diameter at fixed Oil Concentrations of 30, 40, 50 and 60 wt%

4.3 Rheology of Nanocrystalline Cellulose (NCC) Dispersions

From Table 2 in Section 3.3, NCC dispersions were prepared for concentrations ranging from 1.03 to 7.41 wt%. These can be seen in Figure 20 below where the NCC concentration increase when going from left to right. The increasing cloudiness with an increase in nanocrystal concentrations suggests an aggregation of nanocrystals.

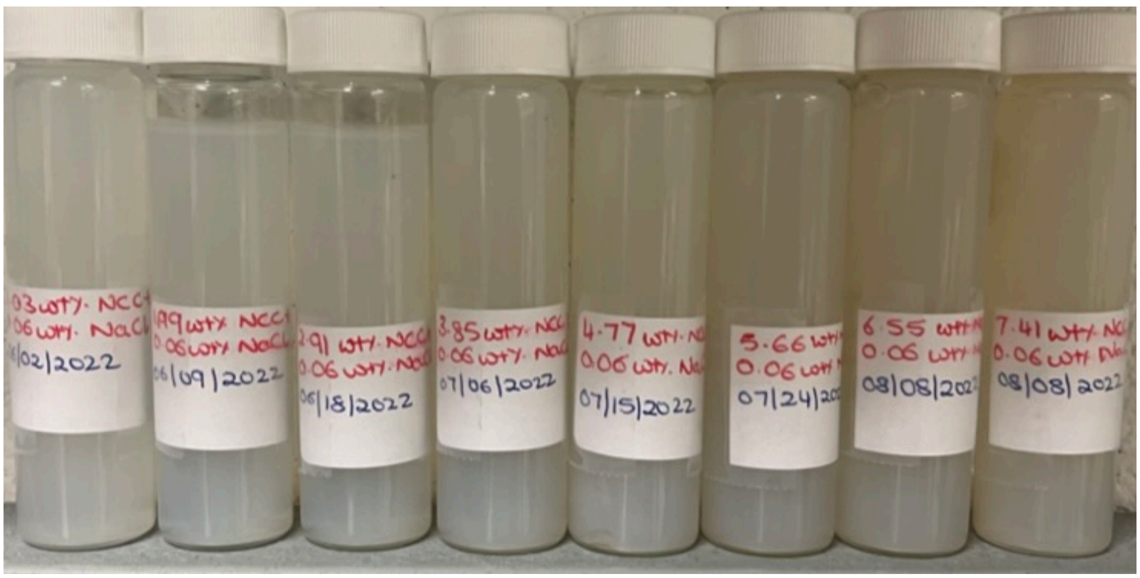

Figure 20 Physical appearance of NCC dispersions ranging from 1.03 to 7.41 wt%

The viscosity data is shown plotted in the Figure 21 below for all the NCC concentrations in this study.

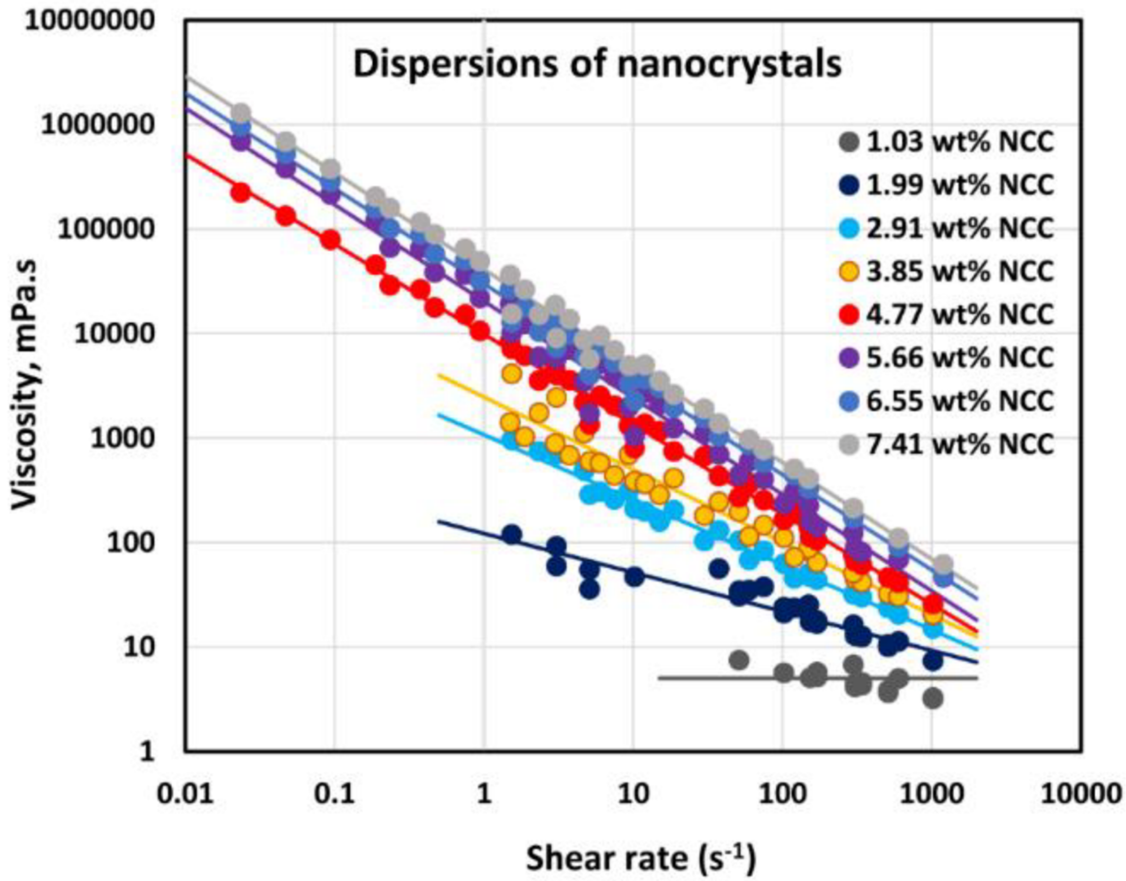

Figure 21 Viscosity versus Shear Rate data for all NCC dispersions made from 1.03 to 7.41 wt%

From Figure 21, a few observations can be made. Firstly, the NCC dispersion is only Newtonian at one concentration, i.e., the lowest concentration used in this study, 1.03 wt%. This can be noted by the fact that the viscosity remains constant independent of the shear rate. Secondly, at all other NCC concentrations, the dispersions behave as non-Newtonian shear-thinning. This can be observed by the fact that the viscosity decreases with an increase in shear rate for a given dispersion. Lastly, the viscosity of the dispersions increases with an increase in NCC concentration. This can be observed when going from the bottom to the top of the graph whilst using the y-axis.

From Section 2.1.3, the power-law can be applied to all the non-Newtonian NCC dispersions to describe the viscous behavior. Using the power-law model, values of *K* (consistency index) and *n* (flow-behavior index) can be calculated and plotted. These results can be observed in Figure 22 below.

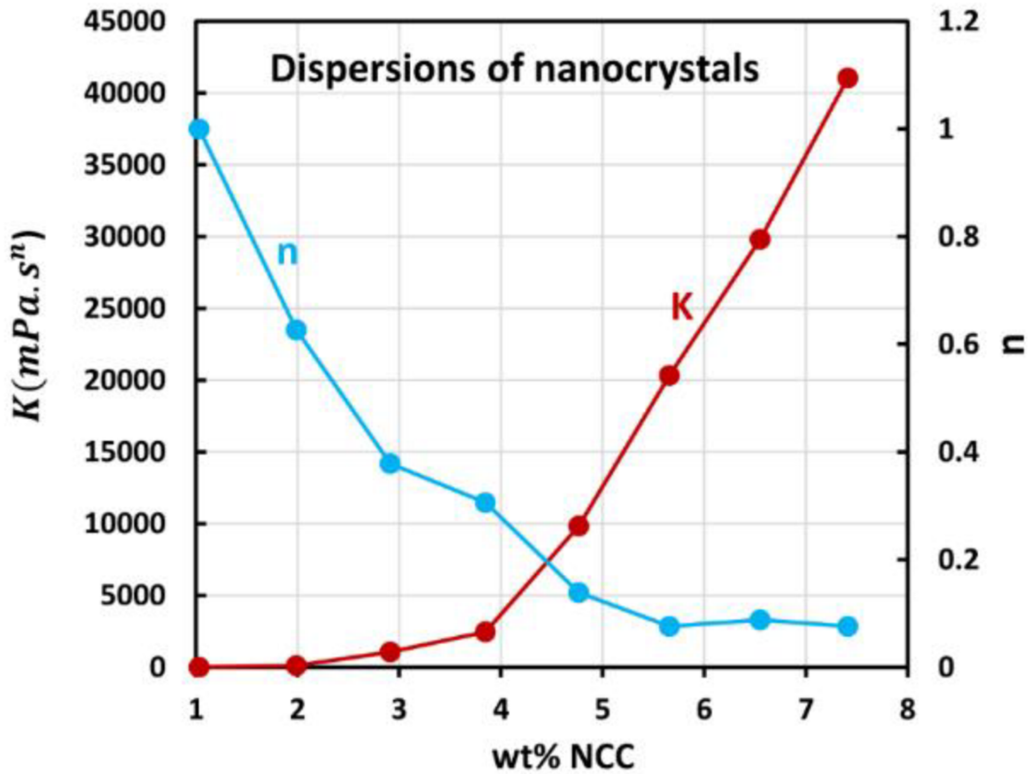

Figure 22 Power-law model values plotted for all NCC dispersions made from 1.03 to 7.41 wt%

4.4 Rheology of O/W Emulsions Stabilized by Nanocrystalline Cellulose (NCC)

From Figure 22, the flow behavior index sharply decreases after the first dispersion which suggests that dispersions are becoming more shear-thinning as the NCC concentration is increased. However, this then plateaus around the 6 wt% mark. The consistency index increases with an increase in NCC concentration. The sharp increase seen around 4 wt% may be attributed to the formation of liquid crystals.

As per Table 2 in Section 3.3, seven or eight oil-in-water emulsions were prepared for each NCC concentration. Their viscous flow behaviour was then plotted and shown in Figures 23-26 below. These figures show viscosities of different O/W emulsions at the same NCC concentration from which the following observations can be made. Firstly, like the NCC dispersions, the O/W emulsions are Newtonian at low NCC concentrations (≤1.03wt%) and low oil concentrations (≤30wt%). Secondly, emulsions are non-Newtonian shear-thinning at NCC concentrations greater than 1.03wt% (≥1.99wt%). The figures also show the *K* and *n* values for each NCC concentration as per the power-law model described in Section 2.1.3.

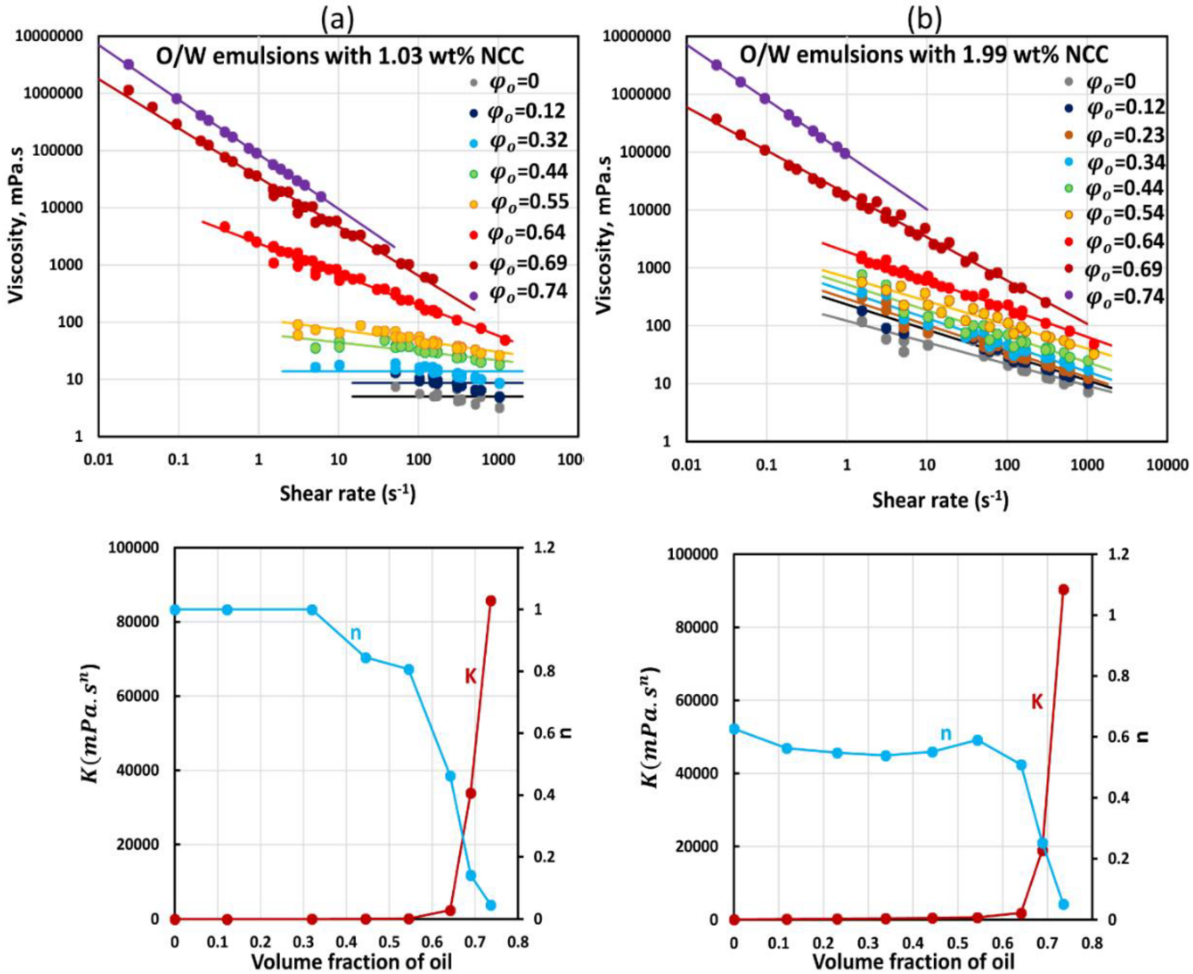

Figure 23 Viscous flow behavior of O/W emulsions at different oil concentrations at a fixed NCC concentration of (a) 1.03 wt% and (b) 1.99 wt%.

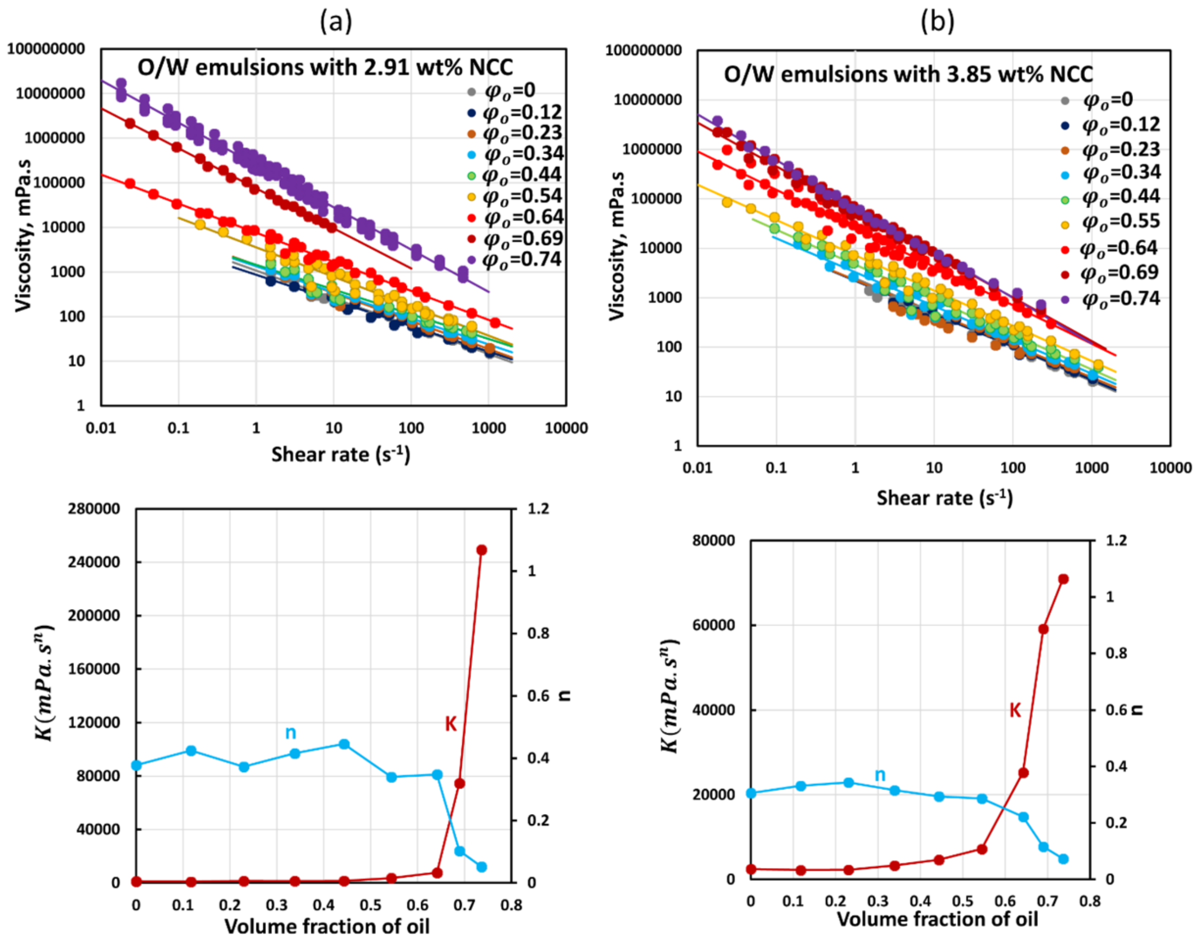

Figure 24 Viscous flow behavior of O/W emulsions at different oil concentrations at a fixed NCC concentration of (a) 2.91 wt% and (b) 3.85 wt%

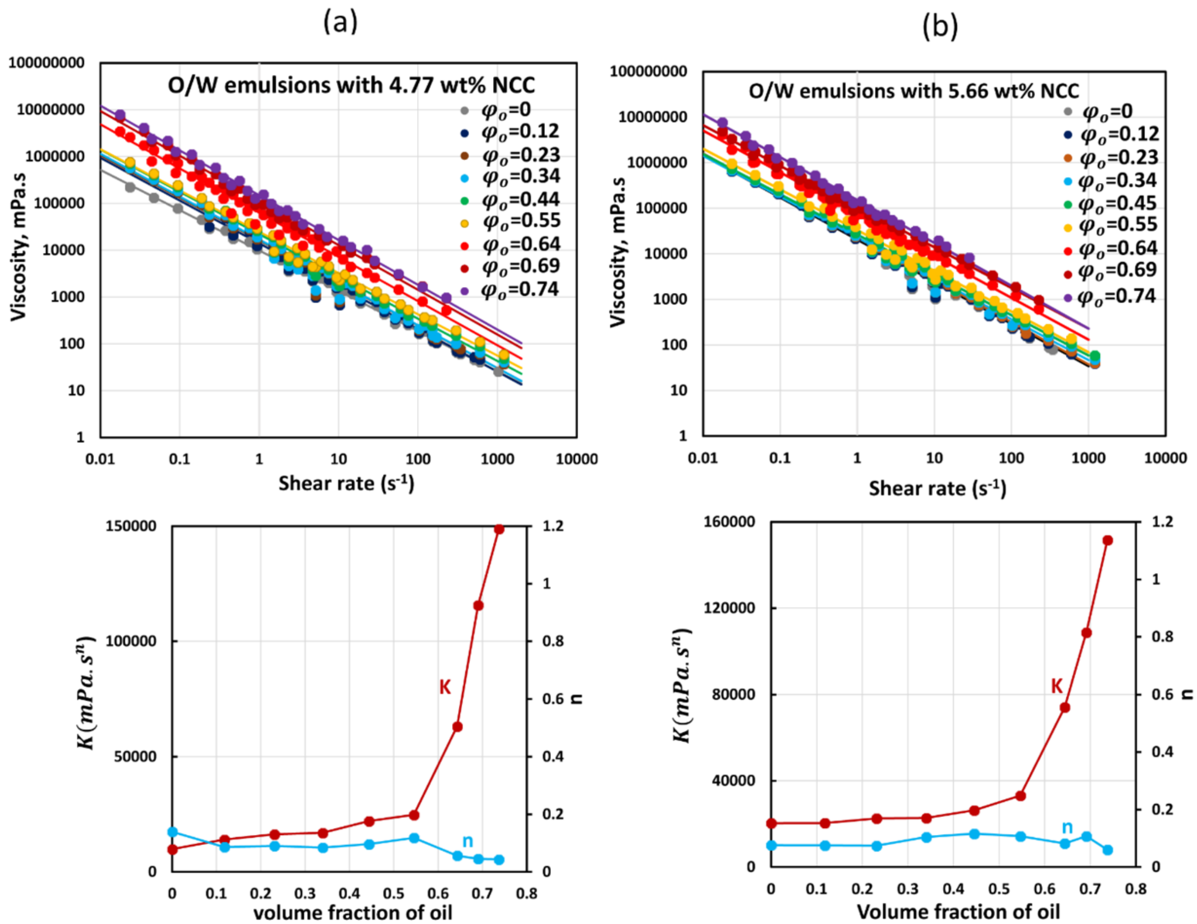

Figure 25 Viscous flow behavior of O/W emulsions at different oil concentrations at a fixed NCC concentration of (a) 4.77 wt% and (b) 5.66 wt%

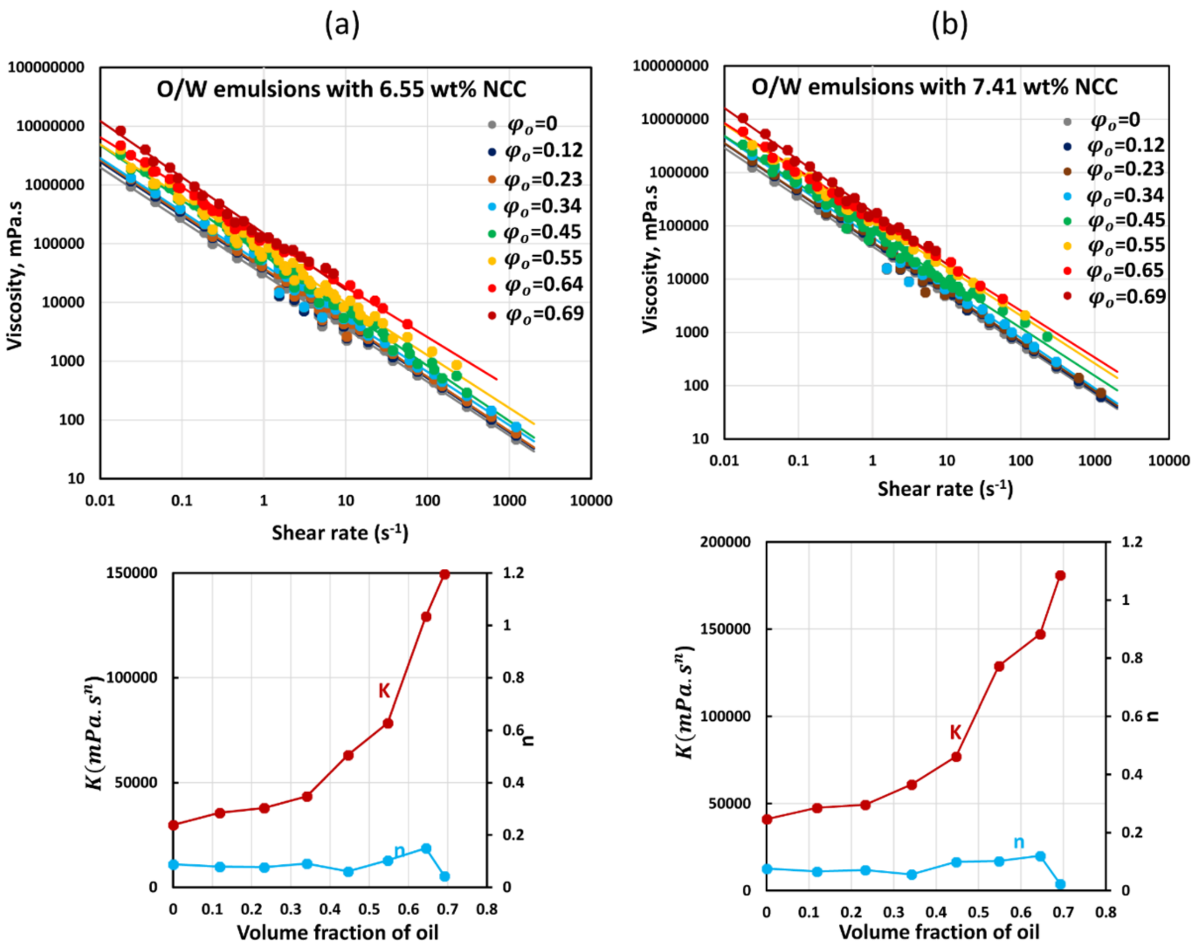

Figure 26 Viscous flow behavior of O/W emulsions at different oil concentrations at a fixed NCC concentration of (a) 6.55 wt% and (b) 7.41 wt%

Using the power-law model from Section 2.1.3, values of *K* and *n* can be calculated and plotted against different oil concentrations in Figures 27 and 28.

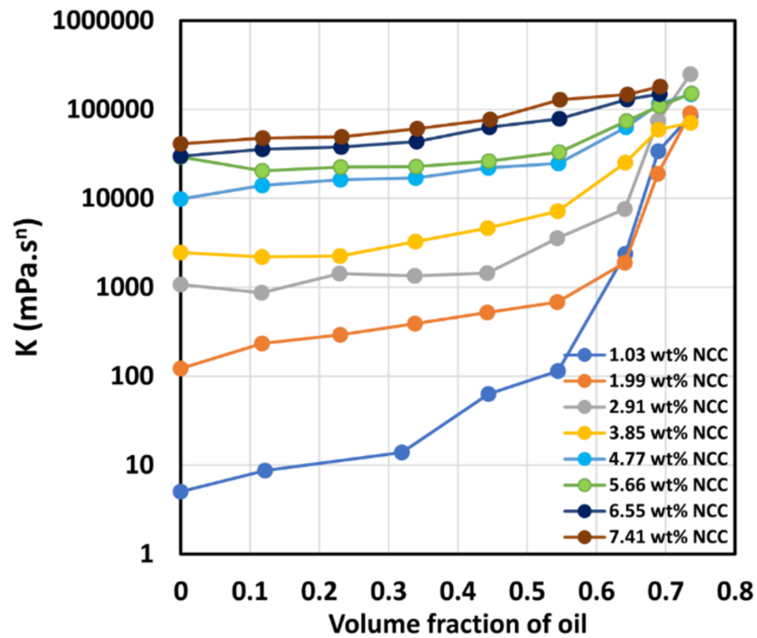

Figure 27 Comparison of *K* (consistency index) values of O/W emulsions for different NCC concentrations

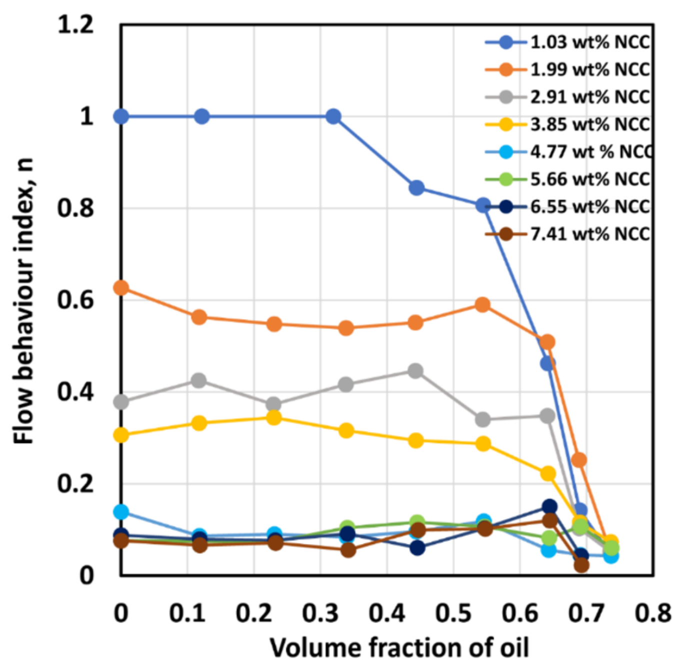

Figure 28 Comparison of *n* (flow behavior index) values of O/W emulsions for different NCC concentrations

From the two figures, some observations regarding the consistency index and the flow behaviour index can be made. Firstly, the consistency index (K) increases with an increase in oil concentration at all NCC concentrations greater than 1.03wt%. This may be due to the oil droplets acting as an obstacle to the flow which increases the flow resistance. This in turn enhances the shear-thinning effect which bring us to the second observation regarding the flow behaviour index. The flow behaviour index (n) decreases and plateaus with an increase in oil concentration at all NCC concentrations greater than 1.03 wt%. This can be attributed to the following two mechanisms that occur when the shear rate is increased: (1) break-up of droplet aggregates and (2) the deformation and change in orientation of the oil droplets[47]. When the shear rate is increased, the droplets undergo the two phenomena which both result in lower emulsion viscosity. When droplet aggregates are broken-up, the entrapped matrix fluid is released which results in lower emulsion viscosity. When the droplets are oriented in the flow direction, the droplets also become more elongated which also results in lower emulsion viscosity.

More observations are noted when analysing the data for a fixed oil concentration and varying NCC concentrations. The primary observation is that viscosity increases with an increase in NCC concentration. This can then be applied to describe the viscous flow behaviour. Because the viscosity of an emulsion is directly proportional to the viscosity of the matrix fluid, both the viscosity of the emulsions and the consistency factor (K) increase in a similar manner[47,48]. Moreover, this increase in NCC concentration at a fixed oil concentration leads to the matrix fluid becoming more shear-thinning. This explains the substantial decrease observed in the flow behaviour index (n) when the NCC concentration is increased.

Chapter 5: Conclusions

Based on a thorough analysis of rheological behaviour, droplet size distribution, and physical appearance results, it may be concluded that cellulose nanocrystals hold significant promise for various industries due to their distinct properties. These conclusions include:

1. **Dispersions of NCC are non-Newtonian shear-thinning at NCC concentrations greater than 1.03 wt%.** This implies that when the concentration of NCC exceeds 1.03 wt%, the behaviour of the dispersion changes. It becomes non-Newtonian, meaning its viscosity decreases as shear rate increases. In other words, as the NCC concentration increases, the dispersion becomes easier to flow under shear stress. Additionally, the consistency index increases, indicating a higher viscosity, while the flow behavior index decreases.
2. **The O/W (oil-in-water) emulsions stabilized and thickened by NCC exhibit different flow properties based on the NCC concentration and oil volume fractions.** At low NCC concentrations (≤1.03 wt%) and low oil volume concentrations (≤30 wt%), the emulsions behave as Newtonian fluids, meaning their viscosity remains constant regardless of shear rate. However, for the rest of the emulsions, they exhibit non-Newtonian shear-thinning behaviour, similar to the NCC dispersions mentioned earlier. This means their viscosity decreases as shear rate increases.
3. **The consistency index and flow behaviour index of the emulsions show different trends with respect to NCC and oil concentrations.** As the NCC and oil concentrations increase, the consistency index also increases, suggesting thicker and more viscous emulsions. On the other hand, the flow behaviour index decreases with increasing NCC and oil concentrations, implying that the emulsions become less resistant to flow under shear stress.
4. **The O/W emulsions produced using cellulose nanocrystals as stabilizers are highly stable, specifically in relation to creaming (separation of oil droplets) and coalescence (merging of droplets).** This indicates that NCC is an effective stabilizer

for O/W emulsions, preventing phase separation and maintaining the emulsion's stability over time.

5. **The average droplet size of O/W emulsions exhibits a relationship with NCC and oil concentrations.** As the concentration of NCC increases, the average droplet size generally decreases, indicating better dispersion and smaller oil droplets. Conversely, increasing the oil concentration leads to an increase in the average droplet size, suggesting larger oil droplets in the emulsion.

References

1. *Studying fundamentals of water as a solvent could lead to greener cellulose-based products*. (n.d.). Studying Fundamentals of Water as a Solvent Could Lead to Greener Cellulose-based Products. https://phys.org/news/2023-05-fundamentals-solvent-greener-cellulose-based-products.html
2. Bhat, A., Khan, I., Usmani, M. A., Umapathi, R., & Al-Kindy, S. M. (2019, May). Cellulose an ageless renewable green nanomaterial for medical applications: An overview of ionic liquids in extraction, separation, and dissolution of cellulose. *International Journal of Biological Macromolecules*, *129*, 750–777. https://doi.org/10.1016/j.ijbiomac.2018.12.190
3. Khalil, H. A., Aprilia, N. S., Bhat, A., Jawaid, M., Paridah, M., & Rudi, D. (2013, June). A Jatropha biomass as renewable materials for biocomposites and its applications. *Renewable and Sustainable Energy Reviews*, *22*, 667–685. https://doi.org/10.1016/j.rser.2012.12.036
4. Ahmad, A., Buang, A., & Bhat, A. (2016, November). Renewable and sustainable bioenergy production from microalgal co-cultivation with palm oil mill effluent (POME): A review. *Renewable and Sustainable Energy Reviews*, *65*, 214–234. https://doi.org/10.1016/j.rser.2016.06.084
5. *Cellulose | Structure, Properties, Function, Facts & Summary*. (2020, April 13). A Level Biology. https://alevelbiology.co.uk/notes/cellulose/
6. Jawaid, M., & Abdul Khalil, H. (2011, August). Cellulosic/synthetic fibre reinforced polymer hybrid composites: A review. *Carbohydrate Polymers*, *86*(1), 1–18. https://doi.org/10.1016/j.carbpol.2011.04.043
7. Vanderfleet, O.M.; Cranston, E.D. Production routes to tailor the performance of cellulose nanocrystals. Nature Reviews/Materials 2021, 6, 124-144.
8. Battista, O. A., Coppick, S., Howsmon, J. A., Morehead, F. F., & Sisson, W. A. (1956, February). Level-Off Degree of Polymerization. Industrial & Engineering Chemistry, 48(2), 333–335. https://doi.org/10.1021/ie50554a046
9. Interface design of stretchable and environment-tolerant strain sensors with hierarchical nanocellulose-supported graphene nanocomplexes. (2022, November 12). Interface Design of Stretchable and Environment-tolerant Strain Sensors With Hierarchical Nanocellulose-

supported Graphene Nanocomplexes - ScienceDirect. https://doi.org/10.1016/j.compositesa.2022.107313

10. Flexible environment-tolerant electroluminescent devices based on nanocellulose-mediated transparent electrodes. (2022, July 21). Flexible Environment-tolerant Electroluminescent Devices Based on Nanocellulose-mediated Transparent Electrodes - ScienceDirect. https://doi.org/10.1016/j.carbpol.2022.119891
11. Recent advances in cellulose-based flexible triboelectric nanogenerators. (2021, May 24). Recent Advances in Cellulose-based Flexible Triboelectric Nanogenerators - ScienceDirect. https://doi.org/10.1016/j.nanoen.2021.106175
12. Fan, F. R., Tian, Z. Q., & Lin Wang, Z. (2012, March). Flexible triboelectric generator. Nano Energy, 1(2), 328–334. https://doi.org/10.1016/j.nanoen.2012.01.004
13. Yao, C., Hernandez, A., Yu, Y., Cai, Z., & Wang, X. (2016, December). Triboelectric nanogenerators and power-boards from cellulose nanofibrils and recycled materials. Nano Energy, 30, 103–108. https://doi.org/10.1016/j.nanoen.2016.09.036
14. Kim, I., Jeon, H., Kim, D., You, J., & Kim, D. (2018, November). All-in-one cellulose based triboelectric nanogenerator for electronic paper using simple filtration process. Nano Energy, 53, 975–981. https://doi.org/10.1016/j.nanoen.2018.09.060
15. Hu, L., Kim, H. S., Lee, J. Y., Peumans, P., & Cui, Y. (2010, April 28). Scalable Coating and Properties of Transparent, Flexible, Silver Nanowire Electrodes. ACS Nano, 4(5), 2955–2963. https://doi.org/10.1021/nn1005232
16. Xu, F., & Zhu, Y. (2012, July 12). Highly Conductive and Stretchable Silver Nanowire Conductors. Advanced Materials, 24(37), 5117–5122. https://doi.org/10.1002/adma.201201886
17. Wang, J., Euring, M., Ostendorf, K., & Zhang, K. (2022, February). Biobased materials for food packaging. Journal of Bioresources and Bioproducts, 7(1), 1–13. https://doi.org/10.1016/j.jobab.2021.11.004
18. Stark, N. M. (2016, October 22). Opportunities for Cellulose Nanomaterials in Packaging Films: A Review and Future Trends. Journal of Renewable Materials, 4(5), 313–326. https://doi.org/10.7569/jrm.2016.634115

19. Huang, S., Liu, X., Chang, C., & Wang, Y. (2020, January 29). Recent developments and prospective food-related applications of cellulose nanocrystals: a review. Cellulose, 27(6), 2991–3011. https://doi.org/10.1007/s10570-020-02984-3
20. El Achaby, M., El Miri, N., Aboulkas, A., Zahouily, M., Bilal, E., Barakat, A., & Solhy, A. (2017, March). Processing and properties of eco-friendly bio-nanocomposite films filled with cellulose nanocrystals from sugarcane bagasse. International Journal of Biological Macromolecules, 96, 340–352. https://doi.org/10.1016/j.ijbiomac.2016.12.040
21. Gan, I., & Chow, W. (2018, September). Antimicrobial poly(lactic acid)/cellulose bionanocomposite for food packaging application: A review. Food Packaging and Shelf Life, 17, 150–161. https://doi.org/10.1016/j.fpsl.2018.06.012
22. Solutions and Dispersions: Differences and Application Areas. (n.d.). Nanografi Nano Technology. https://nanografi.com/blog/solutions-and-dispersions-differences-and-application-areas/
23. Dispersion (chemistry) - Wikipedia. (2013, December 1). Dispersion (Chemistry) - Wikipedia. https://en.wikipedia.org/wiki/Dispersion_(chemistry)
24. Giles Jr, H. F., Wagner, Jr., J. R., Mount III, E. M., Giles Jr, H. F., Wagner, Jr., J. R., & Mount III, E. M. (2013, September 21). Extrusion: The Definitive Processing Guide and Handbook. William Andrew.
25. Strivens, T. (1999). An introduction to rheology. Paint and Surface Coatings, 550–574. https://doi.org/10.1533/9781855737006.550
26. Irgens, F. (2014). Rheology and Non-Newtonian Fluids. https://doi.org/10.1007/978-3-319-01053-3
27. Chhabra, R. P., & Richardson, J. F. (1999, August 1). Non-Newtonian Flow: Fundamentals and Engineering Applications. Butterworth-Heinemann. https://doi.org/10.1604/9780750637701
28. Bird, R. B., Stewart, W. E., & Lightfoot, E. N. (2006, December 11). Transport Phenomena. https://doi.org/10.1604/9780470115398
29. Chhabra, R. P. (2010). Non-Newtonian Fluids: An Introduction. Rheology of Complex Fluids, 3–34. https://doi.org/10.1007/978-1-4419-6494-6_1

30. Morrison, F. A. (2001, March 15). Understanding Rheology. https://doi.org/10.1604/9780195141665
31. BOGER, D. V. (1977, January). Demonstration of upper and lower Newtonian fluid behaviour in a pseudoplastic fluid. Nature, 265(5590), 126–128. https://doi.org/10.1038/265126a0
32. Walters, K. (Ed.). (1989, June 1). An Introduction to Rheology: Vol. Volume 3. https://doi.org/10.1604/9780444871404
33. Chhabra, R. P., & Richardson, J. F. (2008, July 21). Non-Newtonian Flow and Applied Rheology: Engineering Applications. Butterworth-Heinemann. https://doi.org/10.1604/9780750685320
34. Metzner, A. B., & Whitlock, M. (1958, March). Flow Behavior of Concentrated (Dilatant) Suspensions. Transactions of the Society of Rheology, 2(1), 239–254. https://doi.org/10.1122/1.548831
35. Rehm, B., Haghshenas, A., Paknejad, A. S., Al-Yami, A., & Hughes, J. (Eds.). (2013, November 25). Underbalanced Drilling: Limits and Extremes.
36. Tornberg, E. (2017). Influence of Fibers and Particle Size Distribution on Food Rheology. Advances in Food Rheology and Its Applications, 177–208. https://doi.org/10.1016/b978-0-08-100431-9.00008-5
37. Francis, L. F., & Roberts, C. C. (2016). Dispersion and Solution Processes. Materials Processing, 415–512. https://doi.org/10.1016/b978-0-12-385132-1.00006-9
38. Singh, H., & Gallier, S. (2017, July). Nature’s complex emulsion: The fat globules of milk. Food Hydrocolloids, 68, 81–89. https://doi.org/10.1016/j.foodhyd.2016.10.011
39. Shafiei-Sabet, S., Hamad, W. Y., & Hatzikiriakos, S. G. (2012, November 26). Rheology of Nanocrystalline Cellulose Aqueous Suspensions. Langmuir, 28(49), 17124–17133. https://doi.org/10.1021/la303380v
40. Bai, L., Lv, S., Xiang, W., Huan, S., McClements, D. J., & Rojas, O. J. (2019, November). Oil-in-water Pickering emulsions via microfluidization with cellulose nanocrystals: 1. Formation and stability. Food Hydrocolloids, 96, 699–708. https://doi.org/10.1016/j.foodhyd.2019.04.038

41. Miao, C., Mirvakili, M. N., & Hamad, W. Y. (2022, February). A rheological investigation of oil-in-water Pickering emulsions stabilized by cellulose nanocrystals. Journal of Colloid and Interface Science, 608, 2820–2829. https://doi.org/10.1016/j.jcis.2021.11.010
42. Pandey, A., Derakhshandeh, M., Kedzior, S. A., Pilapil, B., Shomrat, N., Segal-Peretz, T., Bryant, S. L., & Trifkovic, M. (2018, December). Role of interparticle interactions on microstructural and rheological properties of cellulose nanocrystal stabilized emulsions. Journal of Colloid and Interface Science, 532, 808–818. https://doi.org/10.1016/j.jcis.2018.08.044
43. Girard, M., Vidal, D., Bertrand, F., Tavares, J. R., & Heuzey, M. C. (2021, March). Evidence-based guidelines for the ultrasonic dispersion of cellulose nanocrystals. *Ultrasonics Sonochemistry*, *71*, 105378. https://doi.org/10.1016/j.ultsonch.2020.105378
44. Shechter, D. (n.d.). Oil-in-Water and Water-in-Oil Emulsions: What's the Difference? Oil-in-Water and Water-in-Oil Emulsions: What's the Difference? https://www.beei.com/blog/oil-in-water-and-water-in-oil-emulsions-whats-the-difference-
45. Creaming - an overview | ScienceDirect Topics. (n.d.). Creaming - an Overview | ScienceDirect Topics. https://doi.org/10.1016/B978-0-12-809438-9.00006-5
46. Coalescence - an overview | ScienceDirect Topics. (n.d.). Coalescence - an Overview | ScienceDirect Topics. https://doi.org/10.1016/j.trac.2013.07.009
47. Pal, R. (2006, November 22). Rheology of Particulate Dispersions and Composites: Vol. Vol. 136. https://doi.org/10.1604/9781574445206
48. Pal, R. (1996, November). Effect of droplet size on the rheology of emulsions. AIChE Journal, 42(11), 3181–3190. https://doi.org/10.1002/aic.690421119

Appendix A: Experimental Data

Appendix A1: Composition Data

The composition data consists of the planned and actual concentrations of both the NCC and oil-in-water emulsions. This was briefly stated in Table 2. Planned NCC concentrations were 1, 2, 3, 4, 5, 6, 7, and 8 wt%. Planned Oil concentrations were 10, 20, 30, 40, 50, 60, 65 and 70 wt%.

Table 4 Actual NCC concentration in NCC Dispersions made

Stated NCC concentration (wt%)	Actual NCC concentration (wt%)
1	1.03
2	1.99
3	2.91
4	3.85
5	4.77
6	5.66
7	6.55
8	7.41

Table 5 Actual Oil Concentrations in O/W Emulsions stabilized by 1.03 wt% NCC

NCC concentration (wt%)	Planned Oil Concentration in Emulsion (wt%)	Actual Oil Concentration in Emulsion (wt%)	Actual Oil Concentration in Emulsion (vol%)	Volume fraction of Oil (φ_0)
1.03	10	10.49	12.17	0.1217
	30	28.42	31.93	0.3193
	40	40.38	44.45	0.4445
	50	50.32	54.47	0.5447
	60	60.28	64.20	0.6420
	65	65.27	68.95	0.6895
	70	70.26	73.62	0.7362

Table 6 Actual Oil Concentrations in O/W Emulsions stabilized by 1.99 wt% NCC

NCC concentration (wt%)	Planned Oil Concentration in Emulsion (wt%)	Actual Oil Concentration in Emulsion (wt%)	Actual Oil Concentration in Emulsion (vol%)	Volume fraction of Oil (φ_0)
1.99	10	10.10	11.75	0.1175
	20	20.16	23.03	0.2303
	30	30.15	33.84	0.3384
	40	40.13	44.27	0.4427
	50	50.12	54.35	0.5435
	60	60.10	64.10	0.6410
	65	65.10	68.85	0.6885
	70	70.12	73.55	0.7355

Table 7 Actual Oil Concentrations in O/W Emulsions stabilized by 2.91 wt% NCC

NCC concentration (wt%)	Planned Oil Concentration in Emulsion (wt%)	Actual Oil Concentration in Emulsion (wt%)	Actual Oil Concentration in Emulsion (vol%)	Volume fraction of Oil (φ_0)
2.91	10	10.01	11.68	0.1168
	20	20.01	22.92	0.2292
	30	30.03	33.79	0.3379
	40	40.05	44.26	0.4426
	50	50.06	54.37	0.5437
	60	60.06	64.12	0.6412
	65	65.07	68.89	0.6889
	70	70.09	73.59	0.7359

Table 8 Actual Oil Concentrations in O/W Emulsions stabilized by 3.85 wt% NCC

NCC concentration (wt%)	Planned Oil Concentration in Emulsion (wt%)	Actual Oil Concentration in Emulsion (wt%)	Actual Oil Concentration in Emulsion (vol%)	Volume fraction of Oil (φ_0)
3.85	10	10.03	11.73	0.1173
	20	20.04	23.01	0.2301
	30	30.06	33.88	0.3388
	40	40.05	44.34	0.4434
	50	50.06	54.45	0.5445
	60	60.06	64.20	0.6420
	65	65.07	68.96	0.6896
	70	70.07	73.63	0.7363

Table 9 Actual Oil Concentrations in O/W Emulsions stabilized by 4.77 wt% NCC

NCC concentration (wt%)	Planned Oil Concentration in Emulsion (wt%)	Actual Oil Concentration in Emulsion (wt%)	Actual Oil Concentration in Emulsion (vol%)	Volume fraction of Oil (φ_0)
4.77	10	10.05	11.79	0.1179
	20	20.04	23.07	0.2307
	30	30.04	33.94	0.3394
	40	40.05	44.42	0.4442
	50	50.06	54.53	0.5453
	60	60.07	64.28	0.6428
	65	65.07	69.03	0.6903
	70	70.07	73.69	0.7369

Table 10 Actual Oil Concentrations in O/W Emulsions stabilized by 5.66 wt% NCC

NCC concentration (wt%)	Planned Oil Concentration in Emulsion (wt%)	Actual Oil Concentration in Emulsion (wt%)	Actual Oil Concentration in Emulsion (vol%)	Volume fraction of Oil (φ_0)
5.66	10	10.02	11.78	0.1178
	20	20.03	23.11	0.2311
	30	30.04	34.01	0.3401
	40	40.07	44.52	0.4452
	50	50.09	54.64	0.5464
	60	60.08	64.36	0.6436
	65	65.08	69.10	0.6910
	70	70.07	73.75	0.7375

Table 11 Actual Oil Concentrations in O/W Emulsions stabilized by 6.55 wt% NCC

NCC concentration (wt%)	Planned Oil Concentration in Emulsion (wt%)	Actual Oil Concentration in Emulsion (wt%)	Actual Oil Concentration in Emulsion (vol%)	Volume fraction of Oil (φ_0)
6.55	10	10.01	11.81	0.1181
	20	20.04	23.17	0.2317
	30	30.04	34.07	0.3407
	40	40.05	44.58	0.4458
	50	50.06	54.68	0.5468
	60	60.07	64.43	0.6443
	65	65.08	69.16	0.6916
	70	70.07	73.81	0.7381

Table 12 Actual Oil Concentrations in O/W Emulsions stabilized by 7.41 wt% NCC

NCC concentration (wt%)	Planned Oil Concentration in Emulsion (wt%)	Actual Oil Concentration in Emulsion (wt%)	Actual Oil Concentration in Emulsion (vol%)	Volume fraction of Oil (φ_0)
7.41	10	10.03	11.86	0.1186
	20	20.06	23.25	0.2325
	30	30.05	34.15	0.3415
	40	40.07	44.67	0.4467
	50	50.06	54.76	0.5476
	60	60.07	64.49	0.6449
	65	65.07	69.22	0.6922

Appendix A2: DLS (Dynamic Light Scattering) Data

Particle size measurement was performed using the DLS method on a 1 wt% NCC sample. This was shown in the form of a plot in Figure 11. Instrument specifications can be found in Section 3.4. The diameter and number percent values are shown in the table below. The number percent values given are an average of four measurements of the same sample. The mean hydrodynamic diameter of nanocrystals is approximately 24 nm (23.76 nm).

Table 13 DLS Data

Diameter (nm)	Number %
0.4	0
0.463	0
0.536	0
0.621	0
0.719	0
0.833	0
0.965	0
1.12	0
1.29	0
1.5	0
1.74	0
2.01	0
2.33	0
2.7	0
3.12	0
3.62	0
4.19	0
4.85	0
5.61	0
6.5	0

7.53	0
8.72	0
10.1	0
11.7	2.2825
13.5	6.825
15.7	11.11
18.2	15.475
21	17.66
24.4	16.1675
28.2	12.8785
32.7	8.688195
37.8	4.86075
43.8	2.306
50.7	0.9780415
58.8	0.400155
68.1	0.179015
78.8	0.09331
91.3	0.0517425
106	0.027325
122	0.012785
142	0.00512775
164	0.00168103
190	0.00040721
220	7.4125E-05
255	7.4303E-05
295	0.00015736
342	0.00023292
396	0.00027157
459	0.00026771

531	0.0002247
615	0.00015688
712	8.6938E-05
825	0.00003512
955	8.3945E-06
1.11E+03	6.8218E-07
1.28E+03	8.7E-09
1.48E+03	0
1.72E+03	0
1.99E+03	0
2.30E+03	0
2.67E+03	0
3.09E+03	0
3.58E+03	0
4.15E+03	0
4.80E+03	0
5.56E+03	0
6.44E+03	0
7.46E+03	0
8.63E+03	0

Appendix A3: Droplet Size Data

The Droplet Size analysis was performed for the emulsions using photomicrographs and was explained in Section 4.2. Figure 18 shows the effect of oil concentration on the Sauter mean diameter at fixed NCC Concentrations of 3.85, 5.66, 6.55 and 7.41 wt%. This data can be found in the tables below.

Table 14 Droplet Size Data for fixed NCC concentration of 3.85 wt%

Oil Concentration in Emulsion (wt%)	Oil Concentration in Emulsion (vol%)	Sauter Mean Diameter (micron or μm)
10.03	11.73	23.66
20.04	23.01	49.71
30.06	33.88	36.92
40.05	44.34	40.85
50.06	54.45	48.60
60.06	64.20	42.80
65.07	68.96	65.50
70.07	73.63	58.04

Table 15 Droplet Size Data for fixed NCC concentration of 5.66 wt%

Oil Concentration in Emulsion (wt%)	Oil Concentration in Emulsion (vol%)	Sauter Mean Diameter (micron or μm)
10.02	11.78	26.73
20.03	23.11	24.76
30.04	34.01	33.11
40.07	44.52	47.24
50.09	54.64	47.85
60.08	64.36	50.56
65.08	69.10	48.13
70.07	73.75	49.30

Table 16 Droplet Size Data for fixed NCC concentration of 6.55 wt%

Oil Concentration in Emulsion (wt%)	Oil Concentration in Emulsion (vol%)	Sauter Mean Diameter (micron or μm)
10.01	11.81	26.80
20.04	23.17	25.36
30.04	34.07	26.88
40.05	44.58	28.12
50.06	54.68	32.11
60.07	64.43	33.07
65.08	69.16	48.09
70.07	73.81	45.70

Table 17 Droplet Size Data for fixed NCC concentration of 7.41 wt%

Oil Concentration in Emulsion (wt%)	Oil Concentration in Emulsion (vol%)	Sauter Mean Diameter (micron or μm)
10.03	11.86	21.64
20.06	23.25	26.05
30.05	34.15	22.65
40.07	44.67	23.64
50.06	54.76	42.35
60.07	64.49	30.52
65.07	69.22	30.93

Figure 19 shows the effect of NCC concentration on the Sauter mean diameter at fixed oil Concentrations of 30, 40, 50 and 60 wt%. This data can be found in the tables below.

Table 18 Droplet Size Data for fixed Oil concentration of 30 wt%

NCC Concentration	Sauter Mean Diameter
1.99	38.65
2.91	57.52
3.85	36.92
4.77	35.15
5.66	33.11
6.55	26.88
7.41	22.65

Table 19 Droplet Size Data for fixed Oil concentration of 40 wt%

NCC Concentration	Sauter Mean Diameter
1.03	101.53
1.99	56.07
2.91	59.71
3.85	40.85
4.77	43.82
5.66	47.24
6.55	28.12
7.41	23.64

Table 20 Droplet Size Data for fixed Oil concentration of 50 wt%

NCC Concentration	Sauter Mean Diameter
1.03	62.10
1.99	48.17
2.91	47.96
3.85	48.60
4.77	55.16
5.66	47.85
6.55	32.11
7.41	42.35

Table 21 Droplet Size Data for fixed Oil concentration of 60 wt%

NCC Concentration	Sauter Mean Diameter
1.03	95.94
1.99	61.65
2.91	72.24
3.85	42.80
4.77	37.34
5.66	50.56
6.55	33.07
7.41	30.52

Appendix A4: Viscometer Calibrations

The rheological data was collected using two different viscometers: the Fann model 35 and the Haake Rotovisco RV 12. This is explained in detail in Section 3.4. All measurements were performed at room temperature. The calibration of each of the viscometers is explained below:

A4.1 Calibration of the Haake viscometer

Using the equipment manual and theory, the shear stress, the shear rate, and the apparent viscosity can be measured and calculated using the following three formulas:

$$Shear\ Rate = M \times n = 2.34n \tag{12}$$

$$Shear\ Stress = (A \times S) + B = 898.07S + 133.38 \tag{13}$$

$$Viscosity = \frac{Shear\ Stress}{Shear\ Rate} \rightarrow \eta = \frac{\tau}{\gamma} \tag{9}$$

Where *M* is the shear rate factor, *n* is the rpm of the rotor bob, *S* is the digital reading, and *A* and *B* are the shear stress factors. Equation 9 from Section 2.1.3 is employed here to calculate the viscosity. The values of the constants are listed in the table below:

Table 22 Constants involved Haake viscometer calculations

Constant	Value
M (shear rate factor)	2.34
A (shear stress factor)	898.07
B (shear stress factor)	133.38

A4.2 Calibration of the Fann viscometer

Similar to the Haake viscometer, the shear stress, the shear rate, and the apparent viscosity can be measured and calculated using the following three formulas:

$$Shear\ Rate = k \times n = 1.7023n \tag{14}$$

$$Shear\ Stress = (C \times S) + D = 98.955S - 212.82 \tag{15}$$

$$Viscosity = \frac{Shear\ Stress}{Shear\ Rate} \rightarrow \eta = \frac{\tau}{\gamma} \tag{9}$$

Where *k* is the spring constant (shear rate factor), *n* is the rpm of the bob, *S* is the dial reading, and *C* and *D* are the shear stress factors. Equation 9 from Section 2.1.3 is employed here to calculate the viscosity. The values of the constants are listed in the table below:

Table 23 Constants involved Fann viscometer calculations

Constant	Value
k (spring constant)	1.7023
C (shear stress factor)	98.955
D (shear stress factor)	-212.82

Appendix A5: Rheological Data

The following section contains all the rheological data obtained from both the viscometers. Section A5.1 contains data for all the NCC dispersions in order of increasing NCC concentration with the last two rows in each table (highlighted) signifying the two data points used to plot the correlation lines seen in the figures in Section 4.3. Sections A5.2-9 contain data for each O/W emulsion made, stabilized by a specific NCC concentration, in order of increasing oil concentration with the last two rows in each table (highlighted) signifying the two data points used to plot the correlation lines seen in the figures in Section 4.4. The last table in each section lists out the *K, n,* and *(n-1)* values as per the Power-Law Model described in Section 2.1.3.

A5.1 Rheological Data of NCC Dispersions

Table 24 Rheological Data of 1.03 wt% NCC Dispersion

Shear Rate (s^{-1})	Shear Stress (mPa)	Viscosity (cP)
51.069	380.91	7.4587
102.138	578.82	5.6670
153.207	776.73	5.0698
306.414	1271.505	4.1496
170.23	974.64	5.7254
340.46	1469.415	4.3160
510.69	1964.19	3.8461
1021.38	3250.605	3.1826
51.069	380.91	7.4587
102.138	578.82	5.6670
153.207	776.73	5.0698
306.414	1370.46	4.4726
170.23	875.685	5.1441
340.46	1568.37	4.6066

510.69	1865.235	3.6524
1021.38	3349.56	3.2794
299.52	2019.327	6.7419
599.04	3007.204	5.0200
15	75.43997	5.0293
2000	10058.66	5.0293

Table 25 Rheological Data of 1.99 wt% NCC Dispersion

Shear Rate (s^{-1})	Shear Stress (mPa)	Viscosity (cP)
1.53207	183	119.4462
3.06414	281.955	92.0177
51.069	1766.28	34.5861
102.138	2458.965	24.0749
153.207	2953.74	19.2794
306.414	4141.2	13.5150
5.1069	281.955	55.2106
10.2138	479.865	46.9820
170.23	3052.695	17.9328
340.46	4339.11	12.7448
510.69	5427.615	10.6280
1021.38	7505.67	7.3486
3.06414	183	59.7231
51.069	1568.37	30.7108
102.138	2162.1	21.1684
153.207	2656.875	17.3417
306.414	3943.29	12.8692
5.1069	183	35.8339
10.2138	479.865	46.9820

170.23	2854.785	16.7702
340.46	4240.155	12.4542
510.69	5130.75	10.0467
1021.38	7505.67	7.3486
37.44	2109.134	56.3337
74.88	2827.59	37.7616
149.76	3815.467	25.4772
299.52	4893.151	16.3366
599.04	6779.098	11.3166
59.904	2109.134	35.2086
119.808	2827.59	23.6010
0.5	78.965	157.93
2000	14320	7.16

Table 26 Rheological Data of 2.91 wt% NCC Dispersion

Shear Rate (s^{-1})	Shear Stress (mPa)	Viscosity (cP)
1.53207	1469.415	959.1043
3.06414	2162.1	705.6140
51.069	5328.66	104.3424
102.138	6417.165	62.8284
153.207	7208.805	47.0527
306.414	9781.635	31.9229
5.1069	1469.415	287.7313
10.2138	2162.1	211.6842
170.23	7505.67	44.0913
340.46	10177.46	29.8932
510.69	12057.6	23.6104
1021.38	15422.07	15.0992

2.34	1749.906	747.8231
4.68	2288.748	489.0487
9.36	2917.397	311.6877
18.72	3815.467	203.8177
37.44	4893.151	130.6931
74.88	6240.256	83.3368
149.76	7587.361	50.6635
299.52	9563.115	31.9281
599.04	12257.33	20.4616
7.488	1929.52	257.6816
14.976	2378.555	158.8245
29.952	3097.011	103.3991
59.904	4084.888	68.1906
119.808	5431.993	45.3392
5.9904	1839.713	307.1102
11.9808	2378.555	198.5306
0.5	826.6775	1653.355
2000	19007	9.5035

Table 27 Rheological Data of 3.85 wt% NCC Dispersion

Shear Rate (s^{-1})	Shear Stress (mPa)	Viscosity (cP)
1.53207	6318.21	4123.9695
3.06414	7505.67	2449.5193
51.069	10078.5	197.3506
102.138	11364.92	111.2702
153.207	12453.42	81.2849
306.414	13739.84	44.8408
5.1069	3052.695	597.7589

10.2138	3943.29	386.0747
170.23	10969.1	64.4369
340.46	14135.66	41.5193
510.69	16510.58	32.3299
1021.38	20864.6	20.4278
2.34	4084.888	1745.6786
4.68	5252.379	1122.3032
9.36	6509.677	695.4783
18.72	7766.975	414.9025
37.44	9203.887	245.8303
74.88	11000.03	146.9021
149.76	13245.2	88.4429
299.52	15220.96	50.8178
599.04	18274.39	30.5061
1.872	1929.52	1030.7265
3.744	2558.169	683.2716
7.488	3276.625	437.5835
14.976	4264.502	284.7557
29.952	5431.993	181.3566
59.904	6868.905	114.6652
119.808	8665.045	72.3244
1.4976	2109.134	1408.3427
2.9952	2647.976	884.0732
5.9904	3456.239	576.9630
11.9808	4354.309	363.4406
0.5	1993.245	3986.491
2000	25222.67	12.6113

Table 28 Rheological Data of 4.77 wt% NCC Dispersion

Shear Rate (s^{-1})	Shear Stress (mPa)	Viscosity (cP)
1.53207	10969.1	7159.6565
3.06414	12255.51	3999.6573
51.069	13838.79	270.9822
102.138	16807.44	164.5562
153.207	17203.26	112.2877
306.414	20369.82	66.4781
5.1069	6911.94	1353.4512
10.2138	8198.355	802.6743
170.23	17796.99	104.5467
340.46	20864.6	61.2835
510.69	23635.34	46.2812
1021.38	26406.08	25.8533
2.34	8305.817	3549.4944
4.68	10281.57	2196.9169
9.36	12257.33	1309.5433
18.72	13963.66	745.9219
37.44	16208.83	432.9282
74.88	19082.66	254.8432
149.76	21148.22	141.2141
299.52	22674.94	75.7043
599.04	24830.31	41.4502
0.234	6779.098	28970.5043
0.468	8305.817	17747.4722
0.936	9922.343	10600.7938
1.872	11538.87	6163.9257

3.744	13424.82	3585.6880
7.488	15310.76	2044.7066
14.976	17555.94	1172.2715
29.952	20070.53	670.0899
59.904	21776.87	363.5294
119.808	22405.52	187.0119
0.0234	5252.379	224460.6410
0.0468	6240.256	133338.8034
0.0936	7407.747	79142.5962
0.1872	8485.431	45328.1571
0.3744	9922.343	26501.9845
0.7488	11359.26	15169.9452
1.4976	12616.55	8424.5146
2.9952	13963.66	4662.0119
5.9904	15220.96	2540.8914
11.9808	16388.45	1367.8925
0.01	5187.362	518736.188
2000	28300.21	14.1501

Table 29 Rheological Data of 5.66 wt% NCC Dispersion

Shear Rate (s^{-1})	Shear Stress (mPa)	Viscosity (cP)
1.53207	15619.98	10195.3436
3.06414	17698.04	5775.8572
51.069	22645.79	443.4351
102.138	23833.25	233.3436
153.207	24624.89	160.7295
306.414	27296.67	89.0843
5.1069	8792.085	1721.6090

10.2138	10672.23	1044.8834
170.23	24130.11	141.7500
340.46	27395.63	80.4665
2.34	14053.47	6005.7543
4.68	16298.64	3482.6154
9.36	18543.82	1981.1768
18.72	23393.39	1249.6471
37.44	26267.22	701.5817
74.88	30398.34	405.9607
149.76	33811.01	225.7679
299.52	37044.06	123.6781
599.04	41085.37	68.5854
1198.08	55634.11	46.4361
0.234	15490.38	66198.1923
0.468	18004.97	38472.1645
0.936	20429.76	21826.6688
1.872	23123.97	12352.5491
3.744	26087.6	6967.8427
7.488	29141.04	3891.6989
14.976	31565.83	2107.7611
29.952	33541.58	1119.8446
59.904	35696.95	595.9026
119.808	36864.44	307.6960
0.0234	16208.83	692685.1709
0.0468	17915.17	382802.6923
0.0936	20070.53	214428.7821
0.1872	22405.52	119687.5855
0.3744	24650.69	65840.5208
0.7488	27704.13	36998.0355

1.4976	28781.81	19218.6251
2.9952	29500.27	9849.1817
5.9904	30757.57	5134.4763
11.9808	32374.09	2702.1645
0.01	14336.28	1433627.58
2000	36250.55	18.1253

Table 30 Rheological Data of 6.55 wt% NCC Dispersion

Shear Rate (s^{-1})	Shear Stress (mPa)	Viscosity (cP)
1.53207	19776.09	12908.0851
3.06414	22348.92	7293.7007
5.1069	20468.78	4008.0626
10.2138	23338.47	2284.9938
2.34	24560.88	10496.1043
4.68	28242.97	6034.8229
9.36	31386.22	3353.2282
18.72	36595.02	1954.8623
37.44	38930	1039.7971
74.88	43599.97	582.2645
149.76	49168	328.3120
299.52	51143.76	170.7524
599.04	54107.39	90.3235
1198.08	56891.4	47.4855
0.234	23662.81	101123.1368
0.468	27165.29	58045.4850
0.936	30039.11	32093.0673
1.872	33092.55	17677.6437
3.744	36684.83	9798.2983

7.488	39379.04	5258.9529
14.976	44947.07	3001.2736
29.952	46294.18	1545.6122
59.904	51502.98	859.7587
119.808	52939.9	441.8728
0.0234	22495.32	961338.5897
0.0468	24560.88	524805.2137
0.0936	26536.64	283511.0897
0.1872	29230.85	156147.6923
0.3744	33002.74	88148.3494
0.7488	37223.67	49711.0991
1.4976	39738.27	26534.6334
2.9952	40815.95	13627.1204
5.9904	42522.28	7098.4048
11.9808	43599.97	3639.1533
0.01	19882.18	1988217.74
2000	58204.23	29.1021

Table 31 Rheological Data of 7.41 wt% NCC Dispersion

Shear Rate (s^{-1})	Shear Stress (mPa)	Viscosity (cP)
1.53207	23635.34	15427.05947
3.06414	27692.49	9037.6060
5.1069	29176.82	5713.2145
2.34	35607.15	15216.7286
4.68	40636.34	8682.9780
9.36	46024.76	4917.1749
18.72	48898.58	2612.1037
37.44	51592.79	1378.0126

74.88	57699.67	770.5618
149.76	61381.75	409.8675
299.52	63986.16	213.6290
599.04	66051.72	110.2626
1198.08	73864.93	61.6528
0.234	37044.06	158307.9359
0.468	41624.21	88940.6282
0.936	46383.99	49555.5395
1.872	49168	26264.9583
3.744	51233.56	13684.1782
7.488	51682.6	6902.0564
14.976	52850.09	3528.9856
29.952	56981.21	1902.4176
59.904	58058.9	969.1990
119.808	60573.49	505.5880
0.0234	29949.3	1279884.7863
0.0468	32284.29	689835.1709
0.0936	35247.92	376580.3098
0.1872	38301.36	204601.2553
0.3744	43330.55	115733.2986
0.7488	48539.35	64822.8539
1.4976	54376.81	36309.3002
2.9952	56083.14	18724.3393
5.9904	57071.02	9527.0797
11.9808	60034.65	5010.9049
0.01	28932.58	2893258.333
2000	73158.62	36.5793

Table 32 Power-Law variable values for different NCC Dispersions

NCC concentration (wt%)	*K*	*n*	*n-1*
1.03	5.029332	1	0
1.99	121.95	0.627	0.373
2.91	1074.3	0.378	0.622
3.85	2464.2	0.306	0.694
4.77	9838.9	0.139	0.861
5.66	20344	0.076	0.924
6.55	29817	0.088	0.912
7.41	41057	0.076	0.924

A5.2 Rheological Data of O/W Emulsions stabilised by 1.03 wt% NCC

Table 33 Rheological Data of 10.49 wt% O/W Emulsion stabilized by 1.03 wt% NCC

Shear Rate (s^{-1})	Shear Stress (mPa)	Viscosity (cP)
51.069	677.775	13.2717
102.138	1073.595	10.5112
153.207	1568.37	10.2369
306.414	2458.965	8.0250
170.23	1667.325	9.7945
340.46	2656.875	7.8038
510.69	3349.56	6.5589
1021.38	5031.795	4.9265
51.069	677.775	13.2717
102.138	974.64	9.5424
153.207	1370.46	8.9452
306.414	2261.055	7.3791
170.23	1469.415	8.6319

340.46	2656.875	7.8038
510.69	3250.605	6.3651
1021.38	5130.75	5.0234
149.76	1749.906	11.6847
299.52	2558.169	8.5409
599.04	3905.274	6.5192
15	130.1337	8.6756
2000	17351.16	8.6756

Table 34 Rheological Data of 28.42 wt% O/W Emulsion stabilized by 1.03 wt% NCC

Shear Rate (s^{-1})	Shear Stress (mPa)	Viscosity (cP)
51.069	974.64	19.0848
102.138	1667.325	16.3242
153.207	2360.01	15.4041
306.414	3943.29	12.8692
5.1069	84.045	16.4571
10.2138	183	17.9169
170.23	2557.92	15.0263
340.46	4141.2	12.1635
510.69	5625.525	11.0155
1021.38	8792.085	8.6080
51.069	776.73	15.2094
102.138	1469.415	14.3866
153.207	2063.145	13.4664
306.414	3448.515	11.2544
5.1069	84.045	16.4571
10.2138	183	17.9169

170.23	2360.01	13.8637
340.46	3745.38	11.0009
510.69	5427.615	10.6280
1021.38	8891.04	8.7049
149.76	2468.362	16.4821
299.52	3725.66	12.4388
599.04	6060.642	10.1173
119.808	2019.327	16.8547
2	27.80425	13.9021
2000	27804.25	13.9021

Table 35 Rheological Data of 40.38 wt% O/W Emulsion stabilized by 1.03 wt% NCC

Shear Rate (s^{-1})	Shear Stress (mPa)	Viscosity (cP)
51.069	1964.19	38.4615
102.138	3448.515	33.7633
153.207	4734.93	30.9054
306.414	8396.265	27.4017
5.1069	183	35.8339
10.2138	479.865	46.9820
170.23	5229.705	30.7214
340.46	8693.13	25.5335
510.69	11661.78	22.8353
1021.38	18786.54	18.3933
3.06414	183	59.7231
51.069	1865.235	36.5238
102.138	3349.56	32.7945
153.207	4635.975	30.2596

306.414	8198.355	26.7558
5.1069	183	35.8339
10.2138	380.91	37.2937
170.23	5031.795	29.5588
340.46	8396.265	24.6615
510.69	11364.92	22.2540
1021.38	18687.59	18.2964
37.44	1839.713	49.1376
74.88	2827.59	37.7616
149.76	4533.923	30.2746
299.52	7228.133	24.1324
599.04	11987.9	20.0119
59.904	2288.748	38.2069
119.808	3546.046	29.5977
2	113.1359	56.5680
1500	30410.77	20.2738

Table 36 Rheological Data of 50.32 wt% O/W Emulsion stabilized by 1.03 wt% NCC

Shear Rate (s^{-1})	Shear Stress (mPa)	Viscosity (cP)
3.06414	281.955	92.0177
51.069	3547.47	69.4643
102.138	5724.48	56.0465
153.207	7208.805	47.0527
306.414	11859.69	38.7048
5.1069	380.91	74.5873
10.2138	677.775	66.3587
170.23	7604.625	44.6726

340.46	12651.33	37.1595
510.69	17005.35	33.2988
1021.38	27098.76	26.5315
3.06414	183	59.7231
51.069	2854.785	55.9005
102.138	4833.885	47.3270
153.207	6615.075	43.1774
306.414	11167.01	36.4442
10.2138	677.775	66.3587
170.23	7208.805	42.3474
340.46	12057.6	35.4156
510.69	16609.53	32.5237
1021.38	26999.81	26.4346
18.72	1660.099	88.6805
37.44	2647.976	70.7259
74.88	4174.695	55.7518
149.76	6509.677	43.4674
299.52	10550.99	35.2263
599.04	17376.32	29.0070
29.952	2109.134	70.4171
59.904	3276.625	54.6979
119.808	5072.765	42.3408
2	200.4132	100.2066
1500	41889.07	27.9260

Table 37 Rheological Data of 60.28 wt% O/W Emulsion stabilized by 1.03 wt% NCC

Shear Rate (s^{-1})	Shear Stress (mPa)	Viscosity (cP)

1.53207	3250.605	2121.7079
3.06414	5031.795	1642.1557
51.069	17203.26	336.8631
102.138	21161.46	207.1850
153.207	25020.71	163.3131
5.1069	4042.245	791.5262
10.2138	6219.255	608.9071
170.23	25020.71	146.9818
1.53207	1667.325	1088.2825
3.06414	2953.74	963.9703
51.069	15521.03	303.9226
102.138	20765.64	203.3096
153.207	24525.93	160.0836
5.1069	3448.515	675.2658
10.2138	5526.57	541.0885
170.23	24624.89	144.6566
2.34	3905.274	1668.9205
4.68	5611.607	1199.0613
9.36	7946.589	848.9946
18.72	10910.22	582.8109
37.44	14322.89	382.5557
74.88	18274.39	244.0491
149.76	24201.66	161.6029
299.52	32912.94	109.8856
599.04	47282.06	78.9297
1198.08	58687.54	48.9847
0.936	2378.555	2541.1912
1.872	3276.625	1750.3339
3.744	4533.923	1210.9837

7.488	6330.063	845.3610
14.976	8575.238	572.5987
29.952	11359.26	379.2486
59.904	14771.92	246.5932
119.808	19801.11	165.2737
0.3744	1749.906	4673.8942
0.7488	2378.555	3176.4890
1.4976	3097.011	2067.9828
2.9952	4174.695	1393.7951
5.9904	5791.221	966.7503
11.9808	7946.589	663.2770
0.2	1132.541	5662.7069
1500	69876.7	46.5845

Table 38 Rheological Data of 65.27 wt% O/W Emulsion stabilized by 1.03 wt% NCC

Shear Rate (s^{-1})	Shear Stress (mPa)	Viscosity (cP)
5.1069	28583.09	5596.9541
1.53207	25317.57	16525.0739
3.06414	25218.62	8230.2424
5.1069	28978.91	5674.4610
2.34	44408.23	18977.8765
4.68	49437.42	10563.5519
9.36	55544.3	5934.2200
18.72	63177.89	3374.8875
37.44	70452.26	1881.7377
74.88	77457.21	1034.4178
149.76	85899.07	573.5782

0.234	29320.66	125301.9444
0.468	30308.53	64761.8205
0.936	33990.62	36314.7639
1.872	36415.41	19452.6752
3.744	39109.62	10445.9450
7.488	43420.35	5798.6584
14.976	49078.2	3277.1231
29.952	55993.33	1869.4356
59.904	63806.54	1065.1466
119.808	73954.73	617.2771
0.0234	26895.87	1149395.9829
0.0468	27075.48	578535.8974
0.0936	27434.71	293105.8547
0.1872	27883.74	148951.6186
0.3744	28871.62	77114.3697
0.7488	30218.73	40356.2033
1.4976	32194.48	21497.3818
2.9952	34978.5	11678.1838
5.9904	38391.16	6408.7810
11.9808	43330.55	3616.6656
0.01	17623.18	1762318.4319
500	81910.23	163.8205

Table 39 Rheological Data of 70.26 wt% O/W Emulsion stabilized by 1.03 wt% NCC

Shear Rate (s^{-1})	Shear Stress (mPa)	Viscosity (cP)
2.34	91018.06	38896.6085
0.234	79522.77	339840.8889

0.468	81498.52	174142.1410
0.936	85001	90813.0288
1.872	89132.12	47613.3104
3.744	93891.89	25077.9615
0.0234	75661.07	3233378.9316
0.0936	76379.52	816020.5449
0.1872	77816.44	415686.0844
0.3744	79702.38	212880.2938
0.7488	82576.21	110278.0529
1.4976	85988.87	57417.7831
2.9952	90209.8	30118.1227
5.9904	94340.92	15748.6851
0.01	69367.84	6936783.6916
50	102638.6	2052.7722

Table 40 Power-Law variable values for different O/W Emulsions stabilized by 1.03 wt% NCC

Oil concentration (wt%)	*K*	*n-1*	*n*
0	5.02933153	0	1
10.49	8.675577814	0	1
28.42	13.90212265	0	1
40.38	62.984	-0.155	0.845
50.32	114.55	-0.193	0.807
60.28	2382.2	-0.538	0.462
65.27	33891	-0.858	0.142
70.26	85735	-0.954	0.046

A5.3 Rheological Data of O/W Emulsions stabilised by 1.99 wt% NCC

Table 41 Rheological Data of 10.1 wt% O/W Emulsion stabilized by 1.99 wt% NCC

Shear Rate (s^{-1})	Shear Stress (mPa)	Viscosity (cP)
1.53207	281.955	184.0353
3.06414	776.73	253.4904
51.069	3052.695	59.7759
102.138	3745.38	36.6698
153.207	4339.11	28.3219
306.414	6219.255	20.2969
5.1069	578.82	113.3408
10.2138	974.64	95.4238
170.23	4537.02	26.6523
340.46	6516.12	19.1392
510.69	8000.445	15.6660
1021.38	10672.23	10.4488
3.06414	281.955	92.0177
51.069	2063.145	40.3992
102.138	3052.695	29.8879
153.207	3745.38	24.4465
306.414	5526.57	18.0363
5.1069	380.91	74.5873
10.2138	776.73	76.0471
170.23	4042.245	23.7458
340.46	5922.39	17.3953
510.69	7406.715	14.5033
1021.38	10474.32	10.2551
37.44	2288.748	61.1311
74.88	3007.204	40.1603
149.76	4174.695	27.8759

299.52	5701.414	19.0352
599.04	8036.396	13.4155
59.904	2198.941	36.7077
119.808	2917.397	24.3506
0.5	158.265	316.53
2000	16880	8.44

Table 42 Rheological Data of 20.16 wt% O/W Emulsion stabilized by 1.99 wt% NCC

Shear Rate (s^{-1})	Shear Stress (mPa)	Viscosity (cP)
1.53207	479.865	313.2135
3.06414	776.73	253.4904
51.069	3151.65	61.7136
102.138	4339.11	42.4828
153.207	4932.84	32.1972
306.414	7307.76	23.8493
5.1069	578.82	113.3408
10.2138	974.64	95.4238
170.23	5130.75	30.1401
340.46	7604.625	22.3363
510.69	9187.905	17.9912
1021.38	12948.2	12.6772
3.06414	578.82	188.9013
51.069	2261.055	44.2745
102.138	3349.56	32.7945
153.207	4339.11	28.3219
306.414	6516.12	21.2657
5.1069	479.865	93.9640

10.2138	776.73	76.0471
170.23	4635.975	27.2336
340.46	6911.94	20.3018
510.69	8792.085	17.2161
1021.38	12849.24	12.5803
37.44	2468.362	65.9285
74.88	3456.239	46.1570
149.76	4803.344	32.0736
299.52	6868.905	22.9330
599.04	9922.343	16.5637
59.904	2378.555	39.7061
119.808	3366.432	28.0986
0.5	200.005	400.01
1800	17778.6	9.877

Table 43 Rheological Data of 30.15 wt% O/W Emulsion stabilized by 1.99 wt% NCC

Shear Rate (s^{-1})	Shear Stress (mPa)	Viscosity (cP)
1.53207	578.82	377.8026
3.06414	1073.595	350.3740
51.069	4042.245	79.1526
102.138	4734.93	46.3582
153.207	6021.345	39.3020
306.414	9385.815	30.6312
5.1069	677.775	132.7175
10.2138	1073.595	105.1122
170.23	6417.165	37.6970
340.46	9880.59	29.0213

510.69	12255.51	23.9979
1021.38	17698.04	17.3276
18.72	2109.134	112.6674
37.44	2917.397	77.9219
74.88	3995.081	53.3531
149.76	5701.414	38.0703
299.52	8485.431	28.3301
599.04	12347.13	20.6115
29.952	1929.52	64.4204
59.904	2647.976	44.2037
119.808	3815.467	31.8465
0.5	268.705	537.41
2000	23484	11.742

Table 44 Rheological Data of 40.13 wt% O/W Emulsion stabilized by 1.99 wt% NCC

Shear Rate (s^{-1})	Shear Stress (mPa)	Viscosity (cP)
1.53207	1172.55	765.3371
3.06414	1568.37	511.8467
51.069	5229.705	102.4047
102.138	7208.805	70.5791
153.207	8495.22	55.4493
306.414	12750.29	41.6113
5.1069	875.685	171.4710
10.2138	1469.415	143.8657
170.23	8792.085	51.6483
340.46	13640.88	40.0660
510.69	17698.04	34.6551

1021.38	25614.44	25.0783
18.72	2109.134	112.6674
37.44	3815.467	101.9088
74.88	5431.993	72.5426
149.76	7946.589	53.0622
299.52	11628.68	38.8244
599.04	17286.52	28.8570
1198.08	41624.21	34.7424
29.952	2288.748	76.4139
59.904	3456.239	57.6963
119.808	5252.379	43.8400
0.5	355.32	710.64
2000	34304.8	17.1524

Table 45 Rheological Data of 50.12 wt% O/W Emulsion stabilized by 1.99 wt% NCC

Shear Rate (s^{-1})	Shear Stress (mPa)	Viscosity (cP)
1.53207	875.685	571.5698
3.06414	1271.505	414.9631
51.069	8396.265	164.4102
102.138	11463.87	112.2390
153.207	14234.61	92.9110
306.414	20666.69	67.4469
5.1069	1172.55	229.6011
10.2138	2360.01	231.0609
170.23	13937.75	81.8760
340.46	21557.28	63.3181
510.69	28682.04	56.1633

4.68	2288.748	489.0487
9.36	3456.239	369.2563
18.72	5162.572	275.7784
37.44	7497.554	200.2552
74.88	10730.61	143.3040
149.76	14592.31	97.4379
299.52	19980.73	66.7092
599.04	29141.04	48.6462
1198.08	39199.43	32.7185
14.976	2558.169	170.8179
29.952	3725.66	124.3877
59.904	5791.221	96.6750
119.808	8844.659	73.8236
0.5	454.1115	908.223
2000	60586	30.293

Table 46 Rheological Data of 60.1 wt% O/W Emulsion stabilized by 1.99 wt% NCC

Shear Rate (s^{-1})	**Shear Stress (mPa)**	**Viscosity (cP)**
1.53207	2458.965	1604.9952
3.06414	4240.155	1383.7994
51.069	18291.77	358.1775
102.138	23734.29	232.3747
153.207	27890.4	182.0439
5.1069	4635.975	907.7865
10.2138	7406.715	725.1674
2.34	2737.783	1169.9927
4.68	3905.274	834.4603

9.36	5791.221	618.7202
18.72	8485.431	453.2816
37.44	12167.52	324.9871
74.88	16747.68	223.6602
149.76	23303.59	155.6062
299.52	33272.16	111.0849
599.04	49078.2	81.9281
1198.08	58687.54	48.9847
1.872	2288.748	1222.6218
3.744	3366.432	899.1538
7.488	4893.151	653.4657
14.976	7228.133	482.6478
29.952	10281.57	343.2683
59.904	14233.08	237.5981
119.808	20070.53	167.5225
1.4976	2198.941	1468.3100
2.9952	3097.011	1033.9914
5.9904	4444.116	741.8730
11.9808	6689.291	558.3343
0.5	1329.245	2658.4900
2000	91276	45.6380

Table 47 Rheological Data of 65.1 wt% O/W Emulsion stabilized by 1.99 wt% NCC

Shear Rate (s^{-1})	Shear Stress (mPa)	Viscosity (cP)
1.53207	24229.07	15814.5940
3.06414	28385.18	9263.6678
2.34	32823.13	14026.9778

4.68	39019.81	8337.5665
9.36	45845.14	4897.9854
18.72	52041.83	2780.0121
37.44	57609.86	1538.7249
74.88	62459.44	834.1271
149.76	67758.05	452.4443
299.52	76559.14	255.6061
0.234	11987.9	51230.3590
0.468	13873.85	29644.9808
0.936	16837.48	17988.7628
1.872	20070.53	10721.4391
3.744	24022.04	6416.1437
7.488	28153.16	3759.7708
14.976	33451.78	2233.6924
29.952	39019.81	1302.7448
59.904	46024.76	768.3086
119.808	55095.26	459.8630
0.0234	8754.852	374138.9744
0.0468	9383.501	200502.1581
0.0936	10191.76	108886.3675
0.1872	11179.64	59720.3045
0.3744	13155.4	35137.2730
0.7488	15580.18	20806.8697
1.4976	18543.82	12382.3551
2.9952	21956.48	7330.5559
5.9904	26177.41	4369.8935
11.9808	31026.99	2589.7259
0.01	5935.07	593506.98
1000	108000	108

Table 48 Rheological Data of 70.12 wt% O/W Emulsion stabilized by 1.99 wt% NCC

Shear Rate (s^{-1})	Shear Stress (mPa)	Viscosity (cP)
0.234	79612.58	340224.7
0.468	84102.93	179707.1
0.936	89850.57	95994.2
0.0234	75481.45	3225703
0.0468	77187.79	1649312
0.0936	79971.8	854399.6
0.1872	83833.5	447828.5
0.3744	88054.43	235188.1
0.7488	92814.2	123950.6
0.01	71166.25	7116625
10	101923.4	10192.34

Table 49 Power-Law variable values for different O/W Emulsions stabilized by 1.99 wt% NCC

Oil concentration (wt%)	*K*	*n-1*	*n*
0	121.95	-0.373	0.627
10.1	233.81	-0.437	0.563
20.16	292.42	-0.452	0.548
30.15	390.42	-0.461	0.539
40.13	520.58	-0.449	0.551
50.12	683.55	-0.41	0.59
60.1	1891.6	-0.491	0.509
65.1	18942	-0.748	0.252

70.12	90422	-0.948	0.052

A5.4 Rheological Data of O/W Emulsions stabilised by 2.91 wt% NCC

Table 50 Rheological Data of 10.01 wt% O/W Emulsion stabilized by 2.91 wt% NCC

Shear Rate (s^{-1})	Shear Stress (mPa)	Viscosity (cP)
1.53207	974.64	636.1589
3.06414	1469.415	479.5522
51.069	5625.525	110.1554
102.138	6417.165	62.8284
153.207	7307.76	47.6986
306.414	10573.275	34.5065
5.1069	1568.37	307.1080
10.2138	2261.055	221.3726
170.23	7901.49	46.4166
340.46	11068.05	32.5091
510.69	12750.285	24.9668
1021.38	16213.71	15.8743
4.68	2019.327	431.4801
9.36	2647.976	282.9034
18.72	3635.853	194.2229
37.44	4623.73	123.4971
74.88	6150.449	82.1374
149.76	7677.168	51.2631
299.52	9473.308	31.6283
599.04	12436.939	20.7614
14.976	2198.941	146.8310
29.952	2917.397	97.4024

59.904	3905.274	65.1922
119.808	5252.379	43.8400
11.9808	2198.941	183.5387
0.5	646.244429	1292.4889
2000	21941.8028	10.9709

Table 51 Rheological Data of 20.01 wt% O/W Emulsion stabilized by 2.91 wt% NCC

Shear Rate (s^{-1})	Shear Stress (mPa)	Viscosity (cP)
1.53207	2557.92	1669.5843
3.06414	3448.515	1125.4430
51.069	6615.075	129.5321
102.138	7505.67	73.4856
153.207	8891.04	58.0329
306.414	11760.735	38.3818
5.1069	1568.37	307.1080
10.2138	2360.01	231.0609
170.23	8891.04	52.2296
340.46	12453.42	36.5782
510.69	15718.935	30.7798
1021.38	20270.865	19.8465
2.34	1839.713	786.2021
4.68	2647.976	565.8068
9.36	3456.239	369.2563
18.72	4713.537	251.7915
37.44	6060.642	161.8761
74.88	7946.589	106.1243
149.76	9922.343	66.2550

299.52	12616.553	42.1226
599.04	15849.605	26.4583
11.9808	2109.134	176.0428
0.5	1098.80521	2197.6104
2000	24237.5707	12.1188

Table 52 Rheological Data of 30.03 wt% O/W Emulsion stabilized by 2.91 wt% NCC

Shear Rate (s^{-1})	Shear Stress (mPa)	Viscosity (cP)
1.53207	1766.28	1152.8716
3.06414	2656.875	867.0867
51.069	7307.76	143.0958
102.138	9187.905	89.9558
153.207	10573.275	69.0130
306.414	14531.475	47.4243
5.1069	1667.325	326.4848
10.2138	2360.01	231.0609
170.23	10474.32	61.5304
340.46	15224.16	44.7164
510.69	19281.315	37.7554
2.34	2019.327	862.9603
4.68	2827.59	604.1859
9.36	3815.467	407.6354
18.72	5162.572	275.7784
37.44	6779.098	181.0657
74.88	8575.238	114.5197
149.76	11179.641	74.6504
299.52	13694.237	45.7206

599.04	19082.657	31.8554
0.5	1007.85238	2015.7048
2000	31758.054	15.8790

Table 53 Rheological Data of 40.05 wt% O/W Emulsion stabilized by 2.91 wt% NCC

Shear Rate (s^{-1})	Shear Stress (mPa)	Viscosity (cP)
1.53207	2360.01	1540.4061
3.06414	3547.47	1157.7376
51.069	8495.22	166.3479
102.138	10375.365	101.5818
153.207	11760.735	76.7637
306.414	18489.675	60.3421
5.1069	1865.235	365.2382
10.2138	2755.83	269.8144
170.23	12849.24	75.4816
340.46	19479.225	57.2144
510.69	25020.705	48.9939
2.34	2378.555	1016.4765
4.68	3276.625	700.1335
9.36	4713.537	503.5830
18.72	6509.677	347.7392
37.44	8934.466	238.6342
74.88	11359.255	151.6995
149.76	15220.956	101.6357
299.52	20160.341	67.3088
599.04	26267.217	43.8489
5.9904	2109.134	352.0857

11.9808	2917.397	243.5060
0.5	1058.38979	2116.7796
2000	42772.4768	21.3862

Table 54 Rheological Data of 50.06 wt% O/W Emulsion stabilized by 2.91 wt% NCC

Shear Rate (s^{-1})	Shear Stress (mPa)	Viscosity (cP)
1.53207	3646.425	2380.0642
3.06414	5229.705	1706.7448
51.069	13344.015	261.2938
102.138	15916.845	155.8367
153.207	18687.585	121.9761
306.414	26406.075	86.1778
5.1069	2458.965	481.4986
10.2138	3943.29	386.0747
170.23	18984.45	111.5224
340.46	28682.04	84.2450
2.34	4174.695	1784.0577
4.68	5701.414	1218.2509
9.36	7677.168	820.2103
18.72	9922.343	530.0397
37.44	12167.518	324.9871
74.88	16388.447	218.8628
149.76	19980.727	133.4183
299.52	27255.094	90.9959
599.04	35696.952	59.5903
9.36	4354.309	465.2040
18.72	6330.063	338.1444

37.44	8934.466	238.6342
74.88	12706.36	169.6896
149.76	17825.359	119.0262
299.52	25099.726	83.7998
599.04	37403.285	62.4387
7.488	9203.887	1229.1516
14.976	11987.904	800.4744
29.952	15041.342	502.1816
59.904	18364.201	306.5605
119.808	20699.183	172.7696
0.1872	2198.941	11746.4797
0.3744	3007.204	8032.0620
0.7488	4174.695	5575.1803
1.4976	5611.607	3747.0666
2.9952	7228.133	2413.2388
5.9904	9383.501	1566.4231
11.9808	11089.834	925.6338
0.1	1627.69104	16276.9104
2000	47197.8453	23.5989

Table 55 Rheological Data of 60.06 wt% O/W Emulsion stabilized by 2.91 wt% NCC

Shear Rate (s^{-1})	Shear Stress (mPa)	Viscosity (cP)
1.53207	10969.095	7159.6565
3.06414	14036.7	4580.9591
5.1069	10870.14	2128.5202
10.2138	15718.935	1538.9899
2.34	6150.449	2628.3970

4.68	8934.466	1909.0739
9.36	12796.167	1367.1119
18.72	18094.78	966.6015
37.44	25369.147	677.5947
74.88	33811.005	451.5359
149.76	41534.407	277.3398
299.52	54287.001	181.2467
599.04	72966.857	121.8063
1198.08	88234.047	73.6462
0.234	4893.151	20910.9017
0.468	6240.256	13333.8803
0.936	8126.203	8681.8408
1.872	10730.606	5732.1613
3.744	13784.044	3681.6357
7.488	17555.938	2344.5430
14.976	22854.551	1526.0785
29.952	29141.041	972.9247
59.904	36505.215	609.3953
119.808	44408.231	370.6617
0.0234	2288.748	97809.7436
0.0468	2647.976	56580.6838
0.0936	3186.818	34047.2009
0.1872	3995.081	21341.2447
0.3744	5072.765	13549.0518
0.7488	6509.677	8693.4789
1.4976	8305.817	5546.0851
2.9952	11000.027	3672.5517
5.9904	15041.342	2510.9078
11.9808	21058.411	1757.6799

0.01	1528.71876	152871.8764
2000	106926.668	53.4633

Table 56 Rheological Data of 65.07 wt% O/W Emulsion stabilized by 2.91 wt% NCC

Shear Rate (s^{-1})	Shear Stress (mPa)	Viscosity (cP)
2.34	76559.137	32717.5799
4.68	82845.627	17702.0571
9.36	93891.888	10031.1846
0.234	55005.457	235066.0556
0.468	61381.754	131157.5940
0.936	68566.314	73254.6090
1.872	77187.786	41232.7917
3.744	86527.714	23111.0347
7.488	94610.344	12634.9284
0.0234	51143.756	2185630.5983
0.0468	55723.913	1190681.9017
0.0936	59855.035	639476.8697
0.1872	66949.788	357637.7564
0.3744	72697.436	194170.5021
0.7488	79432.961	106080.3432
1.4976	84641.767	56518.2739
2.9952	90119.994	30088.1390
5.9904	91646.713	15298.9305
0.01	46472.1407	4647214.0696
100	120003.1589	1200.0316

Table 57 Rheological Data of 70.09 wt% O/W Emulsion stabilized by 2.91 wt% NCC

Shear Rate (s^{-1})	Shear Stress (mPa)	Viscosity (cP)
0.9	251539.65	279488.5
1.8	267861.35	148811.861
3.6	255380.05	70938.9028
7.2	244338.9	33935.9583
14.4	239058.35	16601.2743
28.8	245299	8517.32639
57.6	273141.9	4742.04688
115.2	325947.4	2829.40451
230.4	408996.05	1775.15647
460.8	493004.8	1069.88889
0.09	227537.15	2528190.56
0.18	237138.15	1317434.17
0.36	249619.45	693387.361
0.72	267861.35	372029.653
1.44	287063.35	199349.549
2.88	287063.35	99674.7743
5.76	292823.95	50837.4913
11.52	260180.55	22585.1172
23.04	245779.05	10667.4935
46.08	259220.45	5625.44379
0.009	159370.05	17707783.3
0.018	153129.4	8507188.89
0.036	146888.75	4080243.06
0.072	162250.35	2253477.08
0.144	173291.5	1203413.19
0.288	187693	651711.806
0.576	201134.4	349191.667
1.152	214095.75	185847.005

2.304	219856.35	95423.763
4.608	213135.65	46253.3963
0.01	196294.729	19629472.9
1000	357197.687	357.197687

Table 58 Power-Law variable values for different O/W Emulsions stabilized by 2.91 wt% NCC

Oil concentration (wt%)	*K*	*n-1*	*n*
0	1074.3	-0.622	0.378
10.01	867.63	-0.575	0.425
20.01	1423	-0.627	0.373
30.03	1344.7	-0.584	0.416
40.05	1441.8	-0.554	0.446
50.06	3561	-0.66	0.34
60.06	7591.5	-0.652	0.348
65.07	74678	-0.897	0.103
70.09	249407	-0.948	0.052

A5.5 Rheological Data of O/W Emulsions stabilised by 3.85 wt% NCC

Table 59 Rheological Data of 10.03 wt% O/W Emulsion stabilized by 3.85 wt% NCC

Shear Rate (s^{-1})	Shear Stress (mPa)	Viscosity (cP)
1.53207	5526.57	3607.257
3.06414	6812.985	2223.457
51.069	10177.46	199.2883
102.138	11463.87	112.239
153.207	12552.38	81.93082
306.414	15224.16	49.68494

5.1069	2854.785	559.0055
10.2138	4240.155	415.1398
170.23	12156.56	71.41253
340.46	15817.89	46.46035
510.69	19281.32	37.75542
1021.38	23833.25	23.33436
2.34	3276.625	1400.267
4.68	4084.888	872.8393
9.36	5431.993	580.3411
18.72	6868.905	366.9287
37.44	8305.817	221.8434
74.88	10191.76	136.108
149.76	12526.75	83.64547
299.52	15310.76	51.11766
599.04	19352.08	32.30515
3.744	2109.134	563.3371
7.488	2917.397	389.6096
14.976	3815.467	254.7721
29.952	4893.151	163.3664
59.904	6599.484	110.1677
119.808	8485.431	70.82525
2.9952	2378.555	794.1223
5.9904	3097.011	516.9957
11.9808	3995.081	333.4569
0.5	1745.611	3491.221
2000	27405.1	13.70255

Table 60 Rheological Data of 20.04 wt% O/W Emulsion stabilized by 3.85 wt% NCC

Shear Rate (s^{-1})	Shear Stress (mPa)	Viscosity (cP)
1.53207	6812.985	4446.915
3.06414	7604.625	2481.814
51.069	10573.28	207.039
102.138	12354.47	120.9586
153.207	14036.7	91.61918
306.414	16708.49	54.52912
5.1069	2557.92	500.8753
10.2138	3547.47	347.3213
170.23	12750.29	74.90034
340.46	17005.35	49.94816
510.69	21557.28	42.21207
1021.38	28286.22	27.69412
2.34	4803.344	2052.711
4.68	5521.8	1179.872
9.36	6689.291	714.6678
18.72	7946.589	424.4973
37.44	9473.308	253.0264
74.88	11628.68	155.2975
149.76	14053.47	93.83991
299.52	17645.75	58.91341
599.04	22854.55	38.15196
3.744	2019.327	539.3502
7.488	2647.976	353.6293
14.976	3635.853	242.7786
29.952	4803.344	160.3681
59.904	6599.484	110.1677
119.808	8934.466	74.5732
2.9952	2019.327	674.1877

5.9904	2827.59	472.0202
11.9808	3725.66	310.9692
0.5	1775.901	3551.803
2000	30798.35	15.39918

Table 61 Rheological Data of 30.06 wt% O/W Emulsion stabilized by 3.85 wt% NCC

Shear Rate (s^{-1})	Shear Stress (mPa)	Viscosity (cP)
1.53207	6120.3	3994.791
3.06414	7604.625	2481.814
51.069	11859.69	232.2287
102.138	14531.48	142.273
153.207	15422.07	100.6617
306.414	19281.32	62.9257
5.1069	2360.01	462.1218
10.2138	4141.2	405.4514
170.23	14432.52	84.78247
340.46	19677.14	57.79573
510.69	25713.39	50.35029
1021.38	28286.22	27.69412
2.34	3995.081	1707.3
4.68	5252.379	1122.303
9.36	6689.291	714.6678
18.72	8575.238	458.079
37.44	10820.41	289.0068
74.88	13694.24	182.8824
149.76	17466.13	116.6275
299.52	20968.6	70.00736
599.04	27255.09	45.49795

0.468	2019.327	4314.801
0.936	2468.362	2637.139
1.872	3007.204	1606.412
3.744	3905.274	1043.075
7.488	5072.765	677.4526
14.976	6779.098	452.6641
29.952	8934.466	298.2928
59.904	11898.1	198.6194
119.808	17286.52	144.2852
0.1872	2288.748	12226.22
0.3744	2827.59	7552.324
0.7488	3546.046	4735.638
1.4976	4354.309	2907.525
2.9952	5521.8	1843.55
5.9904	7138.326	1191.628
11.9808	9563.115	798.2034
0.09	1526.008	16955.64
2000	36069.63	18.03481

Table 62 Rheological Data of 40.05 wt% O/W Emulsion stabilized by 3.85 wt% NCC

Shear Rate (s^{-1})	Shear Stress (mPa)	Viscosity (cP)
1.53207	6417.165	4188.559
3.06414	8198.355	2675.581
51.069	12750.29	249.6678
102.138	15916.85	155.8367
153.207	18687.59	121.9761
306.414	24031.16	78.42708
5.1069	2854.785	559.0055

10.2138	4339.11	424.8282
170.23	17895.95	105.128
340.46	25020.71	73.49088
2.34	3366.432	1438.646
4.68	4803.344	1026.356
9.36	6689.291	714.6678
18.72	9383.501	501.2554
37.44	12436.94	332.1832
74.88	16747.68	223.6602
149.76	21776.87	145.4118
299.52	28242.97	94.29411
599.04	34798.88	58.09108
1198.08	47910.7	39.98957
0.234	2737.783	11699.93
0.468	3635.853	7768.917
0.936	4713.537	5035.83
1.872	6240.256	3333.47
3.744	8036.396	2146.473
7.488	10281.57	1373.073
14.976	12526.75	836.4547
29.952	14861.73	496.1848
59.904	17915.17	299.0646
119.808	22405.52	187.0119
0.0936	2378.555	25411.91
0.1872	3186.818	17023.6
0.3744	4264.502	11390.23
0.7488	5431.993	7254.264
1.4976	6868.905	4586.609
2.9952	8395.624	2803.026

5.9904	10371.38	1731.333
11.9808	12167.52	1015.585
0.05	1920.838	38416.76
2000	43300.84	21.65042

Table 63 Rheological Data of 50.06 wt% O/W Emulsion stabilized by 3.85 wt% NCC

Shear Rate (s^{-1})	Shear Stress (mPa)	Viscosity (cP)
1.53207	7901.49	5157.395
3.06414	10177.46	3321.472
51.069	19776.09	387.2426
102.138	22942.65	224.624
153.207	26307.12	171.7096
2.34	4713.537	2014.332
4.68	6509.677	1390.957
9.36	9383.501	1002.511
18.72	13335.01	712.3402
37.44	18364.2	490.4968
74.88	24650.69	329.2026
149.76	32284.29	215.5735
299.52	40905.76	136.571
599.04	44049	73.53266
1198.08	54197.19	45.23671
0.234	3635.853	15537.83
0.468	4982.958	10647.35
0.936	6868.905	7338.574
1.872	9203.887	4916.606
3.744	11987.9	3201.897
7.488	15310.76	2044.707

14.976	18543.82	1238.236
29.952	22764.74	760.0409
59.904	27614.32	460.9763
119.808	31925.06	266.4685
0.0234	2019.327	86296.03
0.0468	3007.204	64256.5
0.0936	3995.081	42682.49
0.1872	5252.379	28057.58
0.3744	7048.519	18826.17
0.7488	8754.852	11691.84
1.4976	10730.61	7165.202
2.9952	13155.4	4392.159
5.9904	15580.18	2600.859
11.9808	18364.2	1532.803
0.01	1917.925	191792.5
2000	63712.87	31.85644

Table 64 Rheological Data of 60.06 wt% O/W Emulsion stabilized by 3.85 wt% NCC

Shear Rate (s^{-1})	Shear Stress (mPa)	Viscosity (cP)
1.53207	15916.85	10389.11
3.06414	22645.79	7390.584
5.1069	25713.39	5035.029
0.44	10178.12	23132.09
0.88	13942.76	15844.05
1.76	18883.85	10729.46
3.52	25471.97	7236.355
7.04	33236.54	4721.099
14.08	42177.56	2995.565

28.16	52765.61	1873.779
56.32	62883.08	1116.532
112.64	77000.48	683.598
225.28	114411.6	507.8639
0.044	8531.09	193888.4
0.088	11589.86	131703
0.176	15119.21	85904.6
0.352	18883.85	53647.3
0.704	23589.65	33508.03
1.408	28295.45	20096.2
2.816	33471.83	11886.3
5.632	38648.21	6862.253
11.264	46177.49	4099.564
22.528	51589.16	2290.002
0.0044	4295.87	976334.1
0.0088	6178.19	702067
0.0176	8766.38	498089.8
0.0352	11354.57	322573
0.0704	14178.05	201392.8
0.1408	17472.11	124091.7
0.2816	20295.59	72072.41
0.5632	24295.52	43138.35
1.1264	28295.45	25120.25
2.2528	33236.54	14753.44
2.34	20160.34	8615.53
4.68	25548.76	5459.137
9.36	32553.71	3477.96
18.72	41175.18	2199.529
37.44	52131.63	1392.405

74.88	63357.51	846.1206
149.76	75391.65	503.4164
299.52	90209.8	301.1812
0.234	19531.69	83468.77
0.468	23573.01	50369.67
0.936	27883.74	29790.32
1.872	31386.22	16766.14
3.744	36505.22	9750.325
7.488	42612.09	5690.717
14.976	48090.32	3211.159
29.952	58597.74	1956.388
59.904	67937.67	1134.109
119.808	78265.47	653.2575
0.0234	23213.78	992041.8
0.0468	25099.73	536318.9
0.0936	30488.15	325728.1
0.1872	32733.32	174857.5
0.3744	36235.79	96783.64
0.7488	38121.74	50910.44
1.4976	41534.41	27733.98
2.9952	43510.16	14526.63
5.9904	46383.99	7743.053
11.9808	52580.67	4388.744
0.01	9089.427	908942.7
2000	136573.1	68.28655

Table 65 Rheological Data of 65.07 wt% O/W Emulsion stabilized by 3.85 wt% NCC

Shear Rate (s^{-1})	Shear Stress (mPa)	Viscosity (cP)

0.44	36295.31	82489.34
0.88	41942.27	47661.67
1.76	49236.26	27975.15
3.52	55118.51	15658.67
7.04	65000.69	9233.053
14.08	72529.97	5151.276
28.16	82412.15	2926.568
56.32	94882.52	1684.704
112.64	113705.7	1009.461
225.28	131352.5	583.0632
0.044	29471.9	669815.9
0.088	33707.12	383035.5
0.176	37001.18	210234
0.352	40765.82	115812
0.704	45001.04	63921.93
1.408	51824.45	36807.14
2.816	56530.25	20074.66
5.632	62647.79	11123.54
11.264	74412.29	6606.205
22.528	84529.76	3752.209
0.0044	32060.09	7286384
0.0088	36295.31	4124467
0.0176	39589.37	2249396
0.0352	42177.56	1198226
0.0704	43824.59	622508.4
0.1408	46177.49	327965.1
0.2816	47589.23	168995.8
0.5632	49471.55	87840.11
1.1264	53706.77	47680.02

2.2528	61000.76	27077.75
2.34	64435.19	27536.41
4.68	72248.4	15437.69
9.36	82306.79	8793.46
18.72	90299.61	4823.697
0.234	55723.91	238136.4
0.468	62010.4	132500.9
0.936	67668.24	72295.13
1.872	74403.77	39745.6
3.744	79253.35	21168.09
7.488	85719.45	11447.58
14.976	92005.94	6143.559
0.0234	52670.48	2250875
0.0468	56981.21	1217547
0.0936	60124.46	642355.3
0.1872	63267.7	337968.5
0.3744	66770.17	178339.1
0.7488	70272.65	93847.02
1.4976	74763	49921.87
2.9952	81139.29	27089.77
5.9904	87335.98	14579.32
0.01	34687.66	3468766
1500	138229.8	92.15317

Table 66 Rheological Data of 70.07 wt% O/W Emulsion stabilized by 3.85 wt% NCC

Shear Rate (s^{-1})	Shear Stress (mPa)	Viscosity (cP)
0.44	54177.35	123130.3
0.88	57236.12	65041.05

1.76	58883.15	33456.34
3.52	63824.24	18131.89
7.04	70412.36	10001.76
14.08	77000.48	5468.784
28.16	91353.17	3244.076
56.32	112058.7	1989.678
112.64	142175.8	1262.214
225.28	165704.8	735.5505
0.044	49706.84	1129701
0.088	53000.9	602283
0.176	54412.64	309162.7
0.352	56294.96	159928.9
0.704	58412.57	82972.4
1.408	61706.63	43825.73
2.816	68294.75	24252.4
5.632	73471.13	13045.3
11.264	84294.47	7483.529
22.528	97000.13	4305.759
0.0044	64294.82	14612459
0.0088	66412.43	7546867
0.0176	67588.88	3840277
0.0352	68059.46	1933507
0.0704	66883.01	950042.8
0.1408	65471.27	464994.8
0.2816	67118.3	238346.2
0.5632	67824.17	120426.4
1.1264	68765.33	61048.77
2.2528	70177.07	31151.04
0.01	50738.53	5073853

1000	117581.2	117.5812

Table 67 Power-Law variable values for different O/W Emulsions stabilized by 3.85 wt% NCC

Oil concentration (wt%)	*K*	*n-1*	*n*
0	2464.2	-0.694	0.306
10.03	2197.3	-0.668	0.332
20.04	2254.1	-0.656	0.344
30.06	3266	-0.684	0.316
40.05	4634.4	-0.706	0.294
50.06	7191.7	-0.713	0.287
60.06	25266	-0.778	0.222
65.07	59180	-0.884	0.116
70.07	71013	-0.927	0.073

A5.6 Rheological Data of O/W Emulsions stabilised by 4.77 wt% NCC

Table 68 Rheological Data of 10.05 wt% O/W Emulsion stabilized by 4.77 wt% NCC

Shear Rate (s^{-1})	Shear Stress (mPa)	Viscosity (cP)
1.53207	11661.78	7611.78014
3.06414	12948.2	4225.71913
51.069	17203.26	336.863068
102.138	17796.99	174.244551
153.207	18291.77	119.392489
306.414	21359.37	69.7075525

5.1069	5031.795	985.293427
10.2138	6911.94	676.725607
170.23	18390.72	108.034542
340.46	22546.83	66.2246079
510.69	26801.9	52.4817306
2.34	8934.466	3818.14786
4.68	10820.41	2312.05406
9.36	14861.73	1587.79145
18.72	15580.18	832.274786
37.44	18184.59	485.699439
74.88	21058.41	281.228779
149.76	23213.78	155.006537
299.52	26267.22	87.6977063
599.04	28242.97	47.1470536
1198.08	52311.25	43.6625659
0.234	7497.554	32040.8291
0.468	9832.536	21009.6923
0.936	11718.48	12519.7468
1.872	13694.24	7315.29754
3.744	15490.38	4137.38702
7.488	17825.36	2380.52337
14.976	21238.03	1418.13735
29.952	23932.24	799.019598
59.904	25189.53	420.498347
119.808	26536.64	221.493039
0.0234	14053.47	600575.427
0.0468	15131.15	323315.15
0.0936	16568.06	177009.199
0.1872	17735.55	94741.1966

0.3744	18364.2	49049.6822
0.7488	19262.27	25724.1867
1.4976	19980.73	13341.8316
2.9952	21238.03	7090.68677
5.9904	21597.25	3605.31066
11.9808	22674.94	1892.60625
0.01	9423.692	942369.212
2000	26922.15	13.4610728

Table 69 Rheological Data of 20.04 wt% O/W Emulsion stabilized by 4.77 wt% NCC

Shear Rate (s^{-1})	Shear Stress (mPa)	Viscosity (cP)
1.53207	12453.42	8128.49282
3.06414	13541.93	4419.48638
51.069	18489.68	362.052811
102.138	20072.96	196.527786
153.207	21458.33	140.060996
306.414	27395.63	89.4072236
5.1069	5625.525	1101.55378
10.2138	8099.4	792.98596
170.23	21557.28	126.636198
340.46	26702.94	78.431945
2.34	11987.9	5123.0359
4.68	14412.69	3079.63526
9.36	16927.29	1808.47105
18.72	20070.53	1072.14391
37.44	22136.1	591.241854
74.88	24740.5	330.40195
149.76	28242.97	188.588214

299.52	30847.37	102.989363
599.04	36325.6	60.6396918
1198.08	44408.23	37.066165
0.234	11987.9	51230.359
0.468	14053.47	30028.7714
0.936	16208.83	17317.1293
1.872	18813.24	10049.8056
3.744	21148.22	5648.5625
7.488	24022.04	3208.07185
14.976	26357.02	1759.95085
29.952	28242.97	942.941072
59.904	31745.44	529.938635
119.808	32553.71	271.715637
0.0234	12796.17	546844.744
0.0468	14412.69	307963.526
0.0936	16208.83	173171.293
0.1872	17915.17	95700.6731
0.3744	19531.69	52167.9808
0.7488	21058.41	28122.8779
1.4976	22136.1	14781.0463
2.9952	23752.62	7930.2287
5.9904	24291.46	4055.06527
11.9808	25369.15	2117.48356
0.01	10735.61	1073560.78
2000	32204.71	16.102353

Table 70 Rheological Data of 30.04 wt% O/W Emulsion stabilized by 4.77 wt% NCC

Shear Rate (s^{-1})	Shear Stress (mPa)	Viscosity (cP)

1.53207	10375.37	6772.12203
3.06414	12255.51	3999.65733
51.069	18687.59	365.928156
102.138	21359.37	209.122658
153.207	23239.52	151.687031
5.1069	7208.805	1411.58139
10.2138	9286.86	909.246314
170.23	23734.29	139.424837
2.34	11000.03	4700.86624
4.68	13514.62	2887.73996
9.36	16119.03	1722.11816
18.72	17735.55	947.411966
37.44	21238.03	567.254941
74.88	23842.43	318.408494
149.76	29051.23	193.98527
299.52	30308.53	101.190345
599.04	39738.27	66.3365835
1198.08	49796.65	41.5637111
0.234	13694.24	58522.3803
0.468	15849.61	33866.6774
0.936	18004.97	19236.0823
1.872	20429.76	10913.3344
3.744	23213.78	6200.26149
7.488	24740.5	3304.0195
14.976	26446.83	1765.94758
29.952	27434.71	915.955796
59.904	29051.23	484.963174
119.808	29859.5	249.227906
0.0234	13514.62	577547.991

0.0468	15400.57	329072.009
0.0936	17466.13	186603.964
0.1872	19531.69	104335.962
0.3744	21507.45	57445.1015
0.7488	22674.94	30281.7001
1.4976	23752.62	15860.4574
2.9952	24560.88	8200.08146
5.9904	25369.15	4234.96711
11.9808	24022.04	2005.04491
0.01	11490.09	1149008.79
2000	32033.9	16.016952

Table 71 Rheological Data of 40.05 wt% O/W Emulsion stabilized by 4.77 wt% NCC

Shear Rate (s^{-1})	Shear Stress (mPa)	Viscosity (cP)
1.53207	13838.79	9032.74002
3.06414	16708.49	5452.91175
5.1069	14729.39	2884.21254
10.2138	17796.99	1742.44551
2.34	14143.27	6044.13333
4.68	17645.75	3770.45833
9.36	20339.96	2173.07212
18.72	24291.46	1297.62089
37.44	27793.94	742.359402
74.88	30847.37	411.957452
149.76	37133.86	247.955823
299.52	45306.3	151.263024
599.04	54556.42	91.0730869
1198.08	58956.97	49.2095394

0.234	18364.2	78479.4915
0.468	21776.87	46531.7671
0.936	24560.88	26240.2607
1.872	26357.02	14079.6068
3.744	27793.94	7423.59402
7.488	29141.04	3891.69885
14.976	30757.57	2053.79053
29.952	32284.29	1077.86745
59.904	34529.46	576.413278
119.808	36684.83	306.196823
0.0234	16657.87	711874.701
0.0468	19082.66	407749.081
0.0936	21327.83	227861.453
0.1872	24111.85	128802.612
0.3744	26446.83	70637.9033
0.7488	27793.94	37117.9701
1.4976	29051.23	19398.527
2.9952	29859.5	9969.11625
5.9904	30039.11	5014.54177
11.9808	31745.44	2649.69318
0.01	14151.98	1415198.35
2000	45678.96	22.8394793

Table 72 Rheological Data of 50.06 wt% O/W Emulsion stabilized by 4.77 wt% NCC

Shear Rate (s^{-1})	Shear Stress (mPa)	Viscosity (cP)
1.53207	14531.48	9484.86362
3.06414	17203.26	5614.38446
5.1069	22843.7	4473.10404

10.2138	23734.29	2323.74728
2.34	17106.9	7310.64231
4.68	21148.22	4518.85
9.36	24920.11	2662.40513
18.72	28692.01	1532.69263
37.44	34978.5	934.254701
74.88	40277.11	537.888742
149.76	48718.97	325.313615
299.52	58687.54	195.938649
599.04	66770.17	111.461962
1198.08	71440.14	59.6288545
0.234	20519.57	87690.4658
0.468	24111.85	51521.0449
0.936	27344.9	29214.6378
1.872	30398.34	16238.429
3.744	31745.44	8479.01816
7.488	34439.65	4599.31277
14.976	35247.92	2353.62694
29.952	39109.62	1305.74312
59.904	42342.67	706.842114
119.808	44318.42	369.912059
0.0234	18004.97	769443.291
0.0468	20429.76	436533.376
0.0936	23123.97	247050.983
0.1872	24471.08	130721.565
0.3744	25369.15	67759.4738
0.7488	28602.2	38197.3811
1.4976	31655.64	21137.5781
2.9952	33451.78	11168.4619

5.9904	34709.08	5794.11642
11.9808	36864.44	3076.96005
0.01	14357.08	1435707.72
2000	60616.04	30.3080209

Table 73 Rheological Data of 60.07 wt% O/W Emulsion stabilized by 4.77 wt% NCC

Shear Rate (s^{-1})	Shear Stress (mPa)	Viscosity (cP)
0.44	27354.29	62168.8409
0.88	32295.38	36699.2955
1.76	37942.34	21558.1477
3.52	44765.75	12717.5426
7.04	52295.03	7428.27131
14.08	63118.37	4482.83878
28.16	74412.29	2642.48189
56.32	82412.15	1463.28391
112.64	92059.04	817.285511
225.28	119117.4	528.752619
0.044	35118.86	798155.909
0.088	39824.66	452552.955
0.176	41942.27	238308.352
0.352	44765.75	127175.426
0.704	49000.97	69603.6506
1.408	53000.9	37642.6847
2.816	59118.44	20993.7642
5.632	65471.27	11624.8704
11.264	72765.26	6459.98402
22.528	74412.29	3303.10236
0.0044	56294.96	12794309.1

0.0088	59118.44	6718004.55
0.0176	61000.76	3465952.27
0.0352	61941.92	1759713.64
0.0704	62647.79	889883.381
0.1408	53942.06	383111.222
0.2816	56294.96	199911.08
0.5632	60294.89	107057.688
1.1264	64294.82	57079.9183
2.2528	67588.88	30002.1662
2.34	78804.31	33677.0564
4.68	81139.29	17337.456
9.36	90389.42	9656.98878
0.234	65782.3	281120.927
0.468	73146.47	156295.878
0.936	79343.15	84768.3269
1.872	85090.8	45454.4882
3.744	91107.87	24334.3673
0.0234	61920.6	2646179.32
0.0468	64704.61	1382577.2
0.0936	68207.09	728708.184
0.1872	69644	372029.904
0.3744	72966.86	194890.11
0.7488	74942.61	100083.615
1.4976	77187.79	51540.9896
2.9952	85360.22	28499.0061
5.9904	91197.68	15223.9714
0.01	48797.1	4879709.7
2000	96661.09	48.3305425

Table 74 Rheological Data of 65.07 wt% O/W Emulsion stabilized by 4.77 wt% NCC

Shear Rate (s^{-1})	Shear Stress (mPa)	Viscosity (cP)
0.44	81470.99	185161.341
0.88	84059.18	95521.7955
1.76	86647.37	49231.4602
3.52	95117.81	27022.1051
7.04	116058.6	16485.5994
14.08	128529	9128.4794
28.16	144058.1	5115.70064
56.32	164763.7	2925.49094
112.64	193469	1717.58727
225.28	215821.6	958.014826
0.044	92294.33	2097598.41
0.088	95588.39	1086231.7
0.176	95117.81	540442.102
0.352	93235.49	264873.551
0.704	89235.56	126755.057
1.408	94176.65	66886.8253
2.816	96294.26	34195.4048
5.632	118176.2	20982.9954
11.264	140999.4	12517.6989
22.528	155822.6	6916.8426
0.0044	116764.5	26537384.1
0.0088	119352.7	13562804.5
0.0176	121940.9	6928458.52
0.0352	124058.5	3524388.64
0.0704	124529.1	1768878.69
0.1408	125470.2	891123.722

0.2816	119117.4	423002.095
0.5632	118176.2	209829.954
1.1264	107823.5	95723.9613
2.2528	115588	51308.6115
0.01	94056.68	9405668.32
2000	162905.6	81.4527992

Table 75 Rheological Data of 70.07 wt% O/W Emulsion stabilized by 4.77 wt% NCC

Shear Rate (s^{-1})	Shear Stress (mPa)	Viscosity (cP)
0.44	108529.3	246657.591
0.88	112999.9	128408.92
1.76	123352.6	70086.7102
3.52	128529	36513.9176
7.04	139117	19760.9432
14.08	167822.4	11919.206
28.16	169234.2	6009.7358
56.32	176057.6	3126.02219
112.64	187586.8	1665.36559
225.28	220527.4	978.903498
0.044	106176.4	2413100.91
0.088	113235.1	1286762.95
0.176	118411.5	672792.727
0.352	124999.6	355112.614
0.704	132528.9	188251.307
1.408	140528.8	99807.3722
2.816	153940.3	54666.3033
5.632	161704.9	28711.804
11.264	182175.1	16173.2164

22.528	230644.9	10238.1414
0.0044	136528.9	31029284.1
0.0088	137940.6	15675067
0.0176	140999.4	8011327.27
0.0352	146411	4159404.26
0.0704	154881.5	2200020.88
0.1408	158175.5	1123405.75
0.2816	164763.7	585098.189
0.5632	172292.9	305917.844
1.1264	174881.1	155256.676
2.2528	162881.3	72301.7267
0.01	122056	12205600.5
2000	206302	103.151

Table 76 Power-Law variable values for different O/W Emulsions stabilized by 4.77 wt% NCC

Oil concentration (wt%)	***K***	***n-1***	***n***
0	9838.9	-0.861	0.139
10.05	14003	-0.914	0.086
20.04	16249	-0.91	0.09
30.04	16917	-0.916	0.084
40.05	22020	-0.904	0.096
50.06	24721	-0.882	0.118
60.07	63153	-0.944	0.056
65.07	115715	-0.955	0.045
70.07	148785	-0.957	0.043

A5.7 Rheological Data of O/W Emulsions stabilised by 5.66 wt% NCC

Table 77 Rheological Data of 10.02 wt% O/W Emulsion stabilized by 5.66 wt% NCC

Shear Rate (s^{-1})	Shear Stress (mPa)	Viscosity (cP)
1.53207	15323.12	10001.58
3.06414	17203.26	5614.384
51.069	22546.83	441.4974
102.138	23932.2	234.3124
153.207	25218.62	164.6048
5.1069	9781.635	1915.376
10.2138	11562.83	1132.079
170.23	25911.3	152.2135
2.34	16657.87	7118.747
4.68	19711.31	4211.818
9.36	22944.36	2451.32
18.72	26087.6	1393.569
37.44	28063.36	749.5555
74.88	30039.11	401.1633
149.76	31655.64	211.3758
299.52	32823.13	109.5858
599.04	38121.74	63.63806
1198.08	47461.67	39.61477
0.234	15310.76	65430.61
0.468	17915.17	38280.27
0.936	20609.38	22018.56
1.872	23752.62	12688.37
3.744	25638.57	6847.908
7.488	28512.39	3807.745
14.976	29679.88	1981.83
29.952	30308.53	1011.903

59.904	32374.09	540.4329
119.808	34439.65	287.457
0.0234	15220.96	650468.2
0.0468	17466.13	373207.9
0.0936	19621.5	209631.4
0.1872	22046.29	117768.6
0.3744	24471.08	65360.78
0.7488	26716.25	35678.76
1.4976	27255.09	18199.18
2.9952	28781.81	9609.313
5.9904	30847.37	5149.468
11.9808	27165.29	2267.402
0.01	14449.17	1444917
1000	34264.39	34.26439

Table 78 Rheological Data of 20.03 wt% O/W Emulsion stabilized by 5.66 wt% NCC

Shear Rate (s^{-1})	Shear Stress (mPa)	Viscosity (cP)
1.53207	17895.95	11680.89
3.06414	19776.09	6454.043
51.069	24723.84	484.1262
102.138	26208.17	256.5956
153.207	27593.54	180.1062
5.1069	12057.6	2361.041
10.2138	14729.39	1442.106
2.34	16657.87	7118.747
4.68	19980.73	4269.386
9.36	23752.62	2537.673
18.72	26087.6	1393.569

37.44	28871.62	771.1437
74.88	32104.67	428.7483
149.76	34439.65	229.9656
299.52	37942.13	126.6764
599.04	44318.42	73.98241
1198.08	48898.58	40.81412
0.234	16568.06	70803.68
0.468	19352.08	41350.59
0.936	22585.13	24129.41
1.872	26087.6	13935.69
3.744	28602.2	7639.476
7.488	30937.18	4131.568
14.976	32104.67	2143.741
29.952	34080.43	1137.835
59.904	37582.9	627.3855
119.808	38840.2	324.187
0.0234	17825.36	761767.5
0.0468	20070.53	428857.6
0.0936	22495.32	240334.6
0.1872	24920.11	133120.3
0.3744	26985.67	72077.12
0.7488	28692.01	38317.32
1.4976	29500.27	19698.36
2.9952	30757.57	10268.95
5.9904	31835.25	5314.378
11.9808	32912.94	2747.14
0.01	16035.73	1603573
1000	37591.42	37.59142

Table 79 Rheological Data of 30.04 wt% O/W Emulsion stabilized by 5.66 wt% NCC

Shear Rate (s^{-1})	Shear Stress (mPa)	Viscosity (cP)
1.53207	17104.31	11164.18
3.06414	18588.63	6066.508
51.069	24822.8	486.0639
102.138	27890.4	273.0659
5.1069	11760.74	2302.911
10.2138	14927.3	1461.483
2.34	16747.68	7157.126
4.68	20429.76	4365.334
9.36	24560.88	2624.026
18.72	29141.04	1556.68
37.44	32823.13	876.6861
74.88	36864.44	492.3136
149.76	41803.83	279.1388
299.52	46294.18	154.5612
599.04	56801.6	94.82104
1198.08	58058.9	48.45995
0.234	16927.29	72338.84
0.468	20339.96	43461.44
0.936	23752.62	25376.73
1.872	27704.13	14799.21
3.744	30039.11	8023.267
7.488	31835.25	4251.503
14.976	36235.79	2419.591
29.952	38660.58	1290.751
59.904	40726.14	679.8568
119.808	43330.55	361.6666

0.0234	16119.03	688847.3
0.0468	18454.01	394316.4
0.0936	20968.6	224023.5
0.1872	24111.85	128802.6
0.3744	26536.64	70877.77
0.7488	28153.16	37597.71
1.4976	29769.69	19878.27
2.9952	33272.16	11108.49
5.9904	34439.65	5749.141
11.9808	36145.99	3016.993
0.01	14087.33	1408733
1000	46647.53	46.64753

Table 80 Rheological Data of 40.07 wt% O/W Emulsion stabilized by 5.66 wt% NCC

Shear Rate (s^{-1})	Shear Stress (mPa)	Viscosity (cP)
1.53207	17796.99	11616.3
3.06414	19380.27	6324.864
5.1069	21458.33	4201.83
10.2138	24624.89	2410.943
2.34	19262.27	8231.74
4.68	23842.43	5094.536
9.36	26267.22	2806.327
18.72	29859.5	1595.059
37.44	35607.15	951.0455
74.88	41085.37	548.6829
149.76	48090.32	321.1159
299.52	58058.9	193.8398
599.04	65333.26	109.0633

1198.08	70811.49	59.10414
0.234	19352.08	82701.19
0.468	23393.39	49985.88
0.936	27165.29	29022.74
1.872	30937.18	16526.27
3.744	35158.11	9390.521
7.488	38840.2	5186.992
14.976	40636.34	2713.431
29.952	42701.9	1425.678
59.904	43689.78	729.3298
119.808	48898.58	408.1412
0.0234	17466.13	746415.9
0.0468	19980.73	426938.6
0.0936	23213.78	248010.5
0.1872	26716.25	142715
0.3744	30488.15	81432.01
0.7488	33631.39	44913.72
1.4976	36505.22	24375.81
2.9952	38121.74	12727.61
5.9904	39019.81	6513.724
11.9808	40815.95	3406.78
0.01	15415.43	1541543
1000	58607.84	58.60784

Table 81 Rheological Data of 50.09 wt% O/W Emulsion stabilized by 5.66 wt% NCC

Shear Rate (s^{-1})	Shear Stress (mPa)	Viscosity (cP)
1.53207	19380.27	12649.73
3.06414	23437.43	7648.941

5.1069	26307.12	5151.289
10.2138	28583.09	2798.477
2.34	23034.17	9843.66
4.68	29141.04	6226.718
9.36	34888.69	3727.424
18.72	37223.67	1988.444
37.44	44408.23	1186.117
74.88	50245.69	671.0161
149.76	57879.28	386.4802
299.52	67578.44	225.6225
599.04	83384.47	139.1968
0.234	26087.6	111485.5
0.468	31386.22	67064.56
0.936	37223.67	39768.88
1.872	40815.95	21803.39
3.744	45396.11	12125.03
7.488	49706.84	6638.2
14.976	52490.86	3504.999
29.952	54825.84	1830.457
59.904	56172.95	937.7161
119.808	60483.68	504.8384
0.0234	22674.94	969014.4
0.0468	25458.95	543994.7
0.0936	28961.43	309417
0.1872	32912.94	175817
0.3744	38031.93	101581
0.7488	40726.14	54388.55
1.4976	42881.51	28633.49
2.9952	47551.48	15875.89

5.9904	49437.42	8252.775
11.9808	52131.63	4351.265
0.01	20247.23	2024723
1000	69400.98	69.40098

Table 82 Rheological Data of 60.08 wt% O/W Emulsion stabilized by 5.66 wt% NCC

Shear Rate (s^{-1})	Shear Stress (mPa)	Viscosity (cP)
0.44	40059.95	91045.34
0.88	49236.26	55950.3
1.76	59589.02	33857.4
3.52	67118.3	19067.7
7.04	80059.25	11372.05
14.08	94176.65	6688.683
28.16	104058.8	3695.271
56.32	116999.8	2077.411
112.64	135587.7	1203.726
225.28	138646.5	615.4406
0.044	45236.33	1028098
0.088	51118.58	580893
0.176	57471.41	326542.1
0.352	65235.98	185329.5
0.704	72294.68	102691.3
1.408	77471.06	55022.06
2.816	89941.43	31939.43
5.632	97235.42	17264.81
11.264	103117.7	9154.623
22.528	110176.4	4890.641
0.0044	64059.53	14558984

0.0088	68765.33	7814242
0.0176	74412.29	4227971
0.0352	78412.22	2227620
0.0704	80059.25	1137205
0.1408	85235.63	605366.7
0.2816	77706.35	275945.8
0.5632	79823.96	141732.9
1.1264	86412.08	76715.27
2.2528	90882.59	40342.06
2.34	65243.46	27881.82
4.68	75212.03	16070.95
9.36	87695.21	9369.146
0.234	52131.63	222784.8
0.468	58687.54	125400.7
0.936	65872.1	70376.18
1.872	73685.31	39361.81
3.744	82037.36	21911.69
7.488	92814.2	12395.06
0.0234	46024.76	1966870
0.0468	49257.81	1052517
0.0936	53568.55	572313.5
0.1872	57969.09	309663.9
0.3744	63986.16	170903.2
0.7488	69913.42	93367.28
1.4976	74763	49921.87
2.9952	80241.22	26789.94
5.9904	90209.8	15059.06
0.01	50822.78	5082278
1000	130634.7	130.6347

Table 83 Rheological Data of 65.08 wt% O/W Emulsion stabilized by 5.66 wt% NCC

Shear Rate (s^{-1})	Shear Stress (mPa)	Viscosity (cP)
0.44	71353.52	162167.1
0.88	78882.8	89639.55
1.76	96058.97	54578.96
3.52	115823.3	32904.36
7.04	137234.7	19493.57
14.08	153940.3	10933.26
28.16	166410.7	5909.47
56.32	190645.6	3385.042
112.64	212762.8	1888.874
225.28	221703.8	984.1257
0.044	64530.11	1466593
0.088	71353.52	810835.5
0.176	76765.19	436165.9
0.352	84294.47	239472.9
0.704	92059.04	130765.7
1.408	102647.1	72902.76
2.816	113705.7	40378.45
5.632	144293.4	25620.28
11.264	158175.5	14042.57
22.528	176057.6	7815.055
0.0044	84294.47	19157834
0.0088	86647.37	9846292
0.0176	88059.11	5003359
0.0352	88764.98	2521732
0.0704	90882.59	1290946

0.1408	91353.17	648815.1
0.2816	93706.07	332763
0.5632	97235.42	172648.1
1.1264	112529.3	99901.7
2.2528	131117.2	58201.87
0.234	81049.49	346365.3
0.468	87695.21	187382.9
0.936	94610.34	101079.4
0.0234	78983.93	3375381
0.0468	82127.17	1754854
0.0936	85988.87	918684.5
0.1872	90928.26	485727.9
0.3744	93891.89	250779.6
0.01	66413.67	6641367
1000	227644.7	227.6447

Table 84 Rheological Data of 70.07 wt% O/W Emulsion stabilized by 5.66 wt% NCC

Shear Rate (s^{-1})	Shear Stress (mPa)	Viscosity (cP)
0.44	112179.1	254952.6
0.88	117811.7	133877
1.76	124617.8	70805.56
3.52	155127.6	44070.35
7.04	171556	24368.75
14.08	206290.3	14651.3
28.16	233514.5	8292.417
0.044	106882.3	2429143
0.088	112529.3	1278742
0.176	119823.3	680814

0.352	127117.3	361128.6
0.704	131352.5	186580.2
1.408	135587.7	96298.08
2.816	155822.6	55334.74
5.632	180528.1	32053.99
11.264	222645	19766.07
0.0044	133234.8	30280634
0.0088	134646.5	15300742
0.0176	135587.7	7703846
0.0352	136999.4	3892029
0.0704	140293.5	1992805
0.1408	142881.7	1014785
0.2816	149234.5	529952.1
0.5632	153234.4	272078.2
1.1264	160999	142932.4
2.2528	166646	73972.82
0.01	115041.3	11504132
1000	229537.6	229.5376

Table 85 Power-Law variable values for different O/W Emulsions stabilized by 5.66 wt% NCC

Oil concentration (wt%)	*K*	*n-1*	*n*
0	20344	-0.924	0.076
10.02	20410	-0.925	0.075
20.03	22547	-0.926	0.074
30.04	22742	-0.896	0.104
40.07	26300	-0.884	0.116
50.09	33141	-0.893	0.107

60.08	74141	-0.918	0.082
65.08	108707	-0.893	0.107
70.07	151654	-0.94	0.06

A5.8 Rheological Data of O/W Emulsions stabilised by 6.55 wt% NCC

Table 86 Rheological Data of 10.01 wt% O/W Emulsion stabilized by 6.55 wt% NCC

Shear Rate (s^{-1})	Shear Stress (mPa)	Viscosity (cP)
1.53207	20270.87	13231.03
3.06414	22151.01	7229.112
5.1069	24921.75	4880.015
10.2138	25614.44	2507.826
2.34	26626.45	11378.82
4.68	32104.67	6859.973
9.36	37223.67	3976.888
18.72	40636.34	2170.744
37.44	44677.65	1193.313
74.88	50874.34	679.4115
149.76	54556.42	364.2923
299.52	59675.42	199.2368
599.04	62639.05	104.5657
1198.08	66410.95	55.43114
0.234	29949.3	127988.5
0.468	34080.43	72821.42
0.936	37942.13	40536.46
1.872	41893.64	22379.08
3.744	45396.11	12125.03
7.488	47731.09	6374.344
14.976	49706.84	3319.1

29.952	55185.07	1842.45
59.904	58687.54	979.6932
119.808	61830.79	516.0823
0.0234	27793.94	1187775
0.0468	30218.73	645699.3
0.0936	33541.58	358350.3
0.1872	37313.48	199324.1
0.3744	41175.18	109976.4
0.7488	44049	58826.13
1.4976	46294.18	30912.24
2.9952	48449.55	16175.73
5.9904	51413.18	8582.595
11.9808	53478.74	4463.703
0.01	24764.41	2476441
2000	64954.52	32.47726

Table 87 Rheological Data of 20.04 wt% O/W Emulsion stabilized by 6.55 wt% NCC

Shear Rate (s^{-1})	Shear Stress (mPa)	Viscosity (cP)
1.53207	24624.89	16072.95
3.06414	25713.39	8391.715
5.1069	25911.3	5073.783
10.2138	27098.76	2653.152
2.34	29949.3	12798.85
4.68	35786.76	7646.743
9.36	40905.76	4370.273
18.72	45755.34	2444.195
37.44	50874.34	1358.823
74.88	54466.62	727.3853

149.76	57879.28	386.4802
299.52	63716.74	212.7295
599.04	69374.58	115.8096
1198.08	72068.79	60.15357
0.234	31476.02	134512.9
0.468	35966.37	76851.22
0.936	39917.88	42647.31
1.872	43061.13	23002.74
3.744	46383.99	12388.88
7.488	48898.58	6530.259
14.976	51502.98	3439.035
29.952	54287	1812.467
59.904	57879.28	966.2006
119.808	60573.49	505.588
0.0234	30128.92	1287561
0.0468	33811.01	722457.4
0.0936	36864.44	393850.9
0.1872	40815.95	218033.9
0.3744	43150.93	115253.6
0.7488	44857.27	59905.54
1.4976	46204.37	30852.28
2.9952	48090.32	16055.8
5.9904	49886.46	8327.734
11.9808	52490.86	4381.248
0.01	26610.41	2661041
2000	68113.13	34.05657

Table 88 Rheological Data of 30.04 wt% O/W Emulsion stabilized by 6.55 wt% NCC

Shear Rate (s^{-1})	Shear Stress (mPa)	Viscosity (cP)
1.53207	22744.74	14845.76
3.06414	26010.26	8488.599
5.1069	28879.95	5655.084
2.34	38570.78	16483.24
4.68	44318.42	9469.749
9.36	49347.62	5272.181
18.72	52131.63	2784.809
37.44	55903.53	1493.15
74.88	59944.84	800.5454
149.76	68117.28	454.8429
299.52	78534.89	262.2025
599.04	87156.36	145.4934
1198.08	92814.2	77.46912
0.234	39468.85	168670.3
0.468	44947.07	96040.75
0.936	50066.07	53489.39
1.872	52131.63	27848.09
3.744	55993.33	14955.48
7.488	57789.47	7717.611
14.976	60842.91	4062.694
29.952	62279.82	2079.321
59.904	63716.74	1063.647
119.808	73146.47	610.5308
0.0234	31565.83	1348967
0.0468	34439.65	735890
0.0936	37493.09	400567.2
0.1872	41714.02	222831.3
0.3744	46833.02	125088.2

0.7488	52401.05	69980.04
1.4976	57520.05	38408.16
2.9952	58148.7	19413.96
5.9904	59495.81	9931.859
11.9808	62369.63	5205.799
0.01	28630.48	2863048
2000	86940.53	43.47027

Table 89 Rheological Data of 40.05 wt% O/W Emulsion stabilized by 6.55 wt% NCC

Shear Rate (s^{-1})	Shear Stress (mPa)	Viscosity (cP)
0.44	43118.72	97997.09
0.88	47824.52	54346.05
1.76	55589.09	31584.71
3.52	60530.18	17196.07
7.04	65941.85	9366.74
14.08	78412.22	5569.05
28.16	87823.82	3118.744
56.32	97000.13	1722.303
112.64	107588.2	955.1507
225.28	128529	570.53
0.044	44530.46	1012056
0.088	51589.16	586240.5
0.176	57941.99	329215.9
0.352	65706.56	186666.4
0.704	72529.97	103025.5
1.408	77235.77	54854.95
2.816	81000.41	28764.35
5.632	84059.18	14925.28

11.264	88059.11	7817.748
22.528	95823.68	4253.537
0.0044	51824.45	11778284
0.0088	55353.8	6290205
0.0176	58412.57	3318896
0.0352	60294.89	1712923
0.0704	63353.66	899909.9
0.1408	65235.98	463323.7
0.2816	68765.33	244195.1
0.5632	72294.68	128364.1
1.1264	78647.51	69822.01
2.2528	78882.8	35015.45
2.34	42971.32	18363.81
4.68	47282.06	10103
9.36	51682.6	5521.645
18.72	57430.25	3067.855
37.44	57879.28	1545.921
74.88	68476.51	914.4833
149.76	77816.44	519.6076
299.52	87874.82	293.3855
0.234	40815.95	174427.1
0.468	47641.28	101797.6
0.936	54736.04	58478.67
1.872	59765.23	31925.87
3.744	63806.54	17042.35
7.488	69554.19	9288.754
14.976	75750.87	5058.151
29.952	79073.73	2640.015
59.904	81947.56	1367.981

119.808	87874.82	733.4637
0.0234	43779.58	1870922
0.0468	47461.67	1014138
0.0936	52041.83	556002.4
0.1872	57160.83	305346.3
0.3744	62279.82	166345.7
0.7488	67847.86	90608.78
1.4976	72068.79	48122.85
2.9952	76110.1	25410.69
5.9904	77457.21	12930.22
11.9808	79343.15	6622.526
0.01	47752.79	4775279
2000	100545.3	50.27263

Table 90 Rheological Data of 50.06 wt% O/W Emulsion stabilized by 6.55 wt% NCC

Shear Rate (s^{-1})	Shear Stress (mPa)	Viscosity (cP)
0.44	53236.19	120991.3
0.88	64294.82	73062.3
1.76	73941.71	42012.34
3.52	83823.89	23813.61
7.04	98176.58	13945.54
14.08	115117.5	8175.956
28.16	126646.7	4497.396
56.32	147352.2	2616.339
112.64	167587.1	1487.812
225.28	196998.4	874.4601
0.044	46883.36	1065531
0.088	54647.93	620999.2

0.176	62647.79	355953.4
0.352	72529.97	206051.1
0.704	84765.05	120404.9
1.408	96058.97	68223.7
2.816	108058.8	38373.14
5.632	112058.7	19896.78
11.264	121705.6	10804.83
22.528	133705.4	5935.075
0.0044	64059.53	14558984
0.0088	69235.91	7867717
0.0176	71824.1	4080915
0.0352	74647.58	2120670
0.0704	77706.35	1103783
0.1408	79118.09	561918.3
0.2816	80765.12	286808
0.5632	88059.11	156355
1.1264	97941.29	86950.72
2.2528	108294.1	48070.87
2.34	56621.98	24197.43
4.68	69374.58	14823.63
9.36	79253.35	8467.238
18.72	90928.26	4857.279
37.44	92993.82	2483.809
0.234	41534.41	177497.5
0.468	48539.35	103716.6
0.936	57699.67	61644.94
1.872	66680.37	35619.85
3.744	77996.05	20832.28
7.488	88772.89	11855.35

14.976	92993.82	6209.523
0.0234	46383.99	1982222
0.0468	49706.84	1062112
0.0936	53029.7	566556.7
0.1872	58238.51	311103.1
0.3744	64075.96	171143.1
0.7488	71350.33	95286.23
1.4976	79343.15	52980.2
2.9952	88593.28	29578.42
5.9904	93712.27	15643.74
0.01	48853.68	4885368
2000	171752.6	85.87632

Table 91 Rheological Data of 60.07 wt% O/W Emulsion stabilized by 6.55 wt% NCC

Shear Rate (s^{-1})	**Shear Stress (mPa)**	**Viscosity (cP)**
0.44	79118.09	179813.8
0.88	100529.5	114238
1.76	129470.2	73562.59
3.52	153469.7	43599.36
7.04	178175.2	25308.97
14.08	197939.5	14058.21
28.16	227821.4	8090.248
56.32	244056.4	4333.387
0.044	75353.45	1712578
0.088	81706.28	928480.5
0.176	91588.46	520389
0.352	99353.03	282252.9
0.704	112529.3	159842.7

1.408	134881.8	95796.75
2.816	175116.4	62186.23
5.632	211115.8	37485.05
11.264	224056.7	19891.4
22.528	244291.7	10843.91
0.0044	81000.41	18409184
0.0088	81470.99	9258067
0.0176	84294.47	4789459
0.0352	86882.66	2468257
0.0704	90176.72	1280919
0.1408	94882.52	673881.5
0.2816	100764.8	357829.4
0.5632	116999.8	207741.1
1.1264	140764.1	124968.1
2.2528	172057.6	76375.02
0.234	86078.68	367857.6
0.468	93353.05	199472.3
0.0234	76648.94	3275596
0.0468	81229.1	1735665
0.0936	84192.73	899495
0.1872	87156.36	465578.9
0.3744	91467.1	244303.1
0.01	64810.53	6481053
700	345469.9	493.5285

Table 92 Rheological Data of 65.08 wt% O/W Emulsion stabilized by 6.55 wt% NCC

Shear Rate (s^{-1})	Shear Stress (mPa)	Viscosity (cP)
0.44	102882.4	233823.6

0.88	114411.6	130013.2
1.76	145705.2	82787.02
3.52	176998.7	50283.73
7.04	222645	31625.71
0.044	111588.1	2536093
0.088	116764.5	1326869
0.176	118176.2	671455.9
0.352	114411.6	325032.9
0.704	121940.9	173211.5
1.408	144528.7	102648.2
2.816	169469.5	60180.91
5.632	221939.1	39406.8
0.0044	147587.5	33542609
0.0088	150411	17092155
0.0176	149940.4	8519340
0.0352	142881.7	4059139
0.0704	141469.9	2009516
0.1408	134176	952954.2
0.2816	135823	482325.9
0.5632	138175.9	245340.7
1.1264	146411	129981.4
2.2528	179351.6	79612.76
0.01	122729.5	12272951
10	165176.8	16517.68

Table 93 Power-Law variable values for different O/W Emulsions stabilized by 6.55 wt% NCC

Oil concentration (wt%)	***K***	***n-1***	***n***

0	29817	-0.912	0.088
10.01	35631	-0.921	0.079
20.04	37936	-0.923	0.077
30.04	43534	-0.909	0.091
40.05	63241	-0.939	0.061
50.06	78505	-0.897	0.103
60.07	129314	-0.85	0.15
65.08	149606	-0.957	0.043

A5.9 Rheological Data of O/W Emulsions stabilised by 7.41 wt% NCC

Table 94 Rheological Data of 10.03 wt% O/W Emulsion stabilized by 7.41 wt% NCC

Shear Rate (s^{-1})	Shear Stress (mPa)	Viscosity (cP)
1.53207	25119.66	16395.9
3.06414	28187.27	9199.079
2.34	36325.6	15523.76
4.68	42342.67	9047.579
9.36	48718.97	5205.018
18.72	50245.69	2684.064
37.44	58058.9	1550.718
74.88	62549.25	835.3265
149.76	68027.47	454.2433
299.52	70362.45	234.9174
599.04	74852.8	124.9546
1198.08	76020.3	63.45177
0.234	40187.3	171740.6
0.468	45755.34	97767.81
0.936	49706.84	53105.6
1.872	53748.16	28711.62

3.744	56262.75	15027.45
7.488	61920.6	8269.31
14.976	62369.63	4164.639
29.952	67219.21	2244.231
59.904	71440.14	1192.577
119.808	72966.86	609.0316
0.0234	37942.13	1621458
0.0468	41085.37	877892.6
0.0936	44857.27	479244.3
0.1872	49437.42	264088.8
0.3744	53837.97	143798
0.7488	56981.21	76096.7
1.4976	58597.74	39127.76
2.9952	60393.88	20163.55
5.9904	60663.3	10126.75
11.9808	63177.89	5273.262
0.01	35085.87	3508587
2000	78523.61	39.2618

Table 95 Rheological Data of 20.06 wt% O/W Emulsion stabilized by 7.41 wt% NCC

Shear Rate (s^{-1})	Shear Stress (mPa)	Viscosity (cP)
1.53207	24921.75	16266.72
3.06414	27890.4	9102.195
5.1069	29374.73	5751.968
2.34	37493.09	16022.69
4.68	43599.97	9316.232
9.36	48808.77	5214.613
18.72	55185.07	2947.92

37.44	61381.75	1639.47
74.88	67578.44	902.4898
149.76	73146.47	488.4246
299.52	76828.56	256.5056
599.04	84641.77	141.2957
1198.08	88952.5	74.24588
0.234	41534.41	177497.5
0.468	47282.06	101030
0.936	52041.83	55600.24
1.872	58058.9	31014.37
3.744	60663.3	16202.8
7.488	64165.77	8569.147
14.976	66770.17	4458.478
29.952	71080.91	2373.161
59.904	73146.47	1221.062
119.808	77726.63	648.7599
0.0234	39558.65	1690541
0.0468	43420.35	927785.3
0.0936	48000.51	512826
0.1872	53299.12	284717.5
0.3744	58867.16	157230.7
0.7488	63357.51	84612.06
1.4976	65153.65	43505.37
2.9952	65782.3	21962.57
5.9904	67668.24	11296.11
11.9808	70272.65	5865.439
0.01	35580.89	3558089
2000	84642.77	42.32139

Table 96 Rheological Data of 30.05 wt% O/W Emulsion stabilized by 7.41 wt% NCC

Shear Rate (s^{-1})	Shear Stress (mPa)	Viscosity (cP)
1.53207	24723.84	16137.54
3.06414	27593.54	9005.311
2.34	48180.13	20589.8
4.68	56891.4	12156.28
9.36	61381.75	6557.88
18.72	65063.84	3475.633
37.44	69284.77	1850.555
74.88	76110.1	1016.428
149.76	81229.1	542.3952
299.52	85001	283.7907
0.234	53478.74	228541.6
0.468	61381.75	131157.6
0.936	67398.82	72007.29
1.872	71440.14	38162.47
3.744	72158.59	19273.13
7.488	75661.07	10104.31
14.976	79343.15	5298.02
29.952	81678.14	2726.968
59.904	86437.91	1442.94
119.808	94161.31	785.9351
0.0234	50335.49	2151089
0.0468	54646.23	1167654
0.0936	59046.77	630841.6
0.1872	64614.81	345164.6
0.3744	69733.81	186254.8
0.7488	73236.28	97804.86

1.4976	78355.28	52320.56
2.9952	80869.87	26999.82
5.9904	81139.29	13544.89
11.9808	84821.38	7079.776
0.01	47069.38	4706938
2000	93238.7	46.61935

Table 97 Rheological Data of 40.07 wt% O/W Emulsion stabilized by 7.41 wt% NCC

Shear Rate (s^{-1})	Shear Stress (mPa)	Viscosity (cP)
0.44	40059.95	91045.34
0.88	48530.39	55148.17
1.76	56059.67	31852.09
3.52	74647.58	21206.7
7.04	81941.57	11639.43
14.08	102647.1	7290.276
28.16	126646.7	4497.396
56.32	144528.7	2566.206
112.64	173704.7	1542.122
225.28	190410.3	845.216
0.044	45471.62	1033446
0.088	58412.57	663779.2
0.176	64294.82	365311.5
0.352	75824.03	215409.2
0.704	82882.73	117731.2
1.408	89235.56	63377.53
2.816	95823.68	34028.3
5.632	106411.7	18894.13
11.264	114882.2	10199.06

22.528	128764.3	5715.744
0.0044	49000.97	11136584
0.0088	58647.86	6664530
0.0176	59353.73	3372371
0.0352	62177.21	1766398
0.0704	66177.14	940016.2
0.1408	72059.39	511785.4
0.2816	79588.67	282630.2
0.5632	88529.69	157190.5
1.1264	95588.39	84861.85
2.2528	100058.9	44415.35
2.34	58418.12	24965.01
4.68	68566.31	14650.92
9.36	76828.56	8208.179
18.72	90209.8	4818.9
0.234	59495.81	254255.6
0.468	67219.21	143630.8
0.936	70901.3	75749.25
1.872	75391.65	40273.32
3.744	79253.35	21168.09
7.488	81767.94	10919.86
14.976	90119.99	6017.628
0.0234	58867.16	2515691
0.0468	63806.54	1363388
0.0936	67039.6	716235
0.1872	71709.56	383063.9
0.3744	72607.63	193930.6
0.7488	72787.24	97205.19
1.4976	77008.17	51421.06

2.9952	79253.35	26460.12
5.9904	81498.52	13604.85
11.9808	85180.61	7109.76
0.01	48828.89	4882889
2000	163485.3	81.74266

Table 98 Rheological Data of 50.06 wt% O/W Emulsion stabilized by 7.41 wt% NCC

Shear Rate (s^{-1})	Shear Stress (mPa)	Viscosity (cP)
0.44	92493.8	210213.2
0.88	109898.6	124884.8
1.76	120247.4	68322.39
3.52	129655.4	36833.92
7.04	152234.6	21624.23
14.08	170345	12098.37
28.16	186103.4	6608.786
56.32	213386.6	3788.825
112.64	239023.4	2122.012
0.044	78618.32	1786780
0.088	91761.02	1042739
0.176	103026.2	585376.1
0.352	115699.5	328691.8
0.704	127434.1	181014.3
1.408	135883	96507.78
2.816	152546	54171.17
5.632	167096.9	29669.19
11.264	173668.2	15417.99
22.528	195259.8	8667.427
0.0044	96454.84	21921556

0.0088	100914	11467497
0.0176	103495.6	5880431
0.0352	106546.6	3026891
0.0704	109832.2	1560117
0.1408	117342.4	833397.4
0.2816	124852.5	443368.1
0.5632	133770.7	237519.1
1.1264	141750.2	125843.6
2.2528	146913.4	65213.7
0.234	86527.71	369776.6
0.468	95059.38	203118.3
0.0234	77996.05	3333164
0.0468	83294.66	1779800
0.0936	87605.4	935955.1
0.1872	93353.05	498680.8
0.01	80536	8053600
2000	279701.7	139.8508

Table 99 Rheological Data of 60.07 wt% O/W Emulsion stabilized by 7.41 wt% NCC

Shear Rate (s^{-1})	Shear Stress (mPa)	Viscosity (cP)
0.44	113941	258956.8
0.88	130881.9	148729.4
1.76	148763.9	84524.96
3.52	180292.8	51219.54
7.04	196292.5	27882.46
14.08	200527.7	14242.03
28.16	213468.7	7580.564
56.32	245232.8	4354.276

0.044	84294.47	1915783
0.088	92529.62	1051473
0.176	98411.87	559158.4
0.352	107352.9	304979.8
0.704	119352.7	169535.1
1.408	143117	101645.6
2.816	187351.5	66531.07
5.632	216998	38529.48
11.264	238174.1	21144.72
0.0044	99353.03	22580234
0.0088	101000.1	11477280
0.0176	105235.3	5979277
0.0352	108764.6	3089904
0.0704	98882.45	1404580
0.1408	108294.1	769133.9
0.2816	118646.8	421331
0.5632	134646.5	239074.1
1.1264	160293.1	142305.7
2.2528	189939.7	84312.71
0.01	84659.3	8465930
2000	366267.4	183.1337

Table 100 Rheological Data of 65.07 wt% O/W Emulsion stabilized by 7.41 wt% NCC

Shear Rate (s^{-1})	Shear Stress (mPa)	Viscosity (cP)
0.44	130411.3	296389.3
0.88	135587.7	154076.9
1.76	149705.1	85059.71
3.52	188763.2	53625.92

7.04	241703.5	34332.88
0.044	139117	3161751
0.088	146175.7	1661088
0.176	150175.7	853270.9
0.352	153469.7	435993.6
0.704	156763.8	222675.8
1.408	172763.5	122701.4
2.816	201704.2	71627.9
5.632	239821.2	42581.88
0.0044	178645.8	40601309
0.0088	183116.3	20808667
0.0176	188763.2	10725184
0.0352	190175	5402698
0.0704	187822.1	2667927
0.1408	185939.8	1320595
0.2816	187586.8	666146.2
0.5632	189939.7	337250.9
1.1264	199116	176772
2.2528	213939.3	94965.94
0.01	162820.8	16282076
15	192645.9	12843.06

Table 101 Power-Law variable values for different O/W Emulsions stabilized by 7.41 wt% NCC

Oil concentration (wt%)	*K*	*n-1*	*n*
0	41057	-0.924	0.076
10.03	47548	-0.934	0.066
20.06	49342	-0.929	0.071

30.05	60917	-0.944	0.056
40.07	77033	-0.901	0.099
50.06	128822	-0.898	0.102
60.07	147121	-0.88	0.12
65.07	181013	-0.977	0.023

Appendix B: Apparatus Information

Appendix B1: Fann viscometer manual

1 Introduction

Fann Model 35 viscometers are direct-reading instruments which are available in six- speed and twelve- speed designs for use on either 50 Hz or 60 Hz electrical power. The standard power source is 115 volts, but all models may be fitted with a transformer, making operation with 220/230 volts possible.

Fann Model 35 viscometers are used in research and production. These viscometers are recommended for evaluating the rheological properties of fluids, Newtonian and non-Newtonian. The design includes a R1 Rotor Sleeve, B1 Bob, F1 Torsion Spring, and a stainless steel sample cup for testing according to American Petroleum Institute Recommended Practice for Field Testing Water Based Drilling Fluids, API RP 13B-1/ISO 10414-1 Specification.

1.1 Background

Fann Model 35 viscometers are Couette rotational viscometers. In this viscometer, the test fluid is contained in the annular space (shear gap) between an outer cylinder and the bob (inner cylinder). Viscosity measurements are made when the outer cylinder, rotating at a known velocity, causes a viscous drag exerted by the fluid. This drag creates a torque on the bob, which is transmitted to a precision spring where its deflection is measured.

Viscosity measured by a Couette viscometer, such as the Model 35, is a measure of the shear stress caused by a given shear rate. This relationship is a linear function for Newtonian fluids (i.e., a plot of shear stress vs. shear rate is a straight line).

The instrument is designed so that the viscosity in centipoise (or millipascal second) of a Newtonian fluid is indicated on the dial with the standard rotor R1, bob B1, and torsion spring F1 operating at 300 rpm. Viscosities at other test speeds may be measured by using multipliers of the dial reading. A simple calculation that closely approximates the viscosity of a pseudo-plastic fluid, such as a drilling fluid is described in Section 7.

The shear rate may be changed by changing the rotor speed and rotor-bob combination. Various torsion springs are available and are easily interchanged in order to broaden shear stress ranges and allow viscosity measurements in a variety of fluids.

3 Features and Specifications

The Fann direct-indicating viscometers are equipped with the standard R1 rotor sleeve, B1 bob, F1 torsion spring, and a stainless steel sample cup. Other rotor-bob combinations and/or torsion springs can be substituted to extend the torque measuring range or increase the sensitivity of the torque measurement.

Each viscometer is supplied with a 115 volt motor. For operation on 230 volts, a step-down transformer is required.

The viscometers are available in six-speed and twelve-speed models.
See Table 3-1, 3-2, 3-3, and 3-4 for specifications. Table 3-5 lists the recommended environmental conditions for use.

Figure 3-1 is a picture of the viscometer and Figure 3-2 is a detailed drawing that names the individual parts.

Figure 3-1 Model 35SA Viscometer

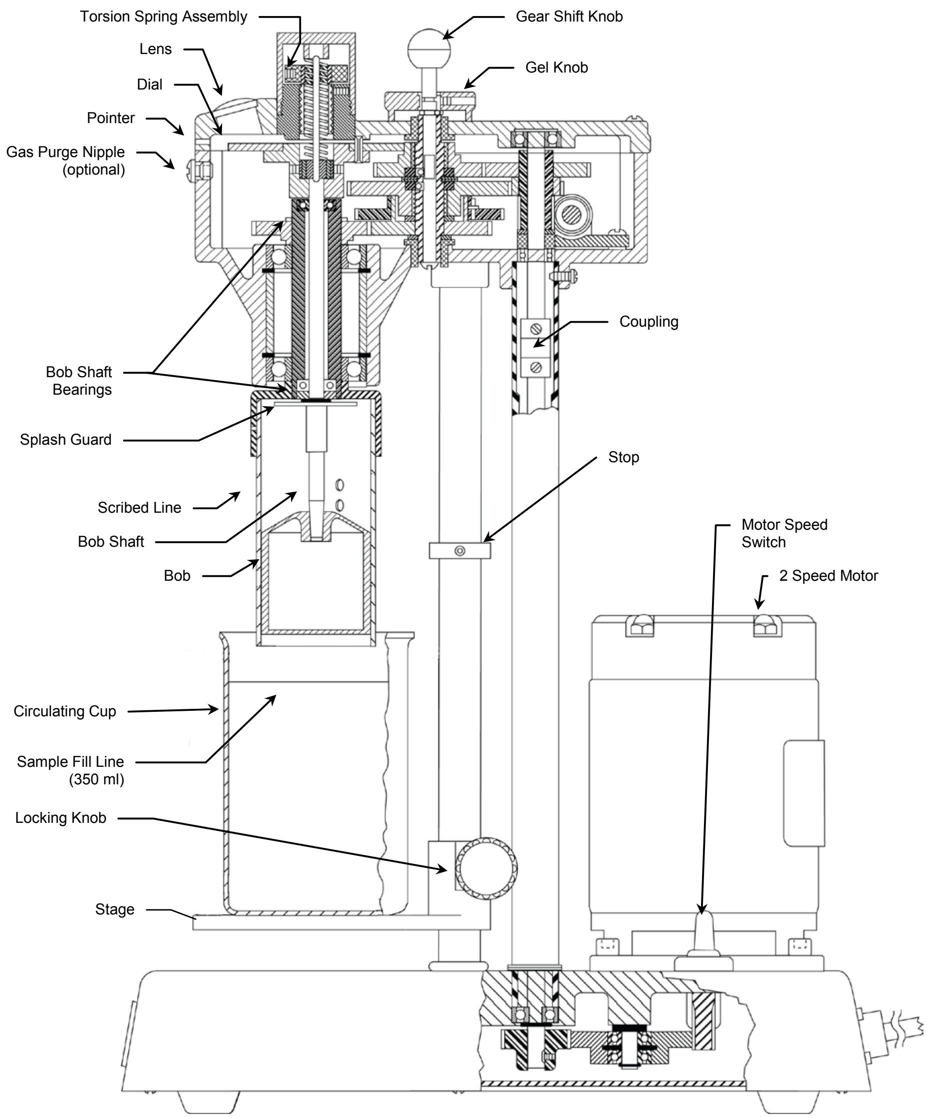

Figure 3-2 Model 35 Viscometer Schematic

Table 3-1 Model 35 Viscometer Specifications

Model No.	Part No.	Electrical	No. of Speeds	Speeds
35A	207198	115V, 60 Hz, 90W	6	600, 300, 200, 100, 6, 3
35SA	207199	115V, 50 Hz, 90W	6	600, 300, 200, 100, 6, 3
35A/SR-12	207200	115V, 60 Hz, 90W	12	600, 300, 200, 180, 100, 90, 60, 30, 6, 3, 1.8, 0.9
35SA/SR-12	207201	115V, 50 Hz, 90W	12	600, 300, 200, 180, 100, 90, 60, 30, 6, 3, 1.8, 0.9

Table 3-2 Model 35 Viscometer Sizes

Model No.	Part No.	Dimensions (LxDxH)	Weight
35A	207198	15.2 x 6 x 10.5 in. 39 x 15 x 27 cm	15 lb 6.8 kg
35SA	207199	15.2 x 6 x 10.5 in. 39 x 15 x 27 cm	15 lb 6.8 kg
35A/SR-12	207200	15.2 x 6 x 10.5 in. 39 x 15 x 27 cm	15 lb 6.8 kg
35SA/SR-12	207201	15.2 x 6 x 10.5 in. 39 x 15 x 27 cm	15 lb 6.8 kg
35A w/ case	101671768	8 x 16 x 19 in. 20.3 x 40.6 x 48.3 cm	26 lb 11.8 kg
35SA w/ case	101671770	8 x 16 x 19 in. 20.3 x 40.6 x 48.3 cm	26 lb 11.8 kg

Table 3-3 Rotor and Bob Dimensions

Unit	Radius (cm)	Length (cm)	Cylinder Area (cm^2) x Radius (cm)
B1	1.7245	3.8	71.005
B2	1.2276	3.8	35.981
B3	0.86225	3.8	17.751
B4	0.86225	1.9	8.876
R1	1.8415	n/a	n/a
R2	1.7589	n/a	n/a
R3	2.5867	n/a	n/a

Table 3-4 Rotor-Bob Specifications

ROTOR-BOB	R1 B1	R2 B1	R3 B1	R1 B2	R1 B3	R1 B4
Rotor Radius, R_0 (cm)	1.8415	1.7588	2.5866	1.8415	1.8415	1.8415
Bob Radius, R_i (cm)	1.7245	1.7245	1.7245	1.2276	0.8622	0.8622
Bob Height, L (cm)	3.8	3.8	3.8	3.8	3.8	1.9
Shear Gap in Annulus (cm)	0.117	0.0343	0.8261	0.6139	0.9793	0.9793
Radii Ratio, R_i/R_0	0.9365	0.9805	0.667	0.666	0.468	0.468
Maximum Use Temperature (°C)	93	93	93	93	93	93
Minimum Use Temperature (°C)	0	0	0	0	0	0

Table 3-5 Range of Environmental Conditions

Maximum Altitude	6562 ft (2000 m)
Temperature Range	41°F to 104°F (5°C to 40°C)
Maximum Relative Humidity (RH)	80% RH at 87.8°F (31°C) or less 50% RH at 104°F (40°C)

5.1 Operating the Model 35A and 35SA

The Model 35A and 35SA viscometers operate at six speeds, ranging from 3 rpm to 600 rpm. To select the desired speed, set the speed switch (located on the right side of the base) to the high or low speed position as desired. Then turn the motor on and move the gear shift knob (located on the top of the instrument) to the position that corresponds to the desired speed.

Table 5-1 lists the positions for the viscometer switch and the gear knob combinations to obtain the desired speed. The viscometer gear shift knob may be engaged while the motor is running. Read the dial for shear stress values.

Table 5-1 Six-Speed Testing Combinations for Models 35A and 35SA

Speed RPM	Viscometer Switch	Gear Shift Knob
600	High	Down
300	Low	Down
200	High	Up
100	Low	Up
6	High	Center
3	Low	Center

5.2 Operating the Model 35A/SR-12 and 35SA/SR-12

The Model 35A/SR-12 and 35SA/SR-12 have twelve speeds for testing capabilities. To achieve this broader testing range from 0.9 rpm to 600 rpm, an additional gear box shift lever is used; it is located on the right side of the gear box. See Figure 5-1. Move this lever to the left or right as determined from Table 5-2.

Never change the gear box shift lever while the motor is running. Changing it while the motor is running will result in gear damage

Only the viscometer gear shift knob (on top of the instrument) can be changed while the motor is running.

After preparing the instrument for 12-speed testing by setting the gear box shift lever, select the proper speed range with the speed shift switch. Then turn on the motor and set the gear shift knob on the top of the instrument. Refer to Table 5-2 for the correct combination of gear box shift lever setting, speed switch selection, and viscometer gear shift knob placement. The shear stress values will appear on the dial.

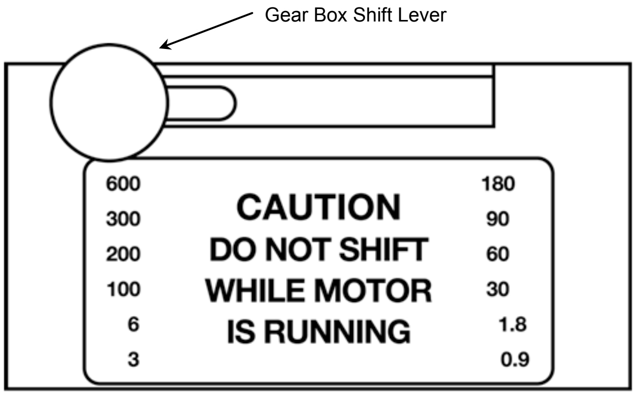

Figure 5-1 Gear Box Shift Lever

Table 5-2 Twelve-Speed Testing Combinations- Models 35A/SR-12 and 35SA/SR-12

RPM	Gear Box Shift Lever	Speed Switch	Gear Shift Knob
600	Left	High	Down
300	Left	Low	Down
200	Left	High	Up
180	Right	High	Down
100	Left	Low	Up
90	Right	Low	Down
60	Right	High	Up
30	Right	Low	Up
6	Left	High	Center
3	Left	Low	Center
1.8	Right	High	Center
0.9	Right	Low	Center

5.4.1 Rotor Removal and Replacement

Refer to Figure 5-2.

To remove the rotor from its socket, twist the rotor clockwise and gently pull it down.

To replace the rotor, align the rotor slot and groove with the lock pin in the main shaft socket. Then push the rotor upward and turn it counterclockwise, locking it into position.

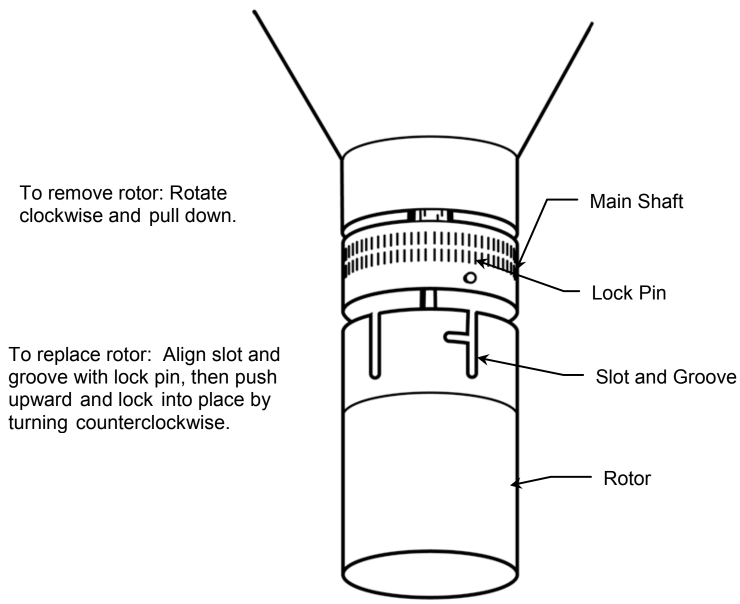

Figure 5-2 Rotor Removal and Installation

Appendix B2: Haake viscometer manual

HAAKE

ROTOVISCO RV 12

Berechnungsfaktoren
Calculation factors
Facteurs de calcul

Nr.: 850195
Datum: 26.4.1985
Kontr.:

M 150
Nr.: 840305
a = 0,0147 (N·cm / Skt)

System	Rotor	D/L (mm)	Nr.	M (min/s)	A (Pa / Skt)	G (mPa·s / Skt·min)
NV	NV	40.2 /60		5.41	0,533	98,6
MV T/MV	MV I	40.08/60		2.34	0,966	412
	MV II	36.8 /60		0.9	1,13	1250
	MV III	30.4 /60		0.44	1,63	3710
SV T/SV	SV I	20.2 /61.4		0.89	3,72	4175
	SV II	20.2 /19.6		0.89	11,3	12670
P	MV I P	40.08/60		2.0	0,966	483
	MV II P	36.8 /60		0.88	1,13	1282
	SV II P	20.2 /19.6		0.78	11,3	14460
DIN 53019	MV	38.7 /58.1		1.29	0,9	700
	SV	21.3 /32		1.29	5,43	4210
HS	HS I	19.95/15				
[redacted]	HS II	19.8 /15				
	PK V,..........°	50 /--				
	PK I,..........°	28 /--				
	PK II,..........°	20 /--				
	MV SP	41.6/40				
	SV SP	20.2 /61.4				

[redacted]KE Mess-Technik GmbH u. Co. · Dieselstraße 6 · D-7500 Karlsruhe 41 · Telefon (07 21) 40 94-1

HAAKE

6.2 Sensor System MV

Application:

The MV is primarily used for viscosity measurements of medium viscous liquids such as heavy oils, paints, varnishes, resins, emulsions, etc. working in the medium shear rate range. Small yield points can be determined.

This coaxial cylinder sensor system consists of an MV cup used with three different rotors to provide different viscosity measuring ranges. MV I and MV II are both available in plastic (phenolic thermoset) and in stainless steel, 18/8. The plastic rotors are low weight and allow higher rates of rotor acceleration. They are mechanically and chemically safe for temperatures up to 100°C.

This sensor system requires the temperature vessel.

The rotors are positively mechanically centered. The top and the bottom surfaces of the rotors are recessed to minimize "end effects", i.e. their influence on torque. An air bubble is retained in the bottom recess, while the upper recess accomodates any excess sample.

The required amount of sample depends on the type of rotor used. For the purpose of reference there are two ring marks on the inside wall of the cup. The lower mark indicates the approximate sample volume required when the MV I and the MV II rotors are used in the cup MV. The upper ring mark is used for the MV III rotor.

Decreasing the temperature of a sample which just fills the annular gap between cup and rotor up to the upper rim of the rotor will cause the sample volume to shrink. This will lead to an only partly filled sensor system, to a reduced torque and to an erroneous viscosity value being below the true viscosity level.

When a sample must be measured at various temperatures, it is advisable to begin at the lowest temperature. When this is not possible, the sensor system MV should be overfilled to such an extent that the sample will be slightly above the rim of the rotor even at the lowest temperature. Rotor alternative: MV DIN (see 6.6).

During a test the liquid level of the sample must just overflow into the upper recess of the rotor. The liquid level must not surpass the upper rim of the rotor by more than 1 or 2 mm. Excess sample may be removed by sucking it back by means of a syringe.

Cleaning: To remove the bottom of the cup, first loosen the knurled screw and remove the cross-bar. (Order no. of sealing 807-0458)

HAAKE

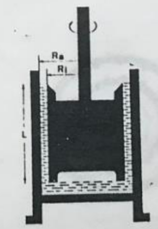

Sensor System	MV I	MV II	MV III
Inner Cylinder (rotor) radius R_i (mm)	20.04	18.4	15.2
height L (mm)	60	60	60
Outer Cylinder (cup) radius R_a (mm)	21	21	21
Radii Ratio R_a/R_i	1.05	1.14	1.38
Sample Volume V (cm³)	40	55	70
Temperature: max. (°C)	100	100	100
min. (°C)	-30	-30	-30
Calculation Factors			
A (Pa/scale grad.)	3.22	3.76	5.44
M (min/s)	2.34	0.9	0.44
G (mPa·s/scale grad.·min)	1374	4171	12375

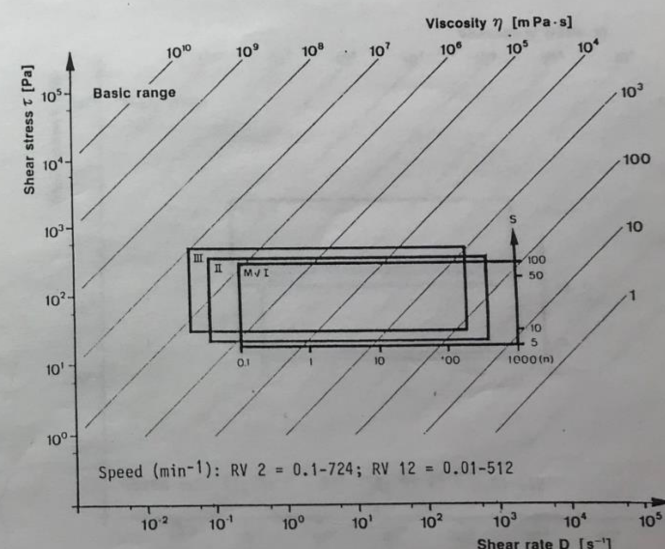

HAAKE

Shear rate D

The shear rate 'D' is linearly linked to speed 'n':

$$D = M \cdot n \quad (7)$$

The proportionality factor M recognizes the characteristic geometry of the sensor system. It is defined as the shear rate per speed unit. The following equations define this M factor:

Cylinder Sensor Systems

$$M = \frac{\pi}{15} \cdot \frac{R_a^2}{R_a^2 - R_i^2} \quad (8)$$

Cone-and-Plate Sensor Systems

$$M = \frac{\pi}{30 \cdot \alpha} \quad (9)$$

Note: The new SI-unit of an angle is the "radiant" rad. This correlates to the normally used "degree angle" (°):

$$1° = \frac{\pi}{180} \text{ rad} = 0.0174 \text{ rad}$$

Viscosity η:

The equation to calculate the viscosity of Newtonian liquids is:

$$\tau = \eta \cdot D \quad (10)$$

When using the equations for τ (2) and D (7) this leads to:

$$A \cdot S = \eta \cdot M \cdot n$$

or with η:

$$\eta = \frac{A \cdot S}{M \cdot n} \quad (11)$$

It is common practice to give viscosity in values of "milli Pascal seconds". Then (11) becomes:

$$\eta = 10^3 \cdot \frac{A \cdot S}{M \cdot n} \quad (11a)$$

To simplify the equation a part of it is combined to a constant G being typical for each sensor system:

$$G = 10^3 \cdot \frac{A}{M} \quad (12)$$

Thus the equation (11a) is changed to:

$$\eta = \frac{G \cdot S}{n} \text{ (mPa·s)} \quad (13)$$

HAAKE

8.2 Determination of instrument constants

Shear rate D, shear stress τ, and viscosity η, are computed from test results of 'n' and 'S' with the sensor factors 'M' (shear rate factor), 'A' (shear stress factor), and 'G' (viscosity factor). These factors are found in the list of calculation factors delivered with each instrument. They were established by means of an absolute test of 'weighing torques' or they are, as for instance 'M' and 'f', calculated by using the geometrical dimensions of the sensor system:

Sensor system	$f \cdot 10^{-4}$ (cm^{-3})	M (min/s)
NV	36.3	5.41
MV I / T I	65.7	2.34
MV II / T II	76.8	0.90
MV III	111	0.44
MV I P	65.8	2.0
MV II P	76.8	0.88
MV SP	87.8	11 *
SV I	253	0.89
SV II	768	0.89
SV II P	768	0.78
SV II FL	572	----
SV SP	253	4.4
MV DIN	55.8	1.29
SV DIN	369.4	1.29
MV-E	61.43	1.29
SV-E	322.1	1.29
HS I	1172	40 *
HS II	1142	10 *
PK V, 1°	305.6	6 *
PK I, 1°	1740	6 *
PKII, 1°	4775	6 *
PK V, 0.5°	305.6	12 *
PK I, 0.5°	1740	12 *
PKII, 0.5°	4775	12 *
PK V, 0.3°	305.6	20 *
PK I, 0.3°	1740	20 *
PKII, 0.3°	4775	20 *

* the factors given are values for reference only; for exact values, see list of calculation factors.

In case that an instrument is expanded by further measuring-drive-units the relevant values A for the range of sensor systems must be calculated:

Example - you need 'A', 'M' for RV 12 with M 150 and MV I.

The value 'a' of the measuring-drive-unit M 150 is 0.0147 Ncm/scale grad.
" " " M 500 is 0.049 Ncm/scale grad.
" " " M 1500 is 0.147 Ncm/scale grad.

Calculation of shear stress factor 'A': $A = f \cdot a = f(MV\ I) \cdot a(M\ 150)$

$A = 65.7 \cdot 10^{-4}\ cm^3 \cdot 0.0147$ Ncm/scale grad. $A = 0.966 \cdot 10^{-4}\ N/cm^2 \cdot$ scale gr

A = 0.966 (Pa/scale grad.)

Calculation of shear stress factor 'M': Taken from the above table.

Calculation of viscosity factor '

$$G = \frac{A}{M} \cdot 1000 = \frac{0.966}{2.34} \cdot 1000 = 413$$

HAAKE

8.3 Calibration

The Rotovisco has been calibrated before delivery. However, the calibration may also be carried out by the customer, which, of course, requires strict adhering to the instructions of the manufacturer. It is of utmost importance to maintain the temperature indicated on the bottle of the standard liquid (±0.01°C, or at least ±0.05°C). The procedure consists of determining the "S" values for each given "n" value. The constant for the particular sensor system can be found using the following equation:

$$G = \frac{\eta \cdot n}{S} \quad \text{(mPa·s/scale grad. · min)}$$

Whereby η represents the viscosity of the standard liquid in mPa·s as noted on bottle.

The shear stress factor A of the rotor can be determined from the following equation:

$$A = 10^{-3} \cdot \frac{\eta \cdot n \cdot M}{S} \quad \text{(Pa/scale grad)}$$

The shear rate factor M can be obtained from the list of calculation factors.

We supply the following standard liquids:

Order designation	Viscosity (mPa·s)	Reference temperature (°C)
7	ca. 4.5	20
200	140	20
2 000	1 840	20
6 000	5 990	20
13 000	14 780	20
30 000	25 780	20
70 000	66 570	10

The viscosity values given above are typical values for reference only. The exact values with reference to temperature and date are noted on each bottle.

The standard liquids can be supplied in quantities of 50, 100 and 250 cm³. The liquids should be stored in a cool and dark place.

Since standard liquids can change with time, the specifications given only apply a period of 3 months after delivery.

HAAKE

9.0 Measurements

To measure viscosity values, speeds or speed programs have to be preset and the resulting torque recorded. Substances, showing a time dependent viscosity value (thixotropic liquids), should be measured with a speed program using an x-y-recorder or, at fixed speed, with a y-t-recorder.

Advice on instrument settings

a) Sensitivity 'E'

The torque reading 'S' should be between 10 and 100 scale grad. which calls for setting E 1 or E 0.3. A further extension/reduction is possible through other measuring-drive-units and different sensor systems

b) Reduction 'R'

The setting of 'R' is given by the required shear rate range and the sensor used. High shear rates are possible in R 1 but for measuring the yield points or the thixotropic recovery, low shear rates should be used with setting R 10 or R 100. A speed resulting with a setting of R 10 is more accurate than a comparable speed with R 1.

c) Time settings using PG 142

Selecting t_1

t_1 is defined as the hold time period. It starts by depressing the push-button ⊕ and ends when tests actually start with rotation. If t_1 is too short, a constant temperature before starting a test cannot be guaranteed and, as a result, the reproducibility of the test results could be low.

The length of t_1 required in order to always guarantee identical test temperatures, will depend on the following:

- type of sample and its specific heat coefficient;
- temperature difference between ambient and required test temperature;
- type of sensor system selected: Gap size between inner cylinder and beaker, surface area of the inner cylinder, wall thickness of the beaker, etc.
- type of circulator used to control the temperature.

Values of t_1 = 2 min will be acceptable for many watery samples to be tested at or slightly above room temperature. Testing pastes or creames at temperatures above 30°C may require a t_1 = 4 min or more. What is suitable as t_1 must be determined by preliminary tests.